II

Pure and mixed films preparation using thermionic vacuum arc method

(original contribution)

OUTLINE

1. TVA principle
2. Fusion Energy; Be coatings on Inconel and marker tiles
3. Hard antireflexive diamond like carbon coatings
4. Preparation of Giant Magnetoresistive (GMR) films
5. High temperature corrosion resistant coatings
6. Tribological coatings

TVA – thermionic vacuum arc - principle

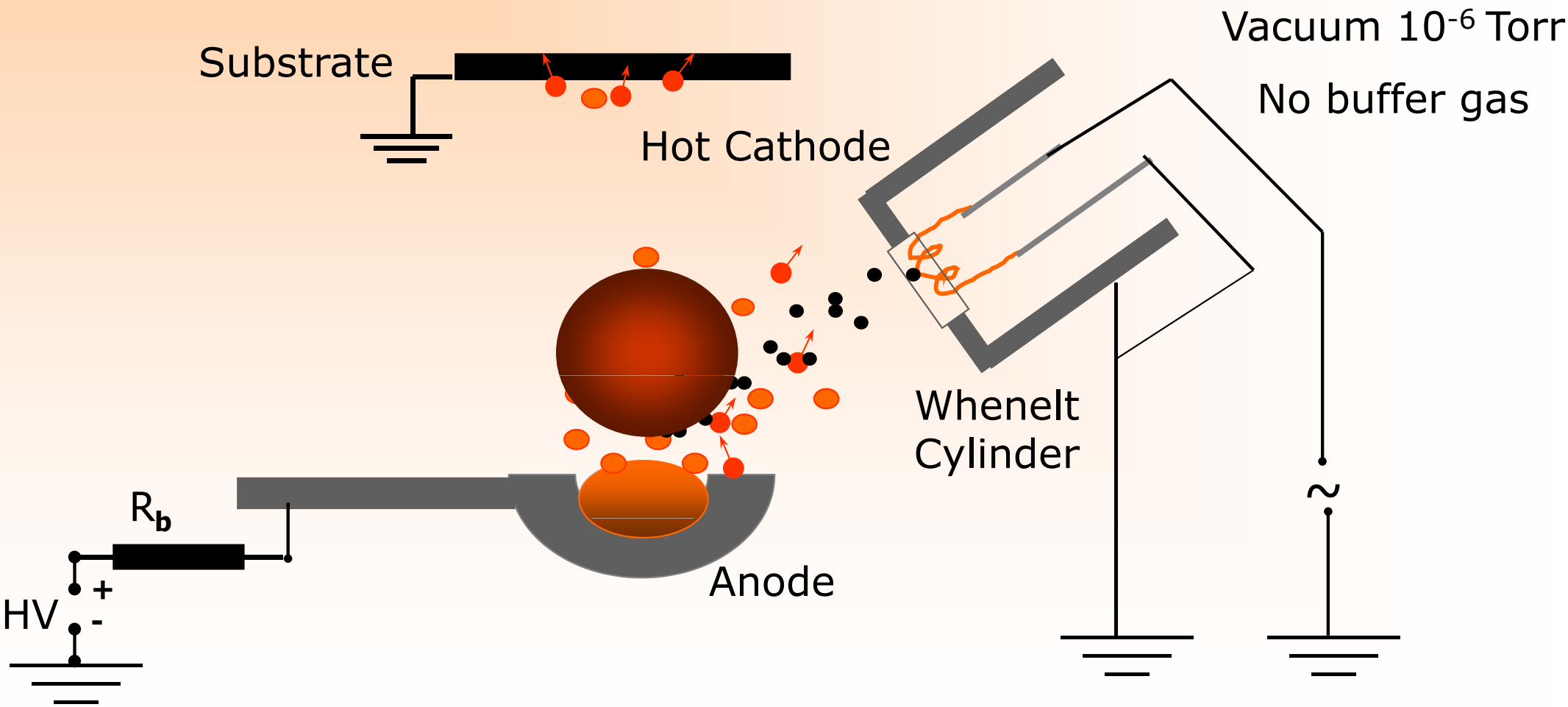

Ignition of the TVA plasma

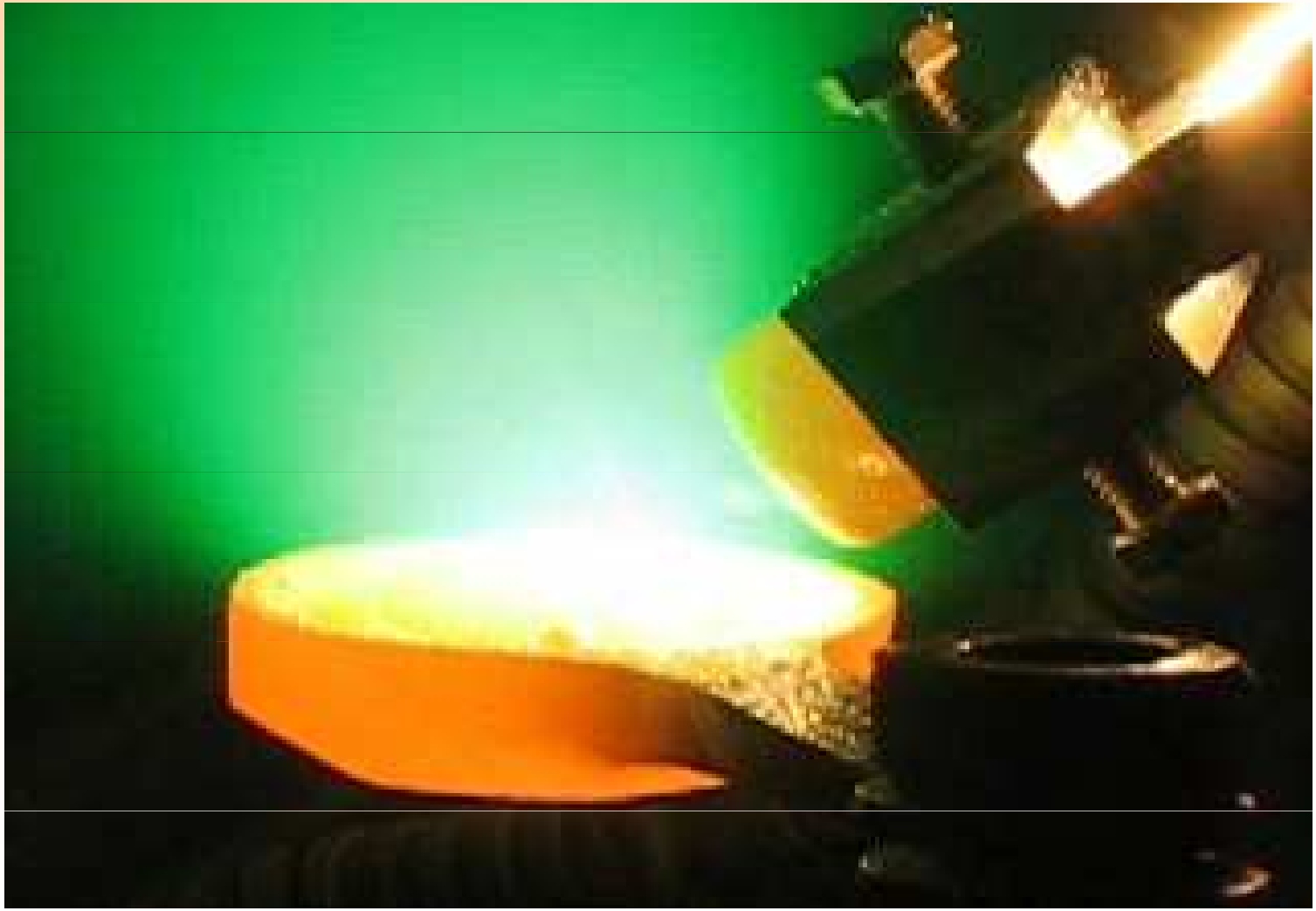

The viewing angle for uniform depositions

20 and 50 degree from the horizontal line.

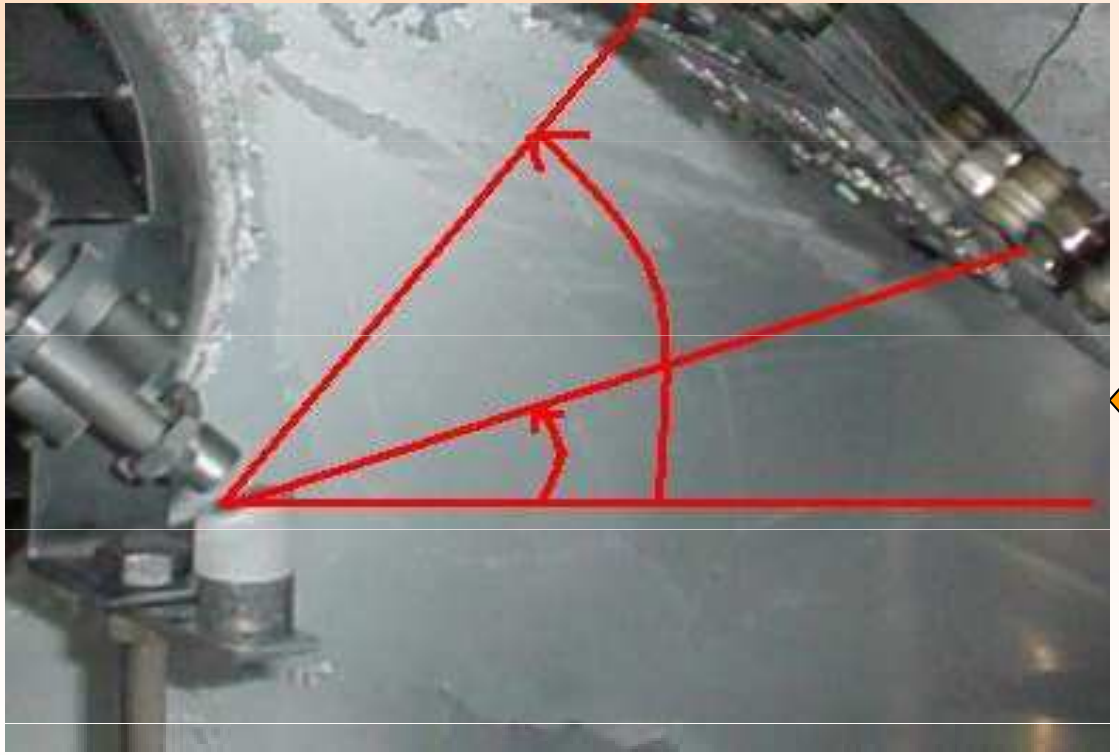

Typical arrangement used for the first Be depositions

Circular TVA

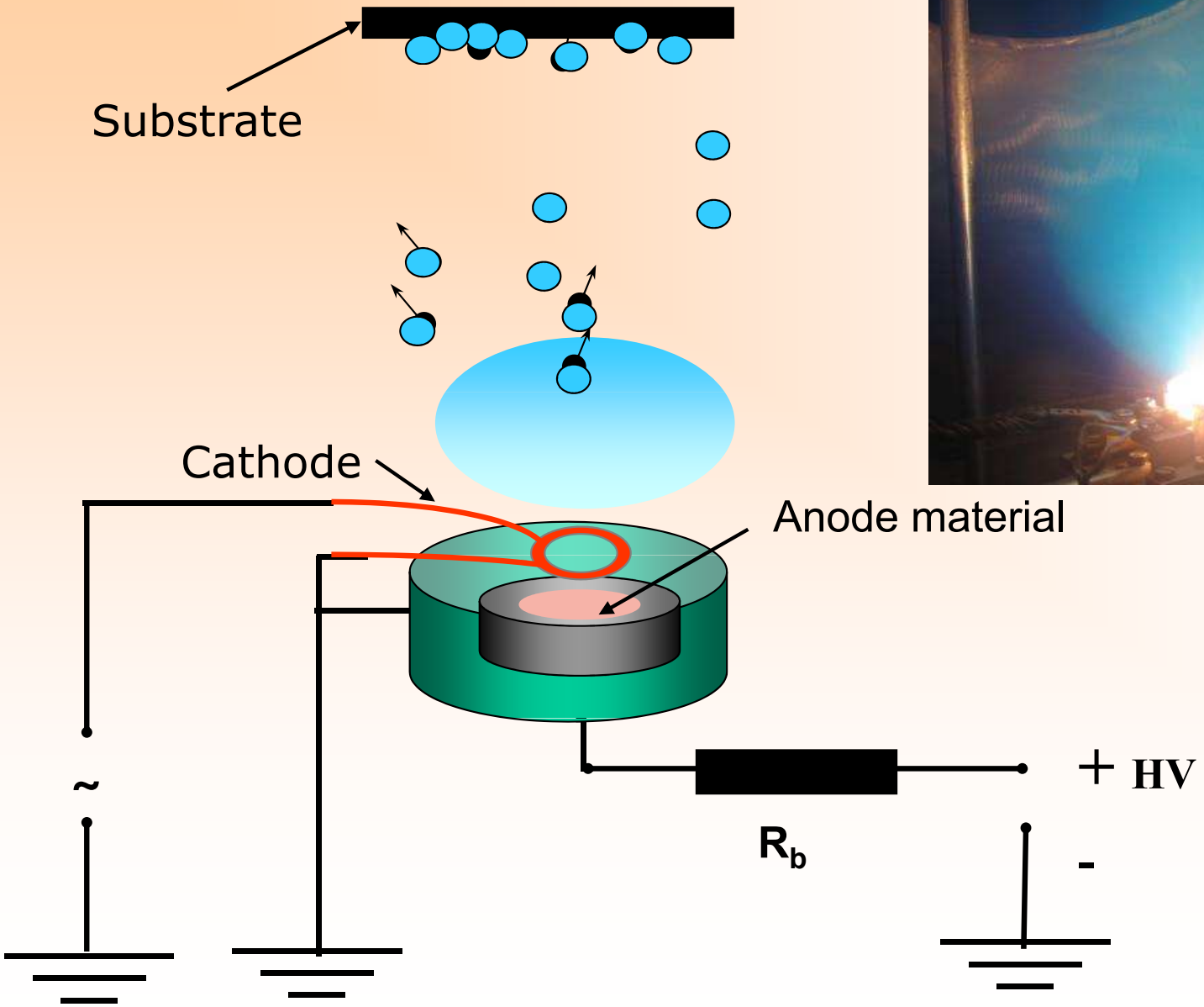

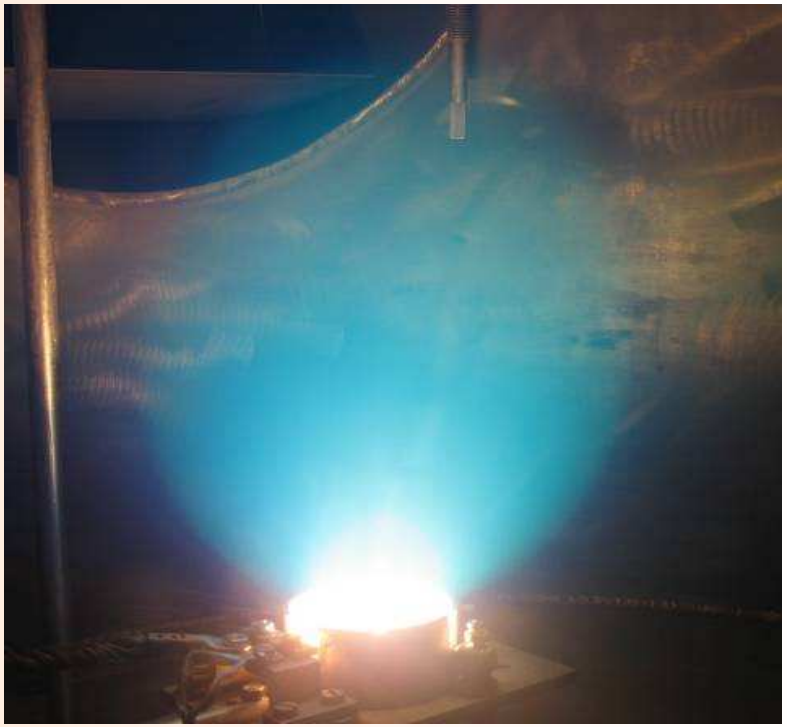

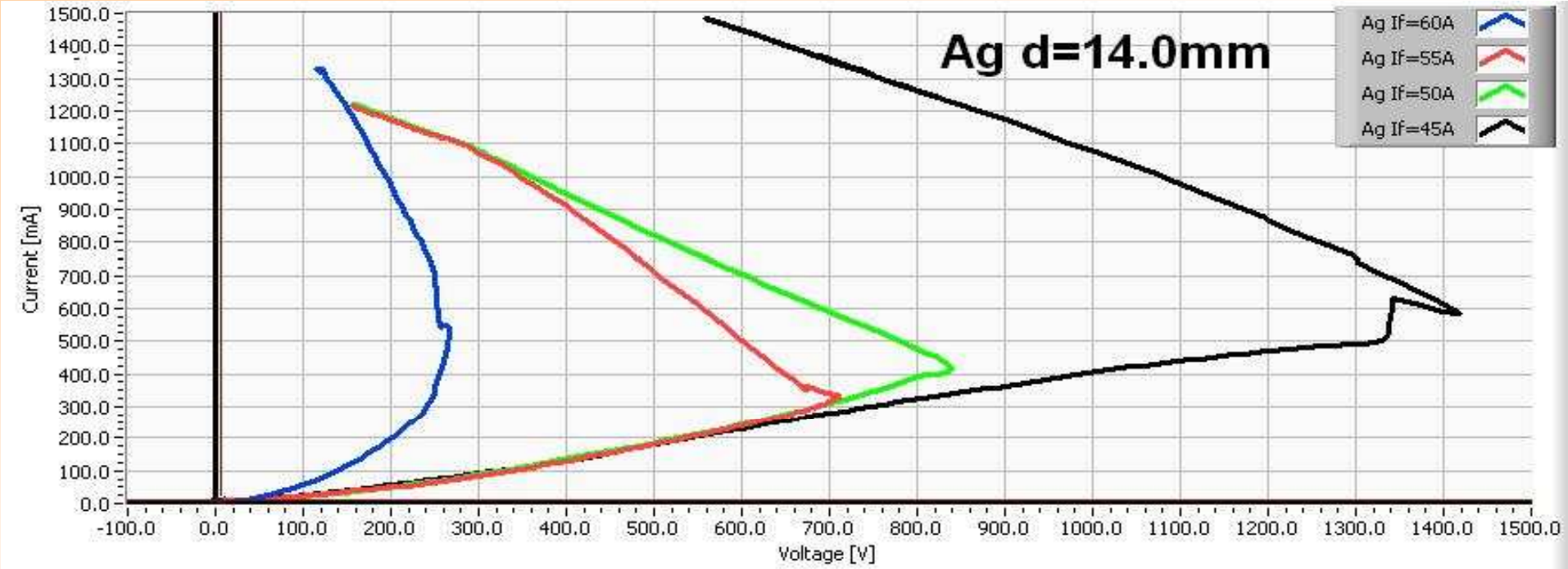

I-V characteristics of the TVA plasma running in Ag vapors for different heating currents

THE ADVANTAGES OF THE TVA TECHNOLOGY

- the high purity of the layers (high vacuum conditions);
- no gas consumption;
- the films are growing from the plasma created in the pure vapors of the evaporating material
- the formed films are continuously bombarded by the genuine ions and the advantages are:
    - no gas inclusions
    - good adherence
    - the ions energy can be controlled by cathode external heating and anode voltage
    - the deposition rates = 1 to 10 nm/sec.

2. Fusion Energy; ITER project

Fusion Energy:

- Climate friendly and yields similar energy production as fission, between 1 and 1.5 gigawatt per plant.

- Do not produce highly radioactive waste or potential nuclear weapon material.

- Its supplies are nearly unlimited. (Main fuel: H^3)

Nuclear fusion development

TECHNOLOGY PROGRAMME

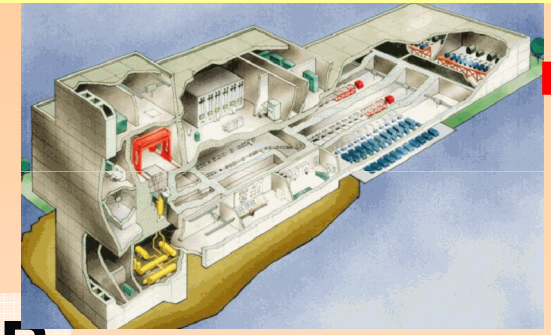

ITER

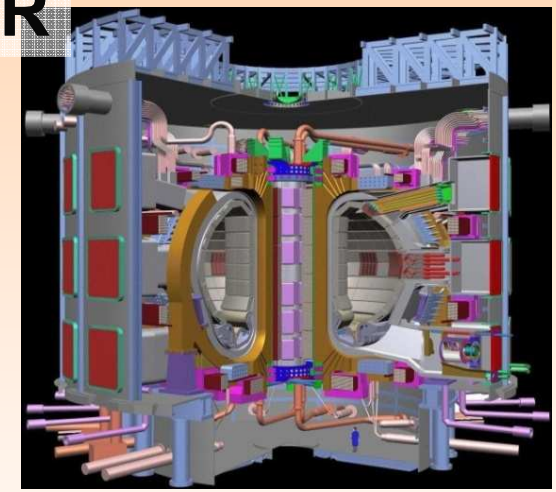

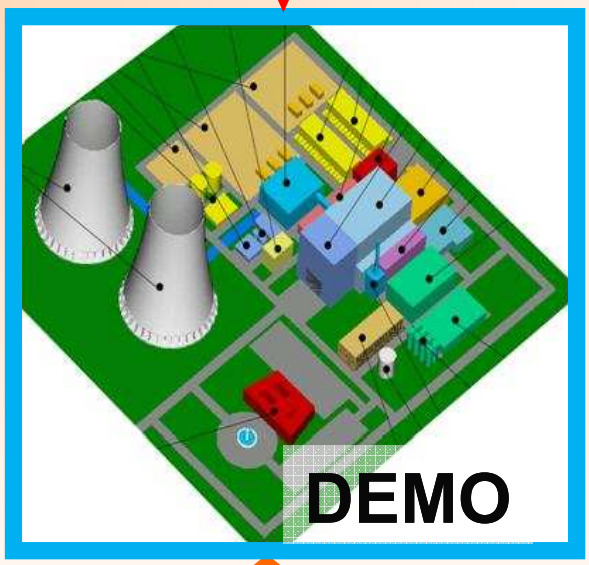

DEMO

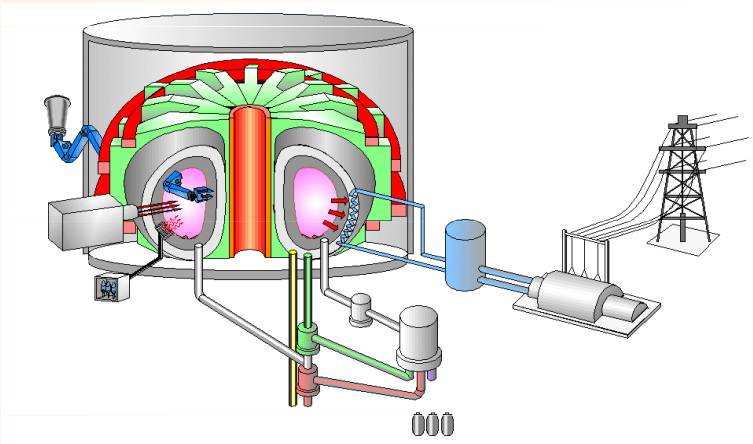

POWER PLANT

JET

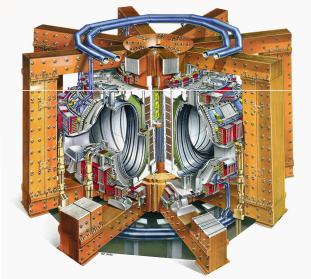

PHYSICS PROGRAMME

EFDA-JET homepage: www.efda.org.

JET ITER-like wall experiment

ITER

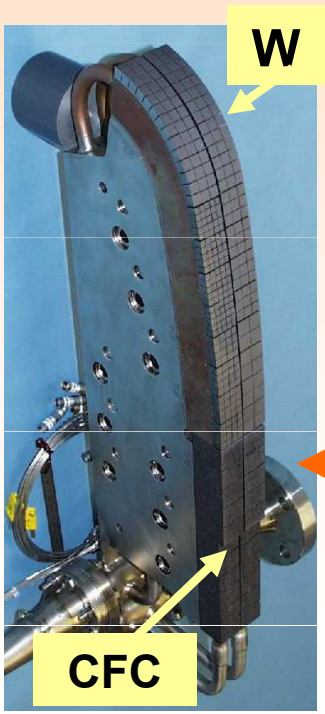

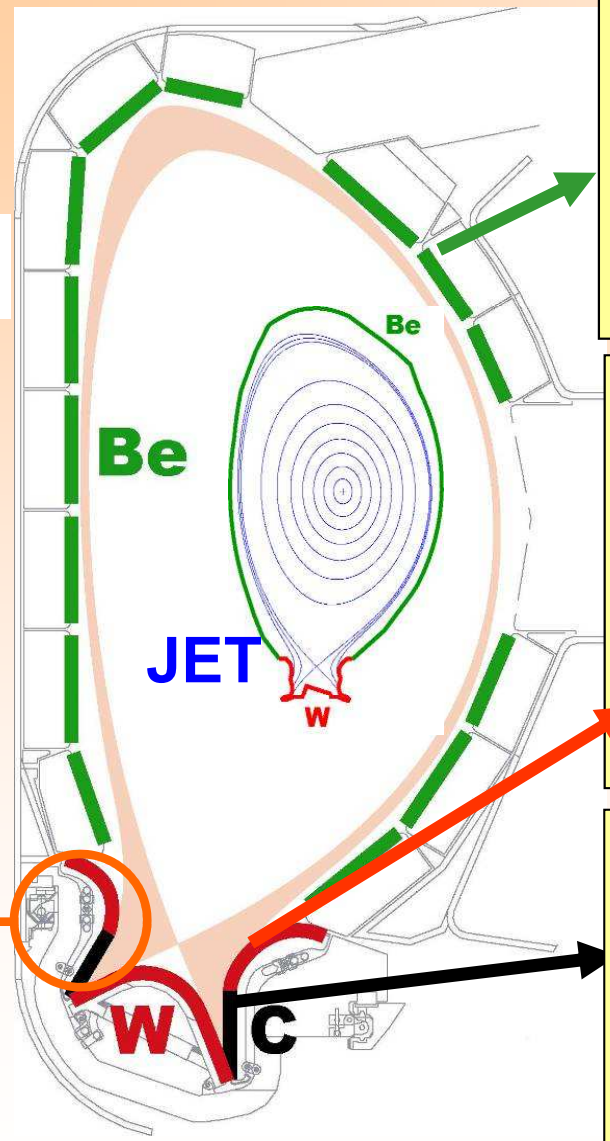

700m² Beryllium first wall

- low Z
- Oxygen getter

Optimise plasma performance

But large erosion & melting

100m² Tungsten

- Low erosion
- high melting T
- Negligible T retention

Optimise lifetime & T- retention

But high Z & melting

50 m² Graphite CFC

- Lowish Z
- No melting in transients
- Superior heat shock behaviour

Optimise heat flux resistance

But large erosion & T retention

ITER-like wall installed at JET

Image taken from EFDA-JET homepage: www.efda.org.

Licensed laboratory to work with beryllium and beryllium containing composites

Vacuum deposition system:
- **stainless steel chamber,**
- **glass, quartz and**
- **germanium windows;**
- **volume; 250 l,**
- **base pressure; $6*10^{-7}$ torr**
- **mechanical pump (60 m^3/h),**
- **buster pump (200 m^3/h),**
- **diffusion pump (3000 l/s)**

BERILLYUM

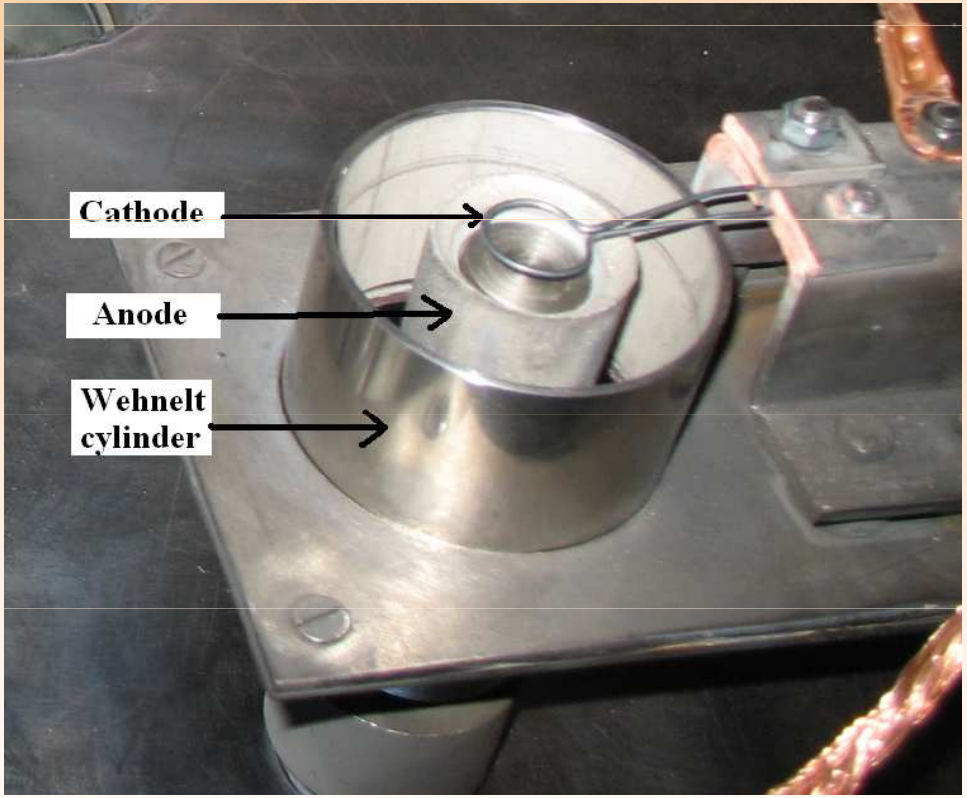

TVA evaporator and plasma running in pure Be vapors

Be/St Steel
Bias: **+430V**

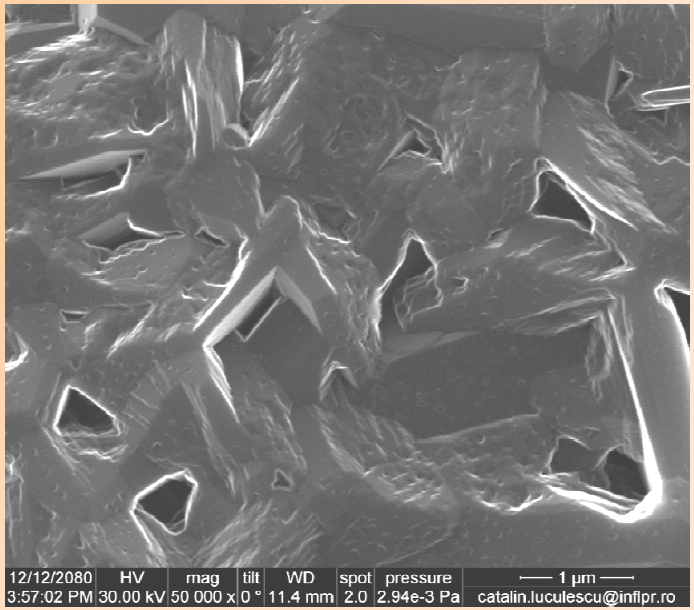

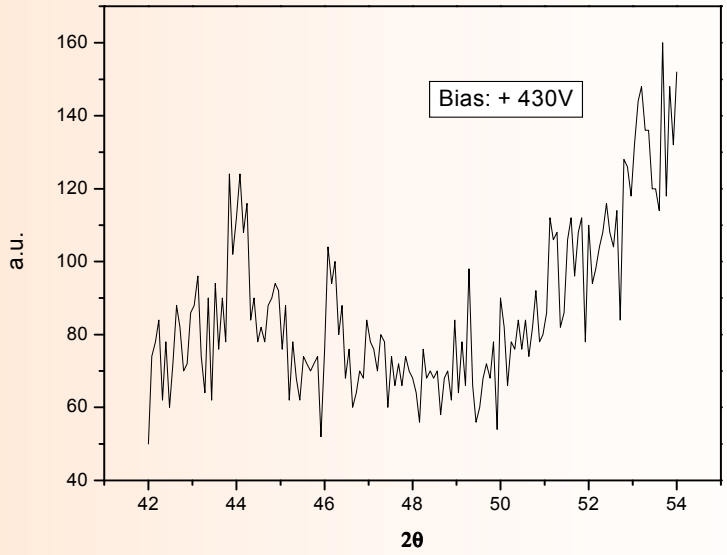

Be/St Steel
Bias: **0 V**

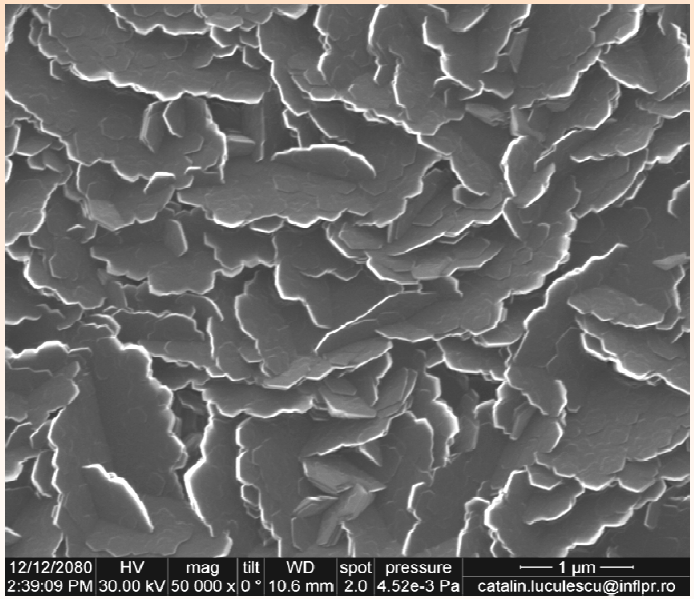

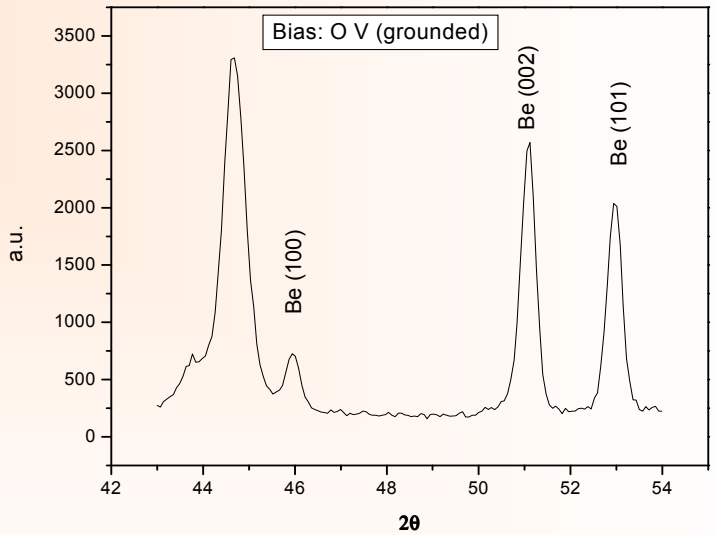

Be/St Steel
Bias: **-285 V**

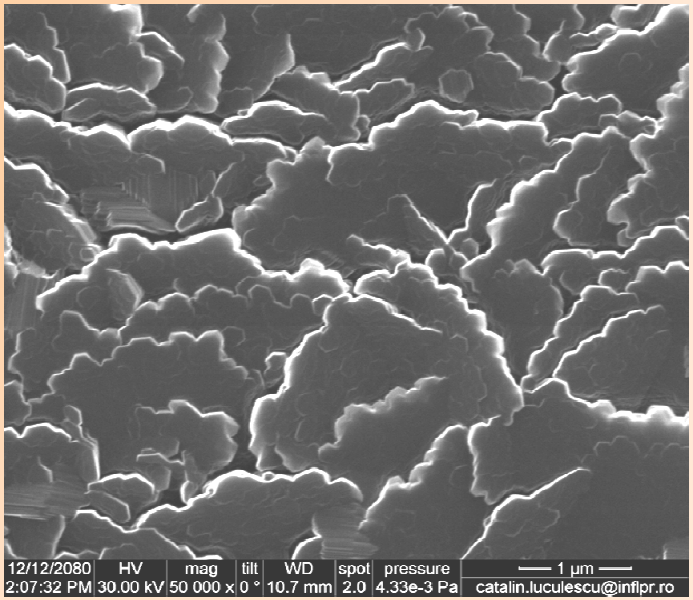

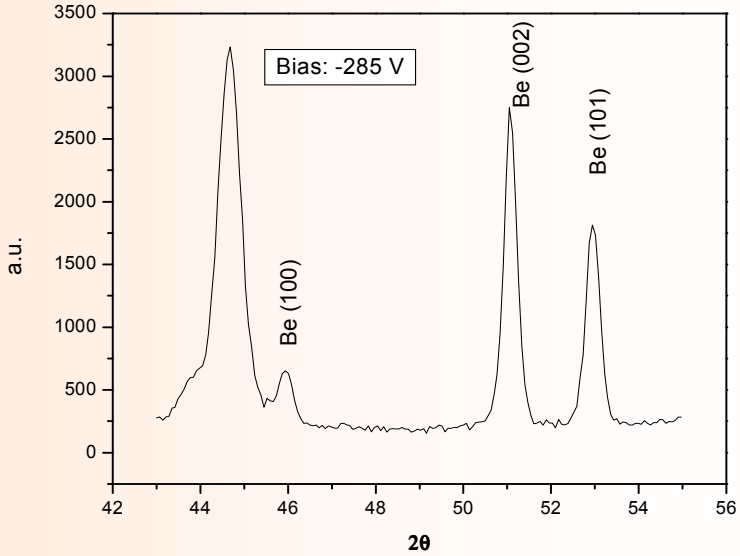

Be/St Steel
Bias: **-750 V**

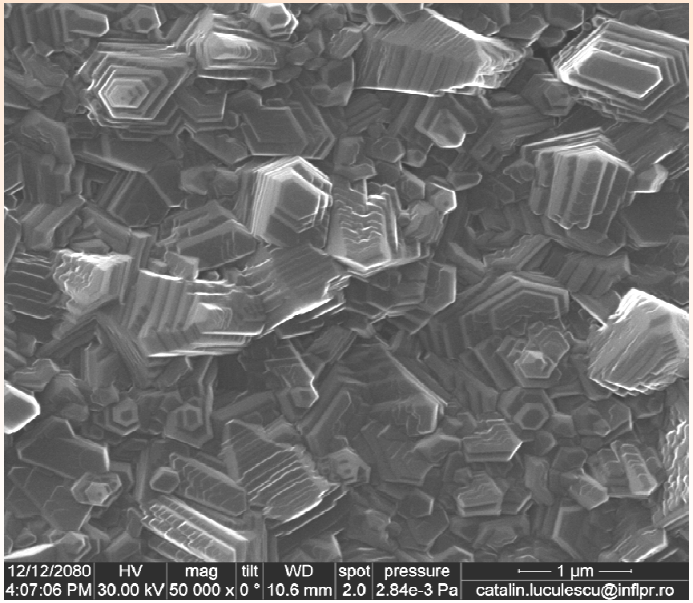

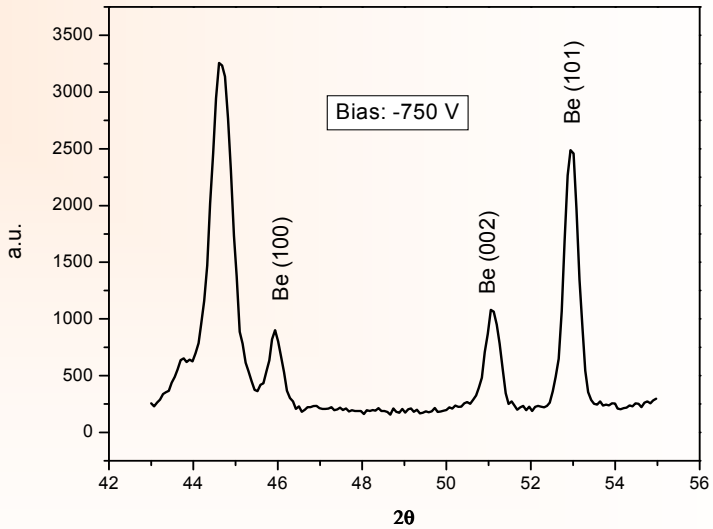

Bias: +430 V

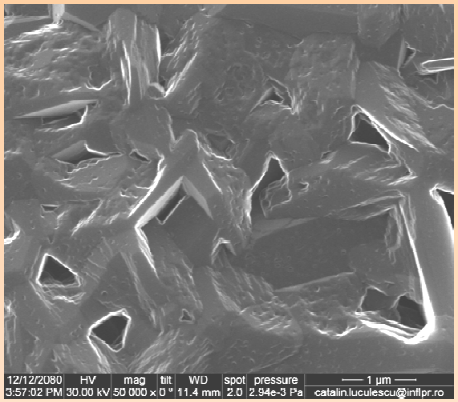

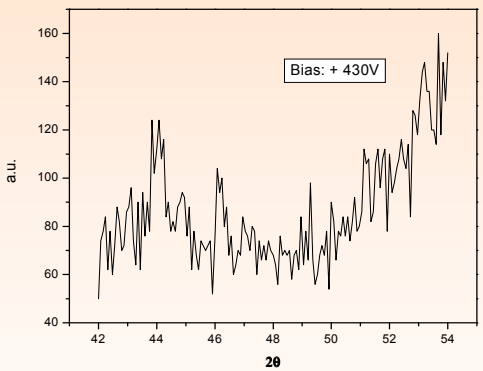

0 V

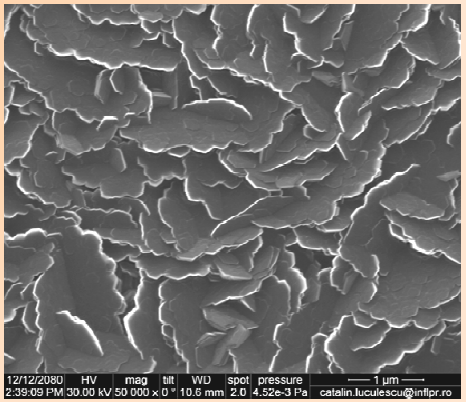

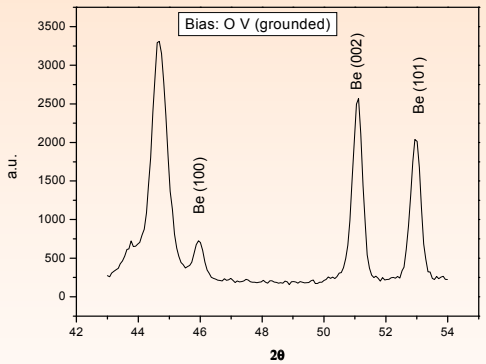

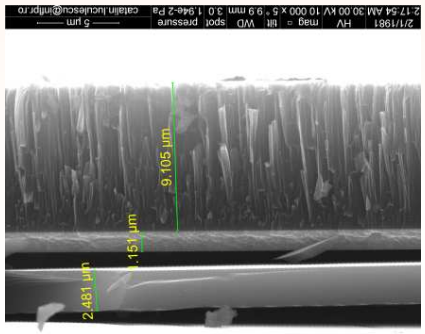

-285V

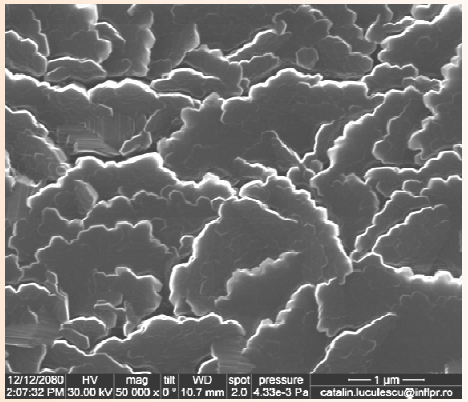

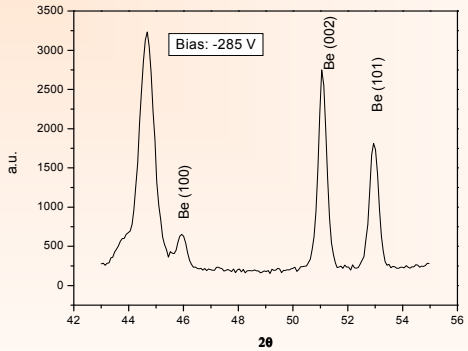

-750 V

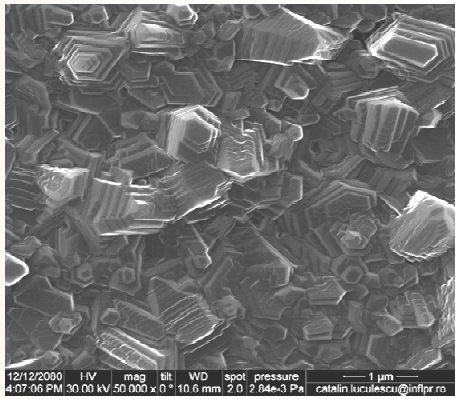

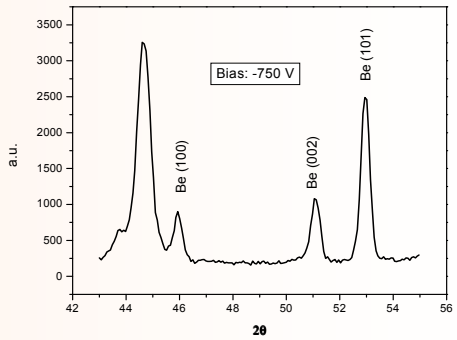

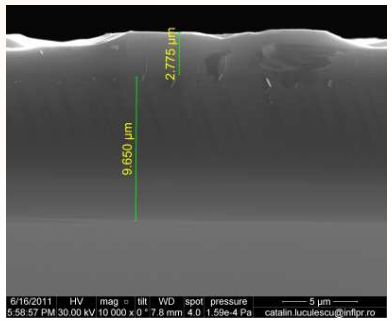

Be Marker coated tiles for ILW

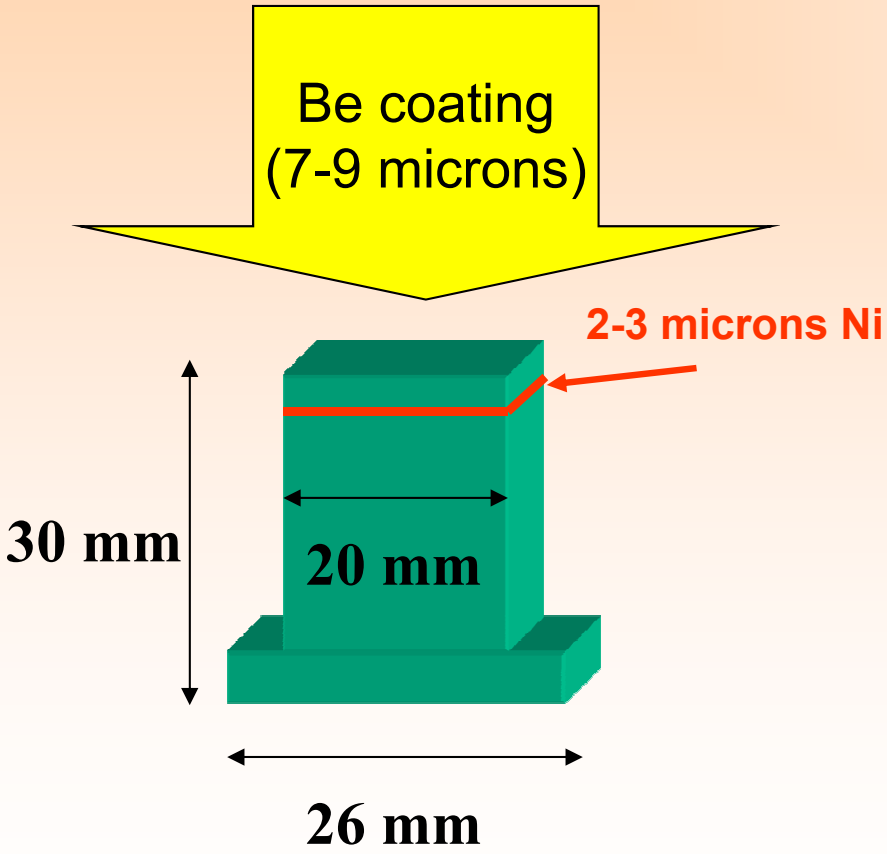

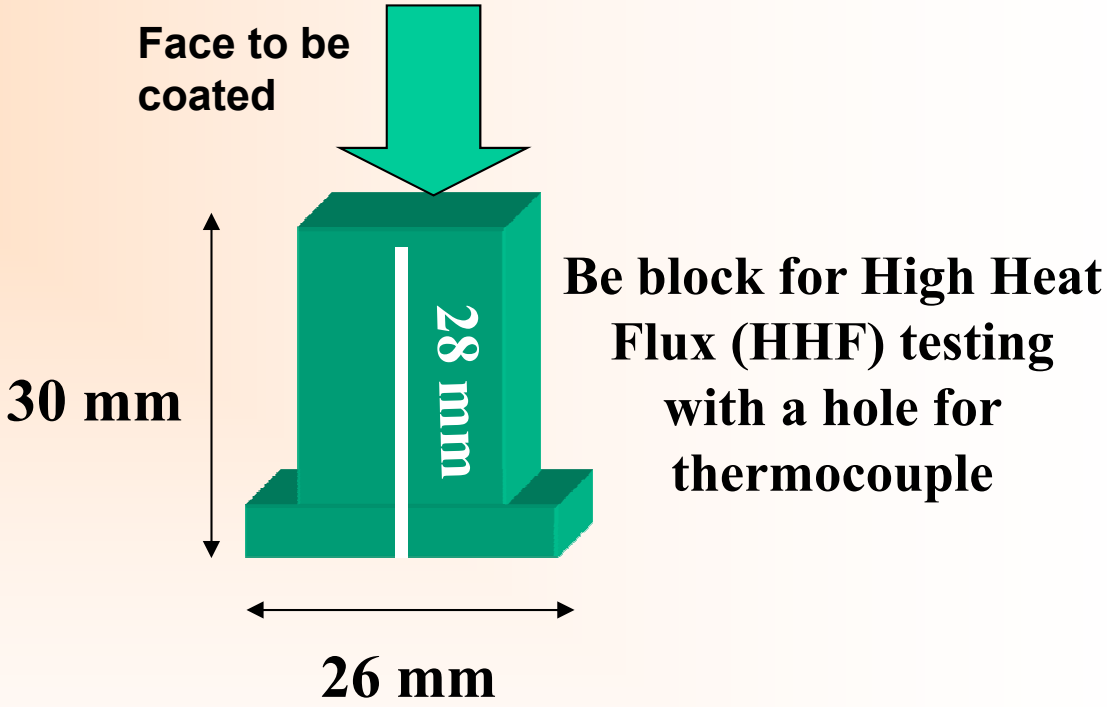

Be plasma

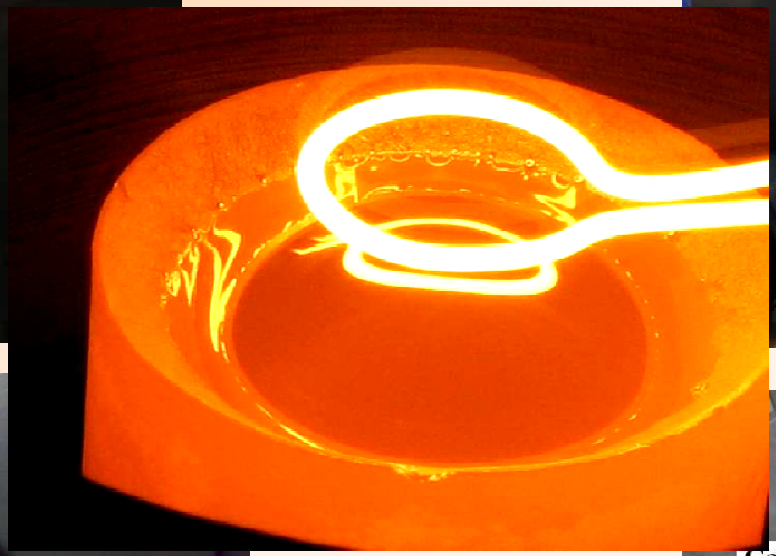

Ni plasma

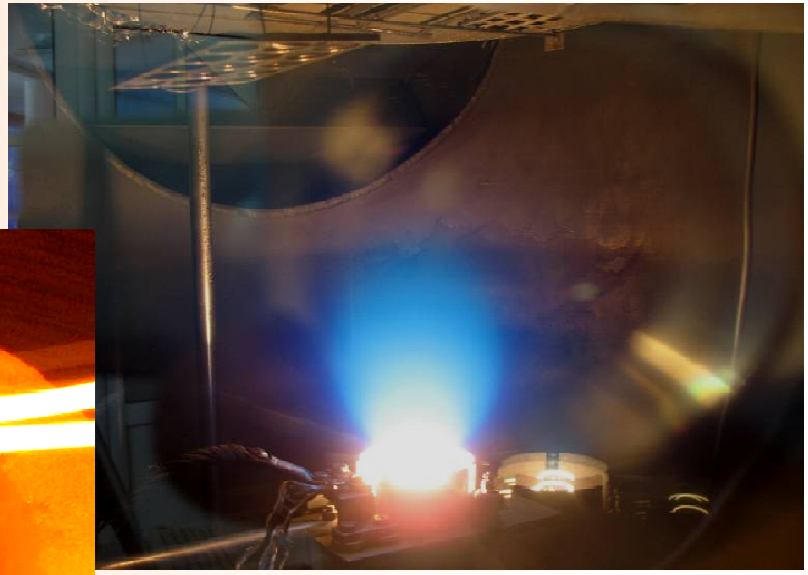

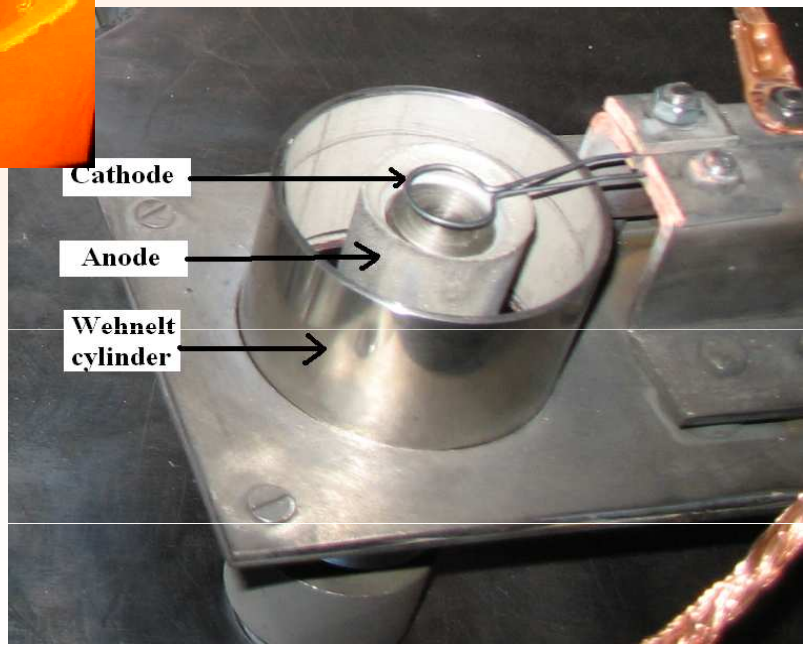

Ni and Be evaporators

Cross-section of Be blocks

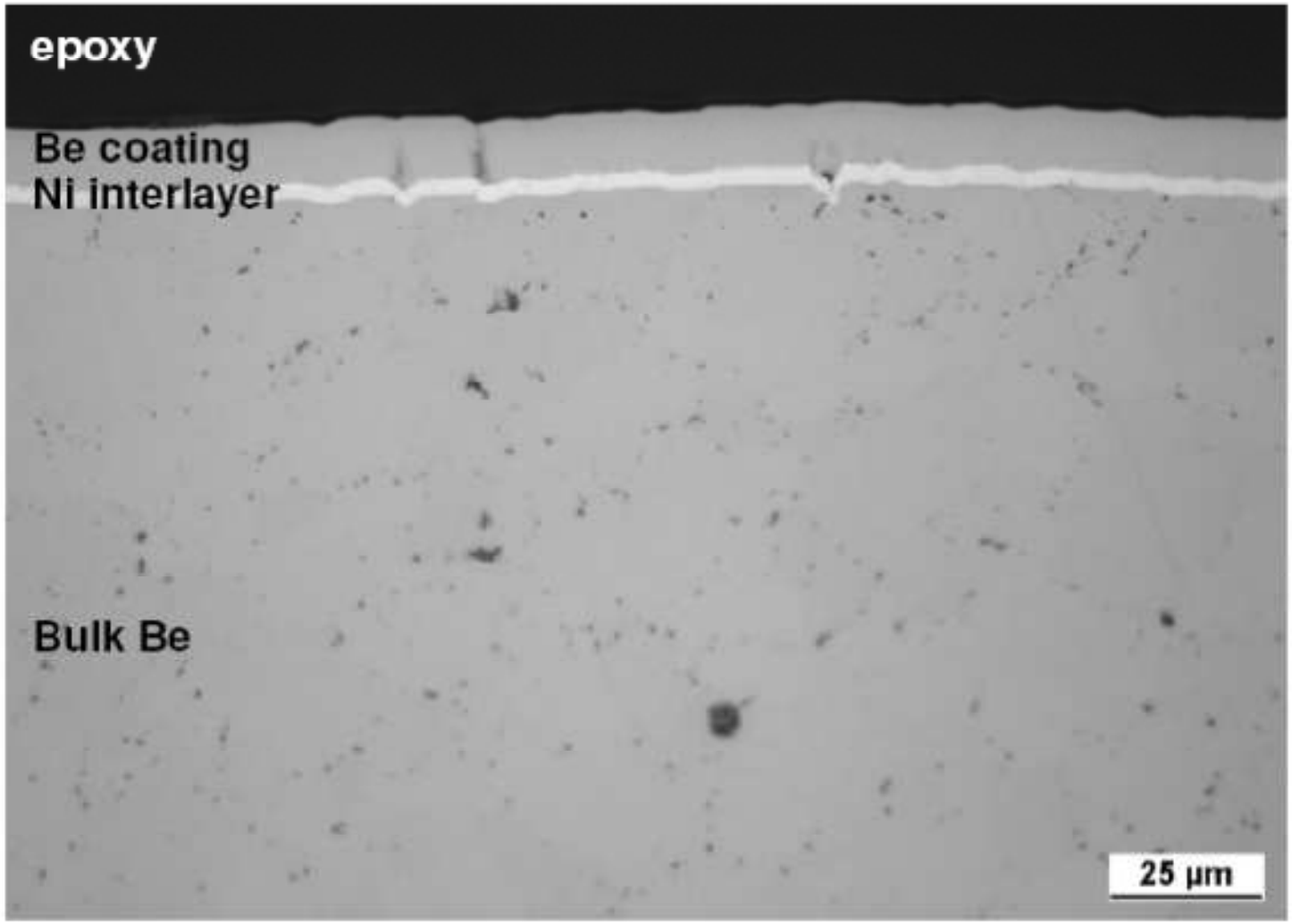

Fig. 16 TC28, 50 cycles of 3.5 MW/m^2 for 10s, optical image.

Impurity analysis of Be blocks

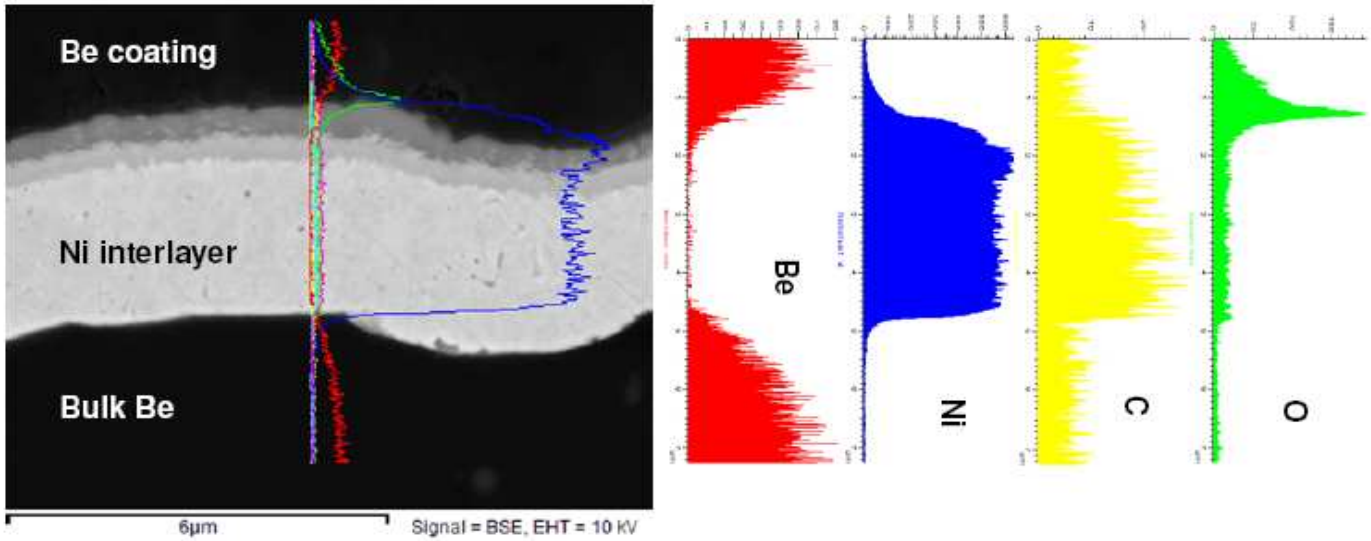

Fig. 25, TC26, 50 cycles of 3.5 MW/m^2 for 10s, BSE image and line scan across the interlayer. O and O background signal at Ni interlayer is caused by artificial effect (high background signal from Ni (high Z) compared with Be (low Z)).

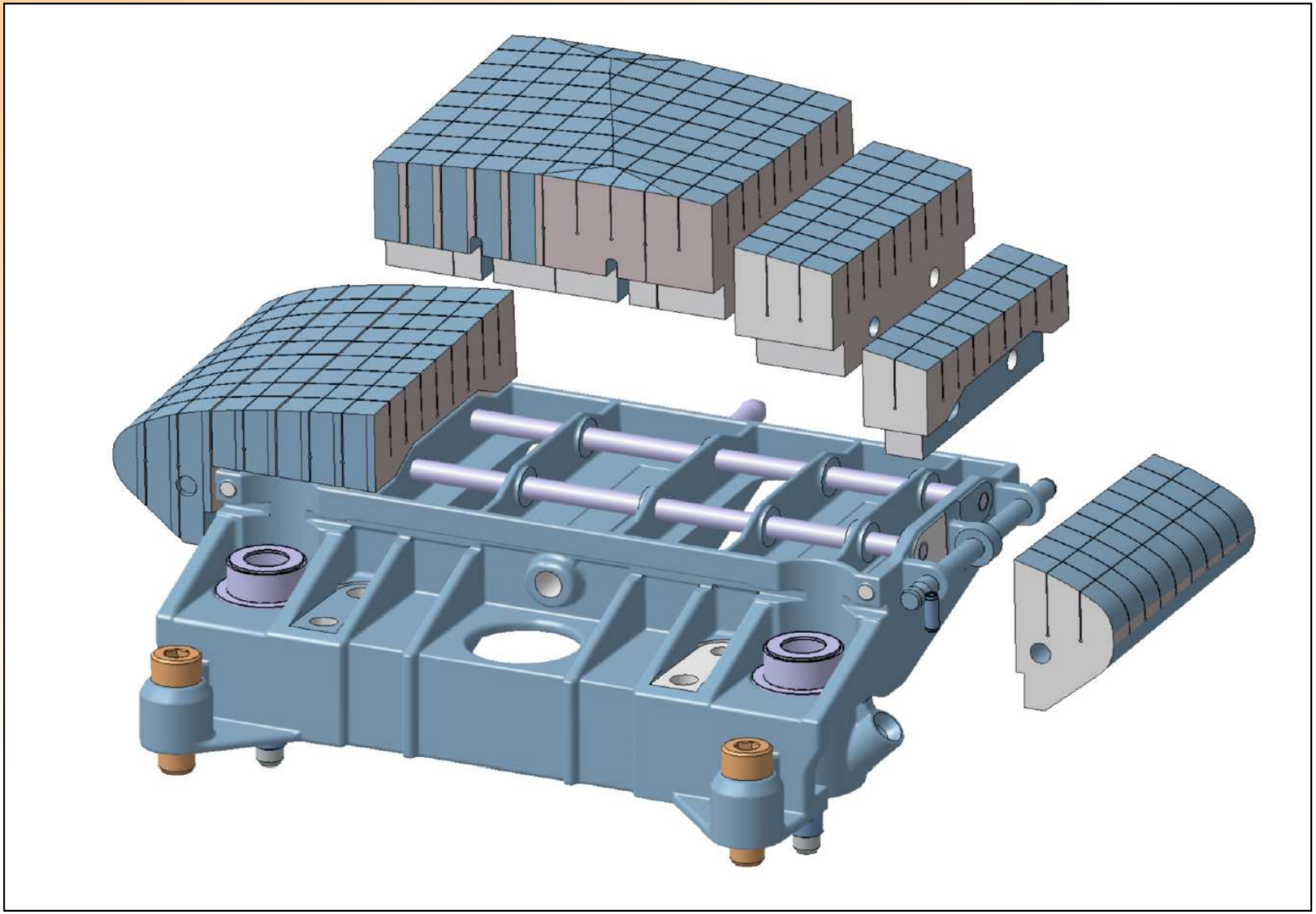

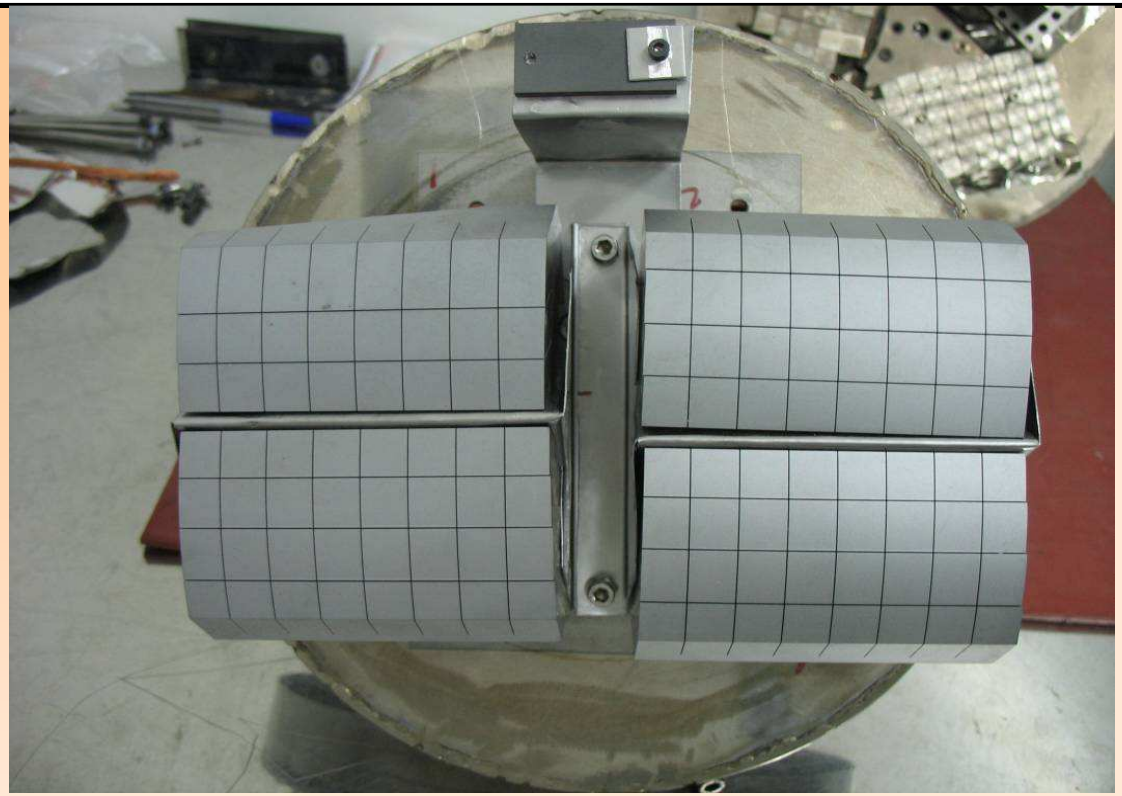

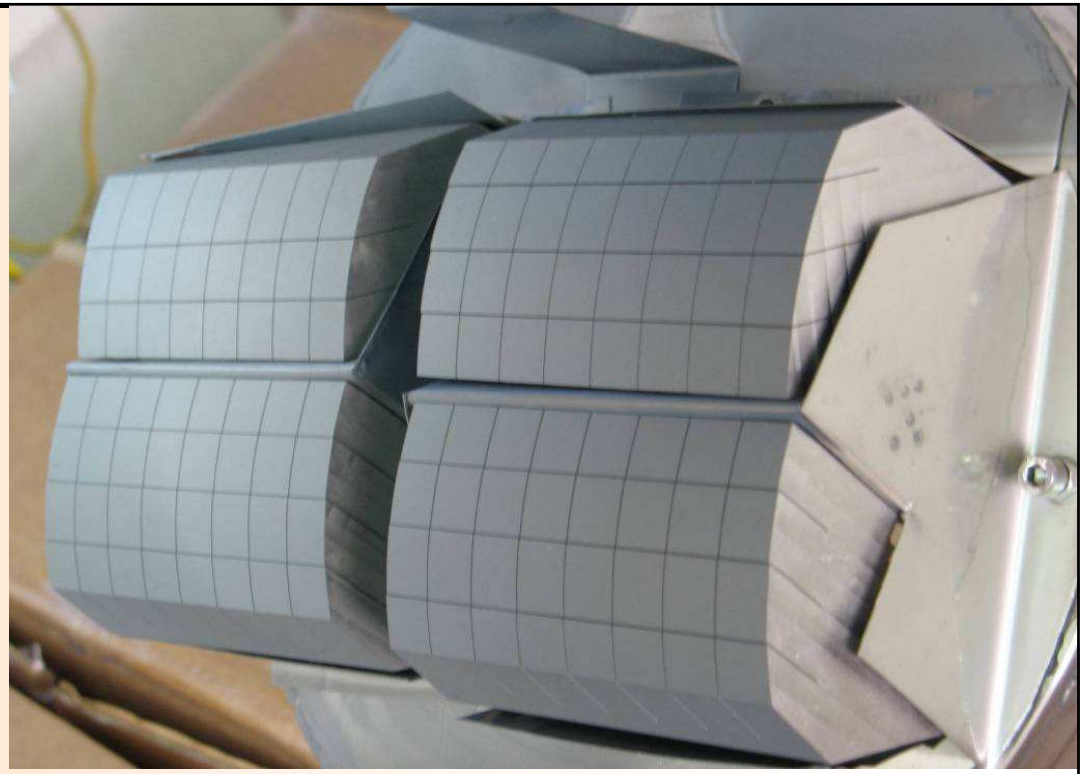

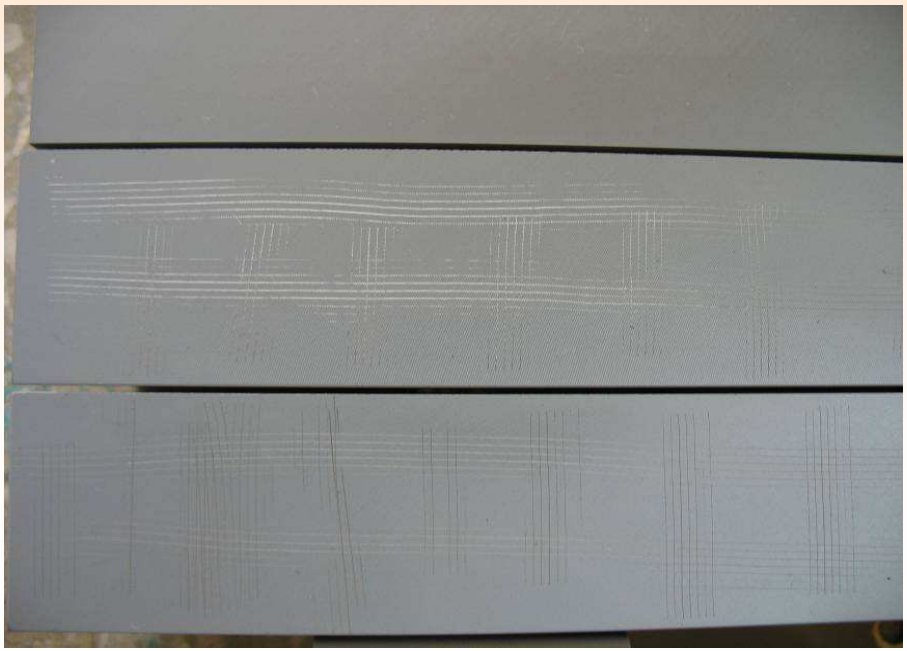

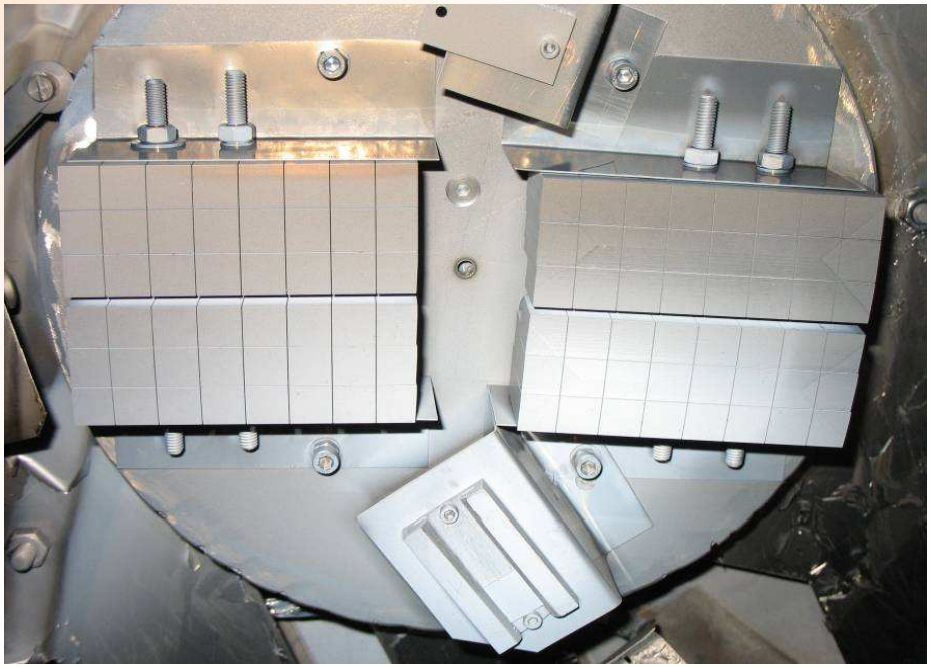

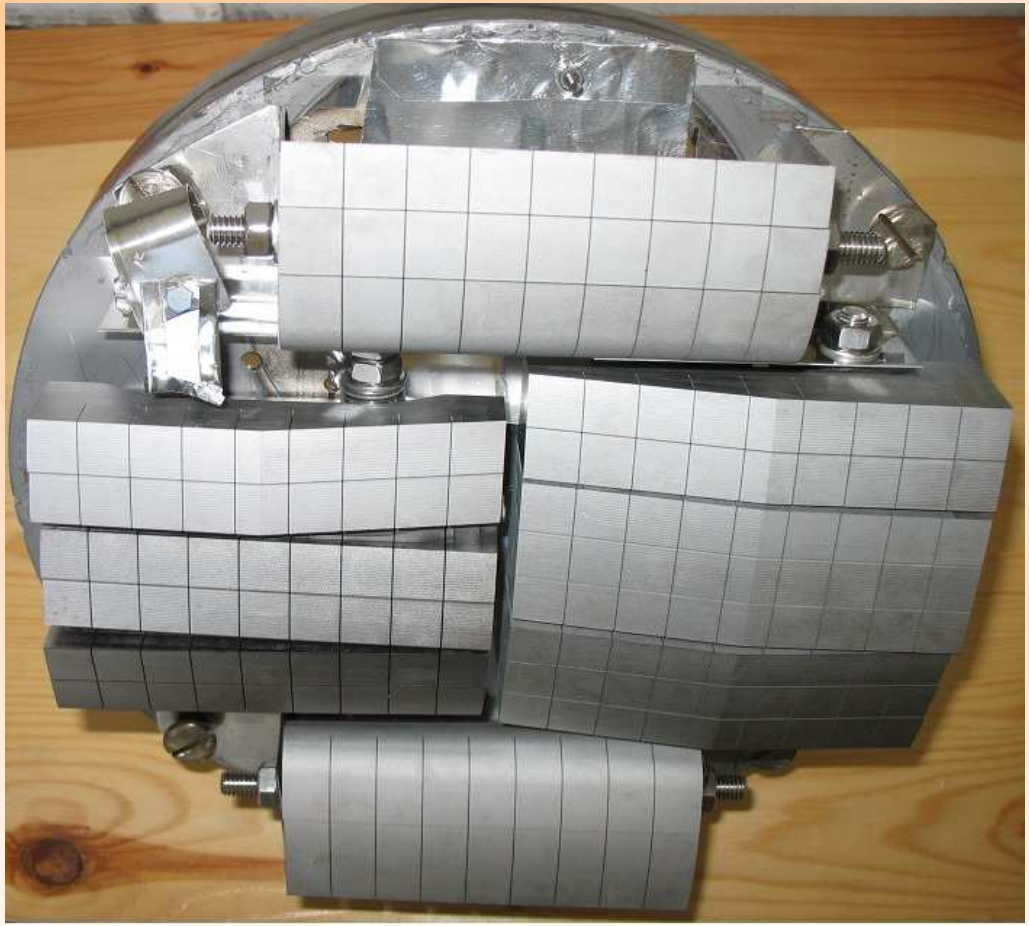

PRODUCTION-Run 5/13.05.2010

IMG_4155 (**Before** Ni+Be deposition)

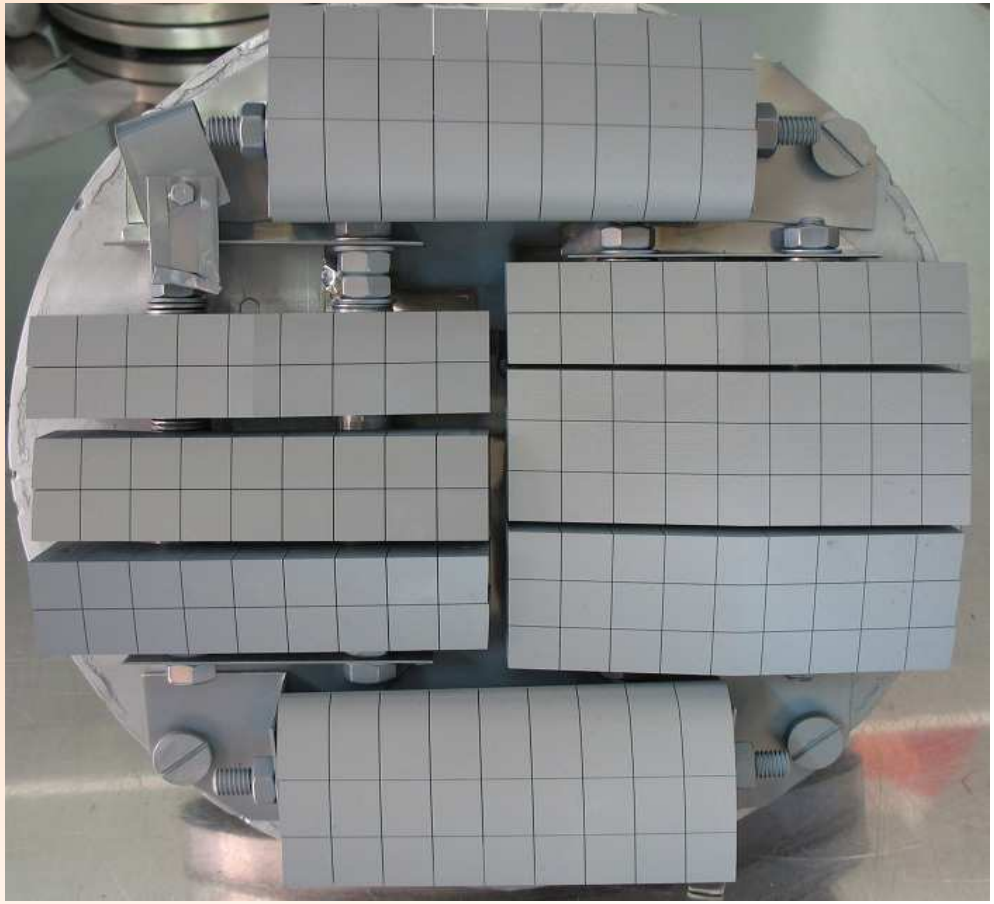

PRODUCTION-Run 5/13.05.2010

IMG_4185 (**After** Ni+Be deposition)

Thermal evaporation in vacuum of Be (Manufacturing of Be / inconel tiles)
(in cooperation with **NUCLEAR FUEL PLANT** (NFP) Mioveni-Pitesti, Romania

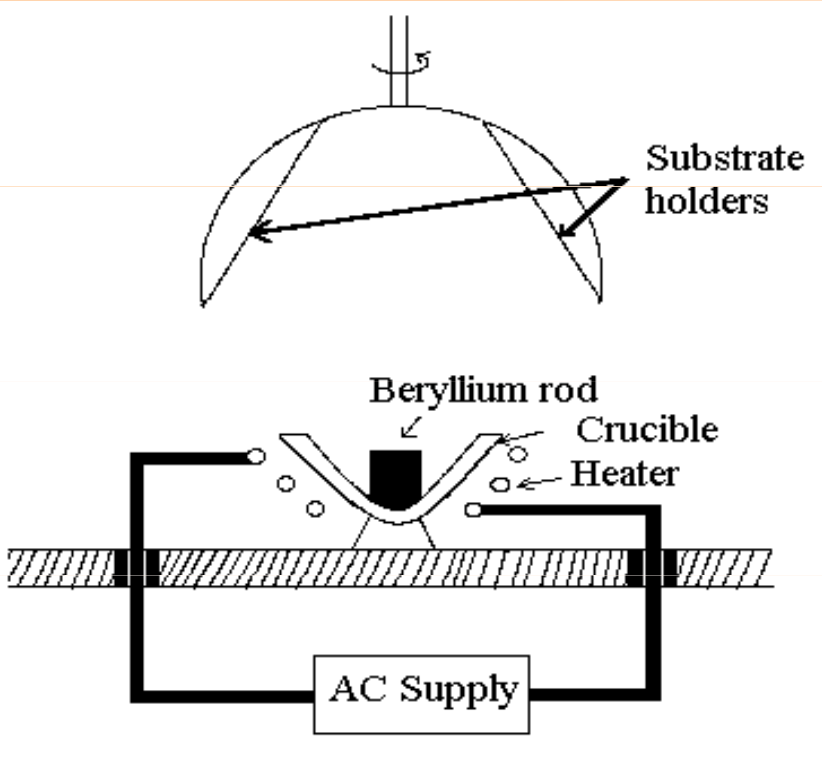

Schematic arrangement for thermal evaporation in vacuum

Photograph of the substrate holder

Scanning Electron Microscopy,

Microscope XL 30 ESEM PHILIPS (1000 x and 5000 x)

	1000x	5000x
Inconel substrate (THERMAL)	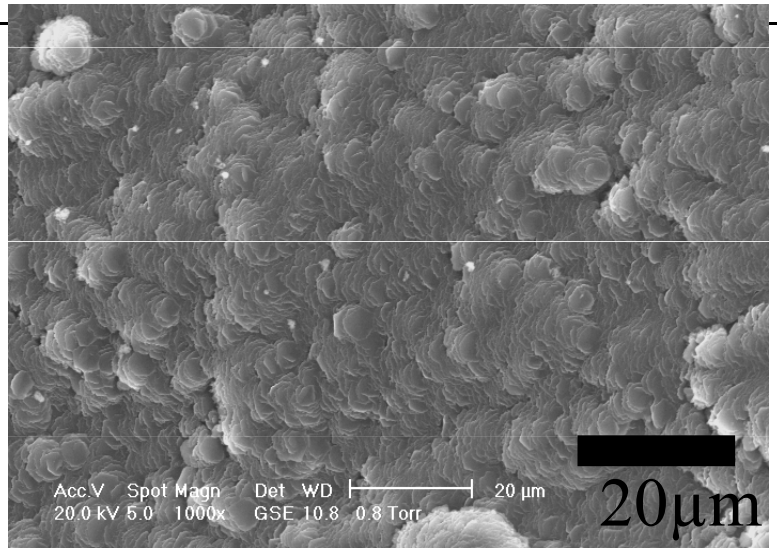	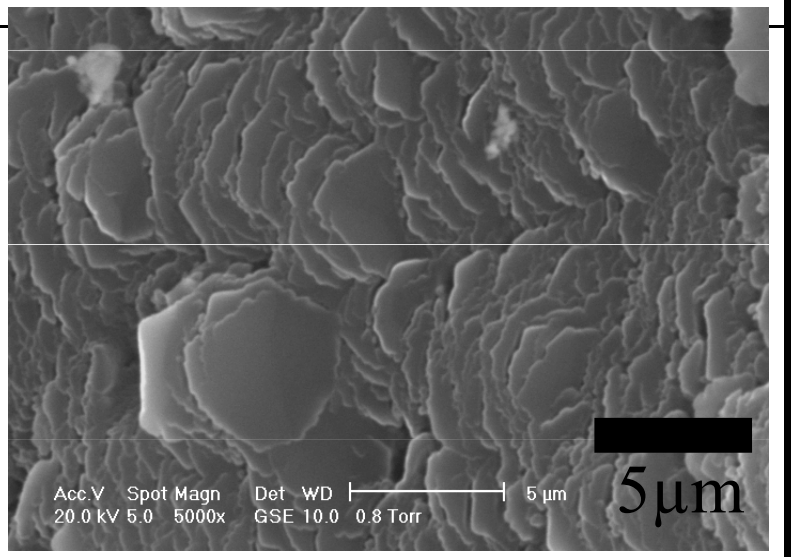
Stainless steel substrate (TVA)	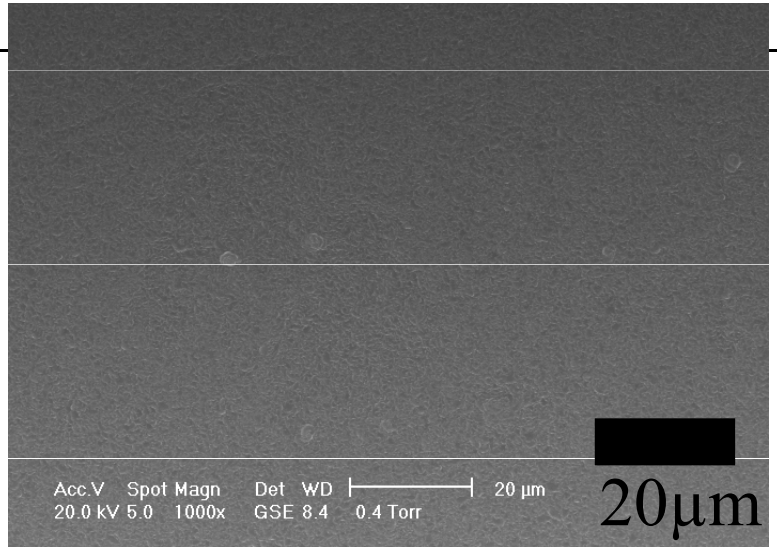	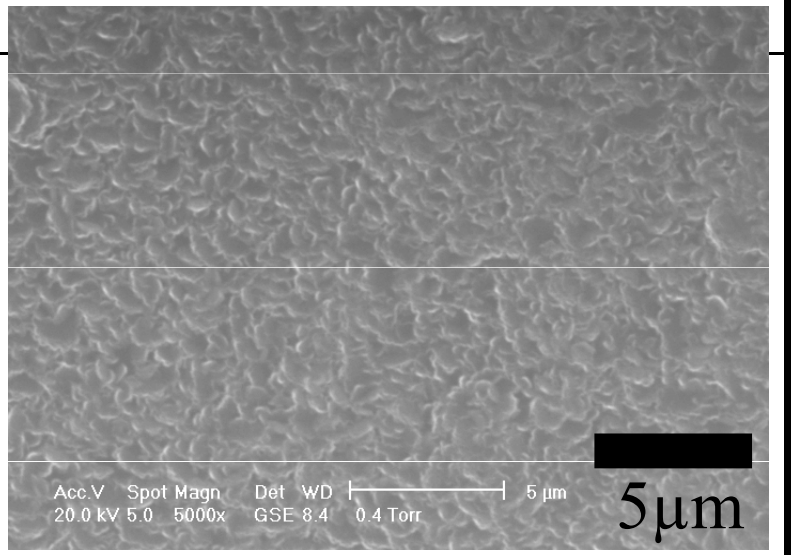

SEM images: microstructure of the Be/Inconel coating from TOP surface

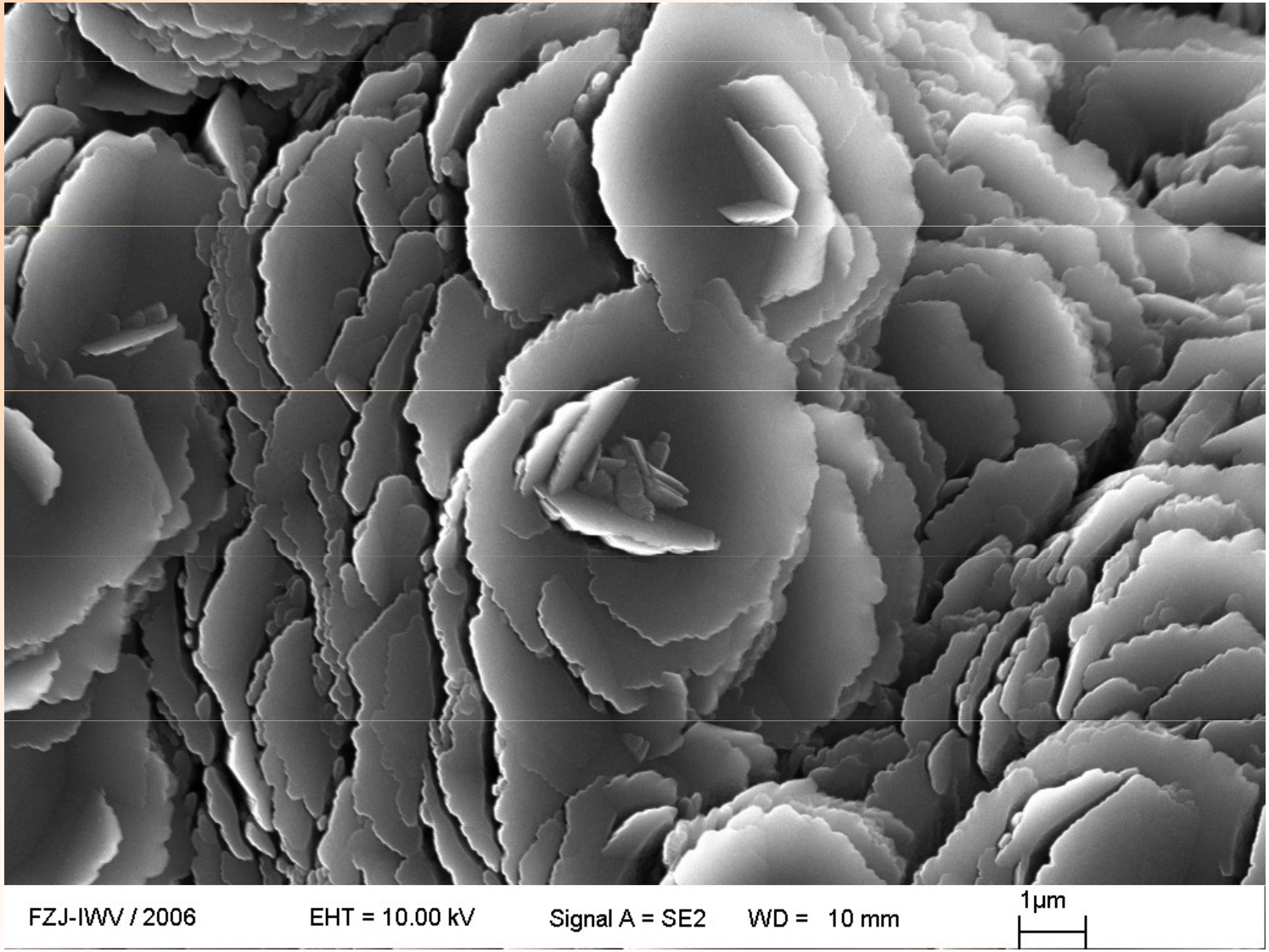

SEM image obtained at FZJ Juelich

- Consists of platelets, occasionally hexagonal morphology, which originated from crystallographic structure

- Size of platelet ~5

2 high heat flux (HHF) test schemes:
✓(i) screening tests,
✓(ii) cyclic heat load tests

JET requirements: 0.5 MW/m^2 for 20 s (10 MJ/m^2)

(i) **Screening** tests

Aim: determine the allowable energy density limit of the Be coating

Tests: energy density of 4 MJ/m^2 to **20 MJ/m^2**, (0.4 MW/m^2 to 1.8 MW/m^2 for 10 s ; **2.6 MW/m^2** for 6.2 s)

(ii) **Cyclic** heat load tests

Aim: study the degradation of the Be coatings by thermal fatigue

Tests: 50 cycles of 1 MW/m^2 in 10 s corresponding to **10 MJ/m^2**.

✓ **Observation during the high heat flux testing**

• Surface temperature was monitored with a **10 Hz infra-red (IR) camera**

• Surface temperature was measured at a black-coloured surface with an emissivity of 0.85.

➢ Surface morphology of Be/Inconel (Inconel_2) after 50 thermal cyclic loads at **1 MW/m², 10 s (10 MJ/m²)**.

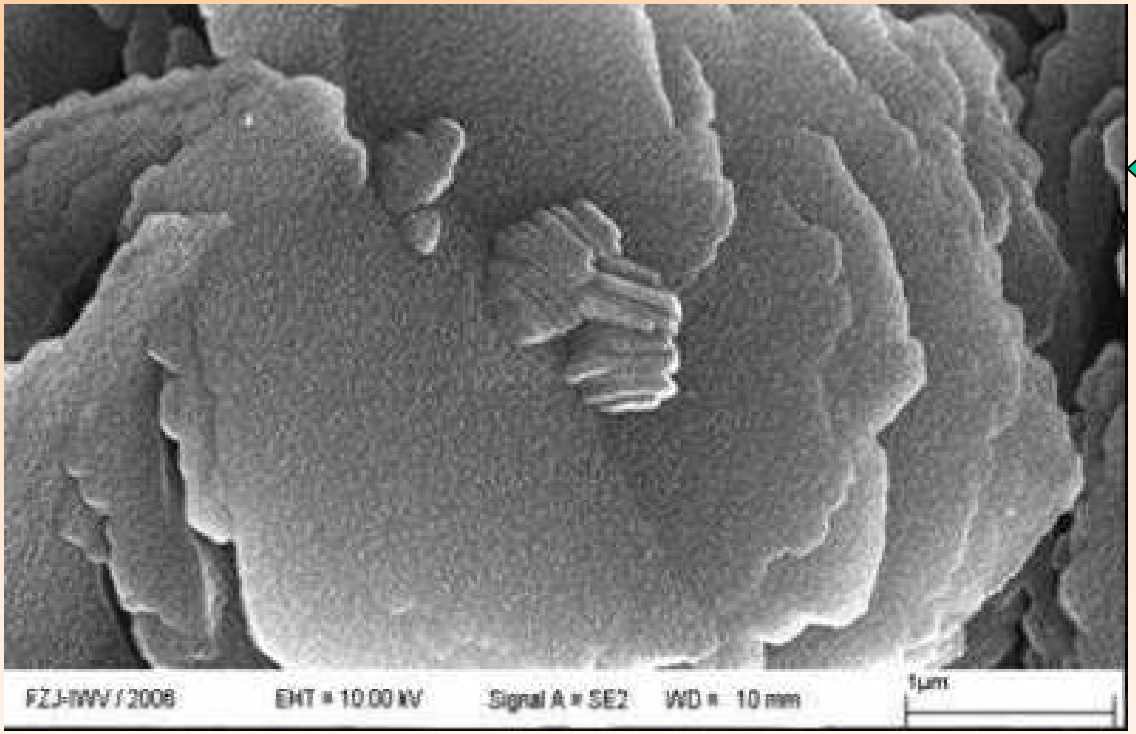

After test

Before

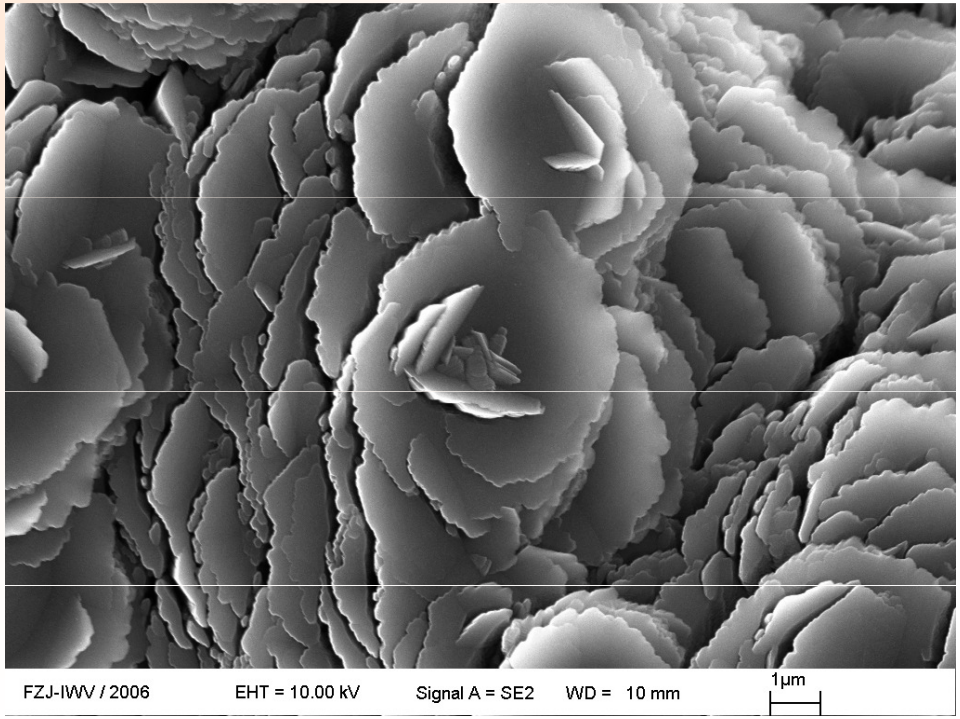

➢ Cross section of Be/Inconel (Inconel_2) after 50 thermal cyclic loads at **1 MW/m², 10 s (10 MJ/m²)**.

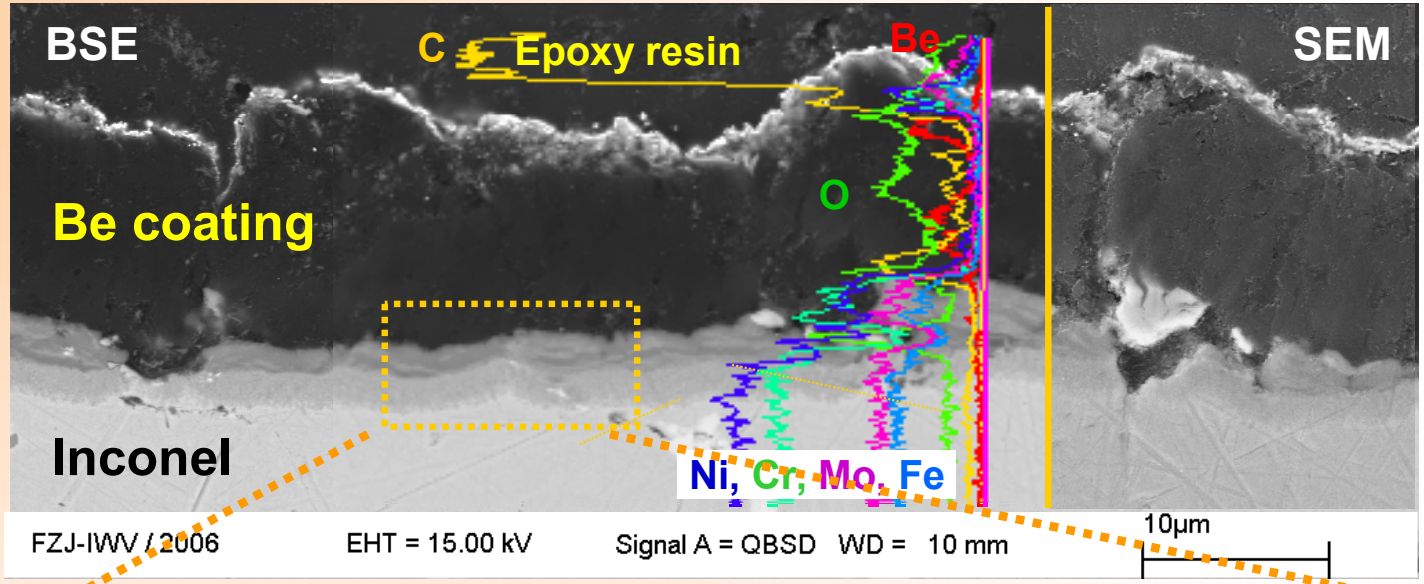

Eutectic alloy formation

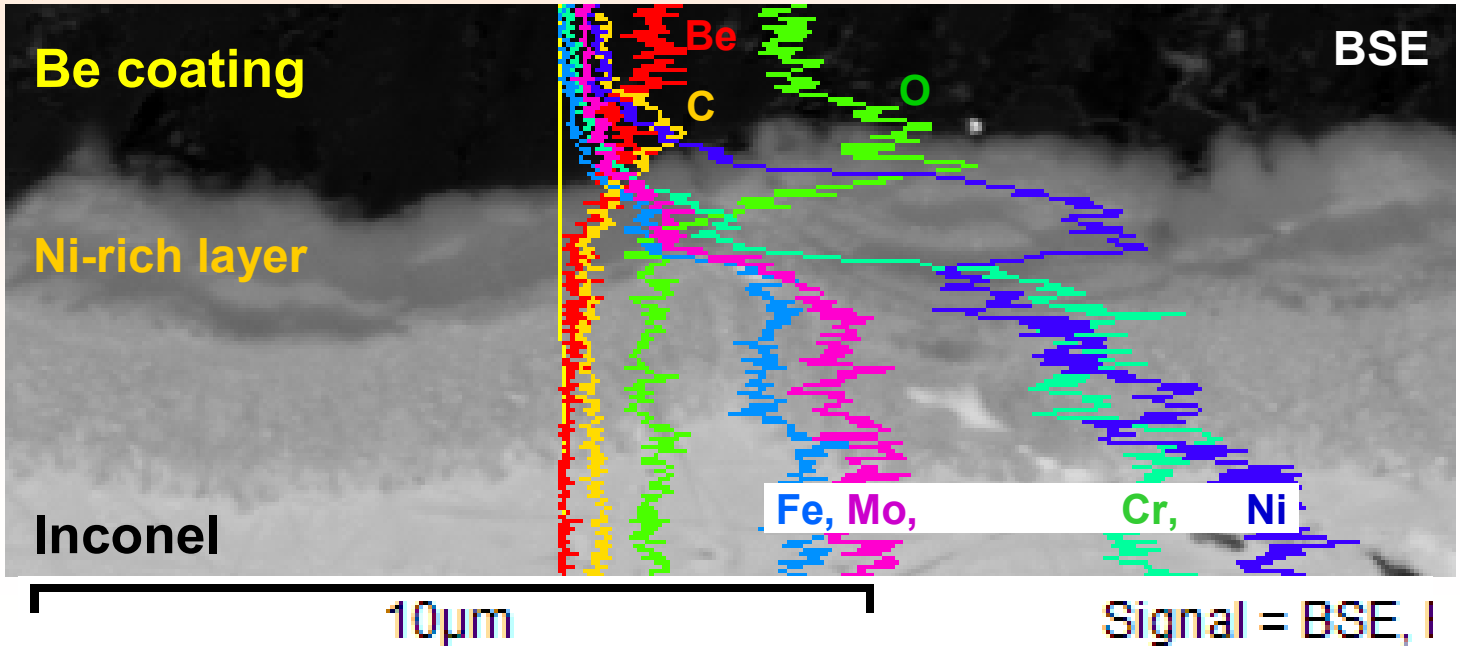

PRODUCTION OF BERYLLIUM COATED INCONEL TILES

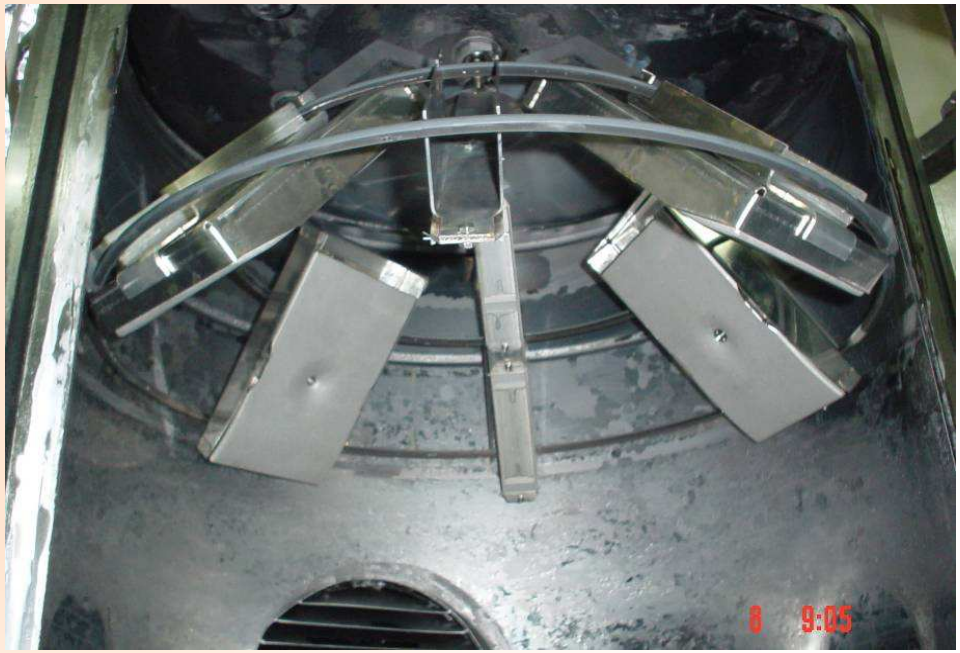

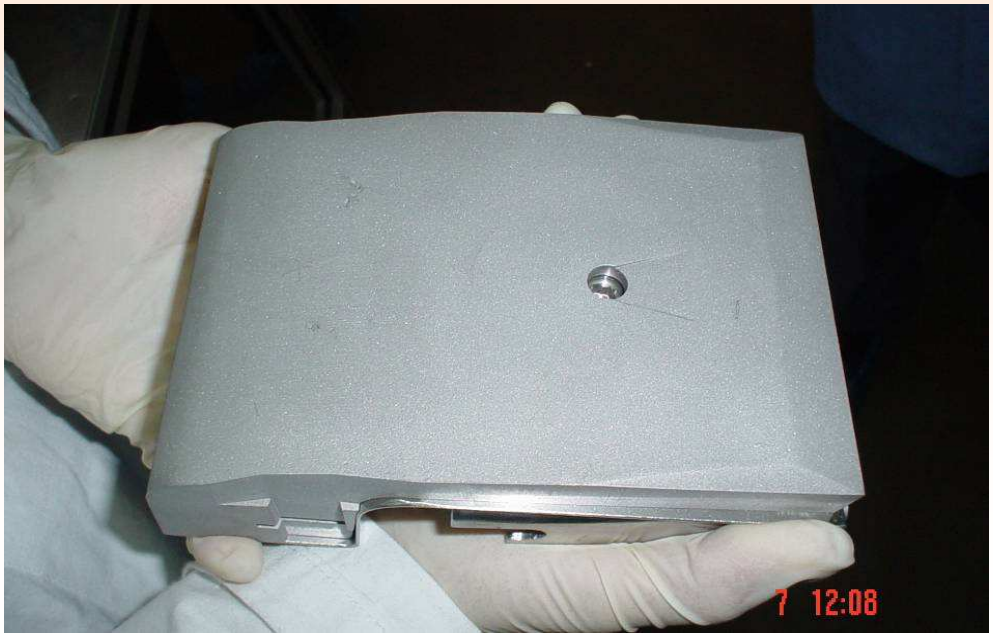

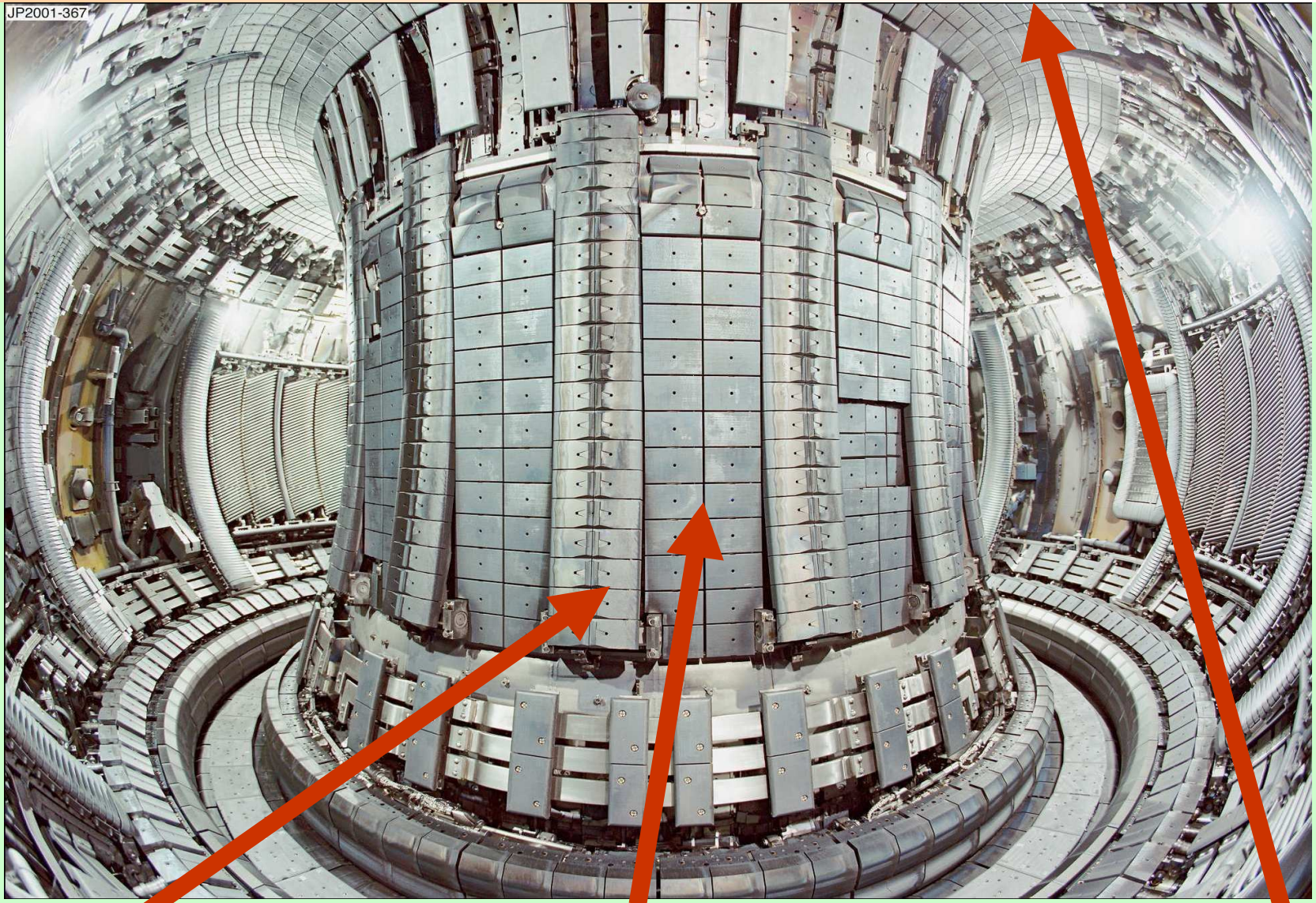

Inner Wall Guard Limiter
112 Be Coated Inconel Tiles

Inner Wall Cladding Tiles
272 Be Coated Inconel Tiles

Dump Plates: 512 Be Coated Inconel Tiles

Summary

- Thermionic vacuum arc (TVA) method developed at the National Institute for Laser, Plasma and Radiation, Bucharest, Romania, was used for:
    - Optimization of deposition of pure films: 2-3 μm Ni, 7-9 μm Be
    - Preparation of marker tiles: test samples, test coupons, qualification of the deposition method, pre-production run, production runs
- Thermal evaporation in vacuum method developed at Nuclear fuel Plant, Mioveni-Pitesti, was used for:
    - Production of Be coatings 7-9 μm on inconel tiles: test samples, qualification of the deposition method, pre-production run, production runs

Hard antireflexive diamond like carbon coatings prepared by TVA method

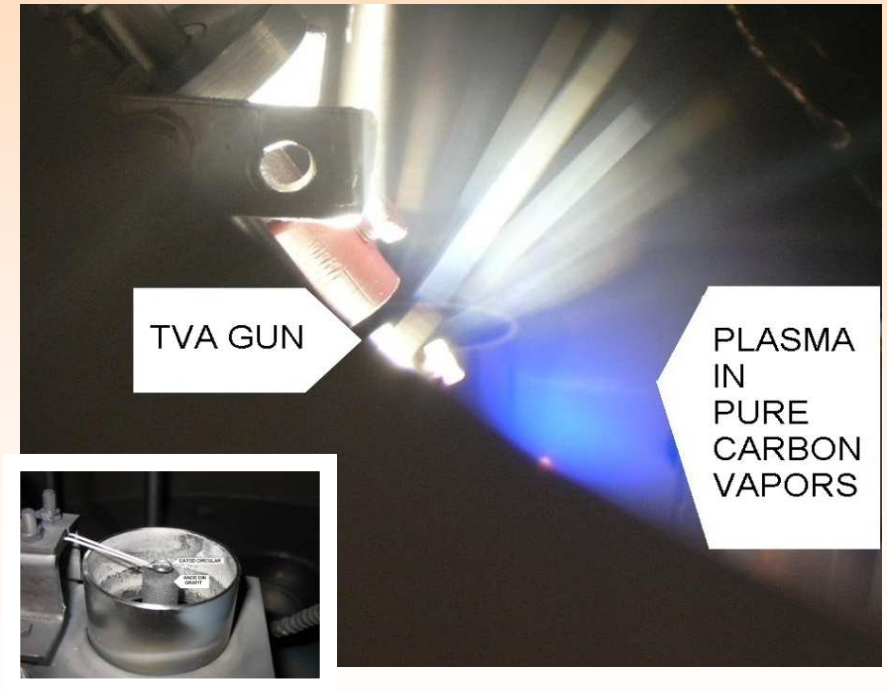

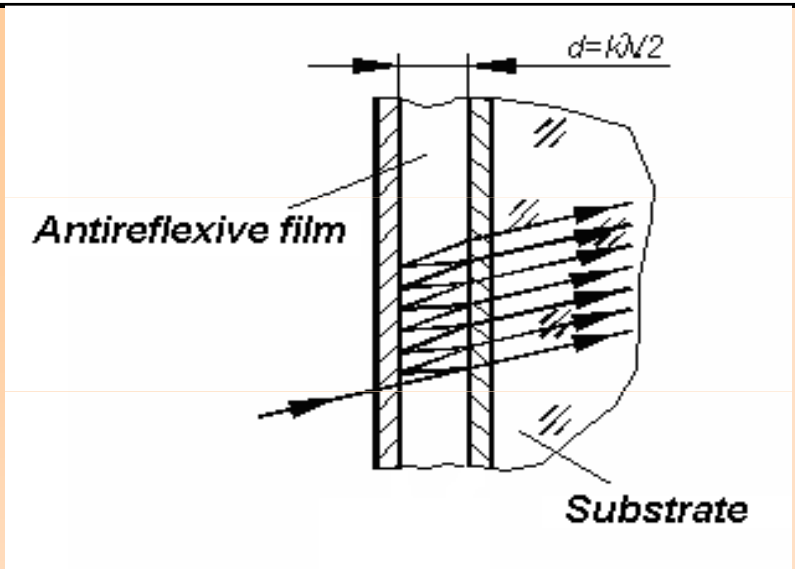
d=kλ/2
Antireflexive film
Substrate

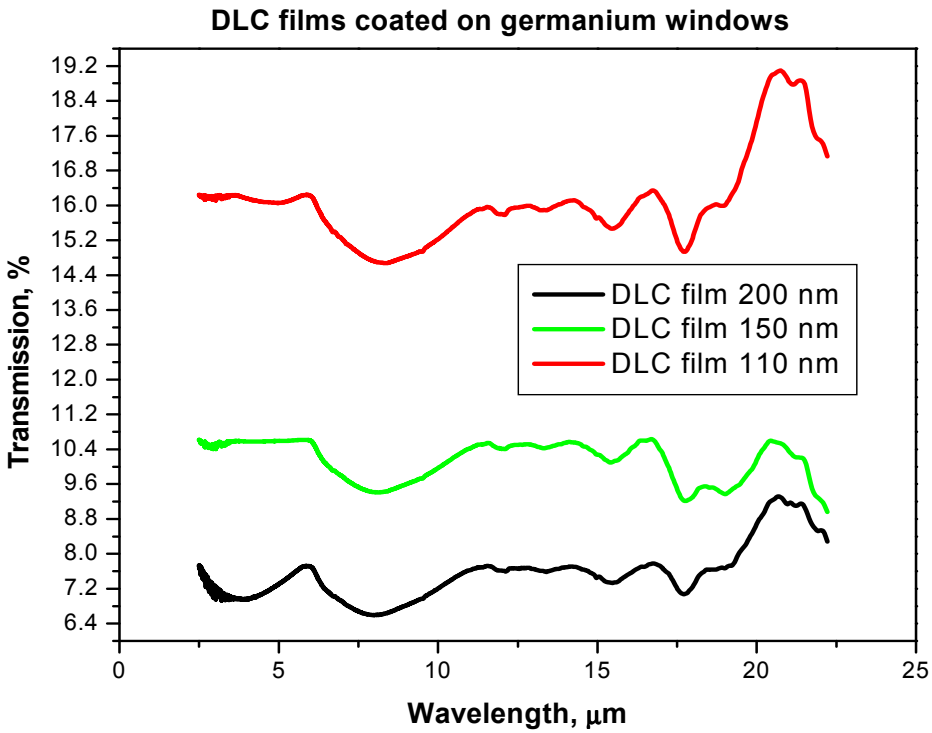
DLC films coated on germanium windows
Transmission, %
Wavelength, µm
DLC film 200 nm
DLC film 150 nm
DLC film 110 nm

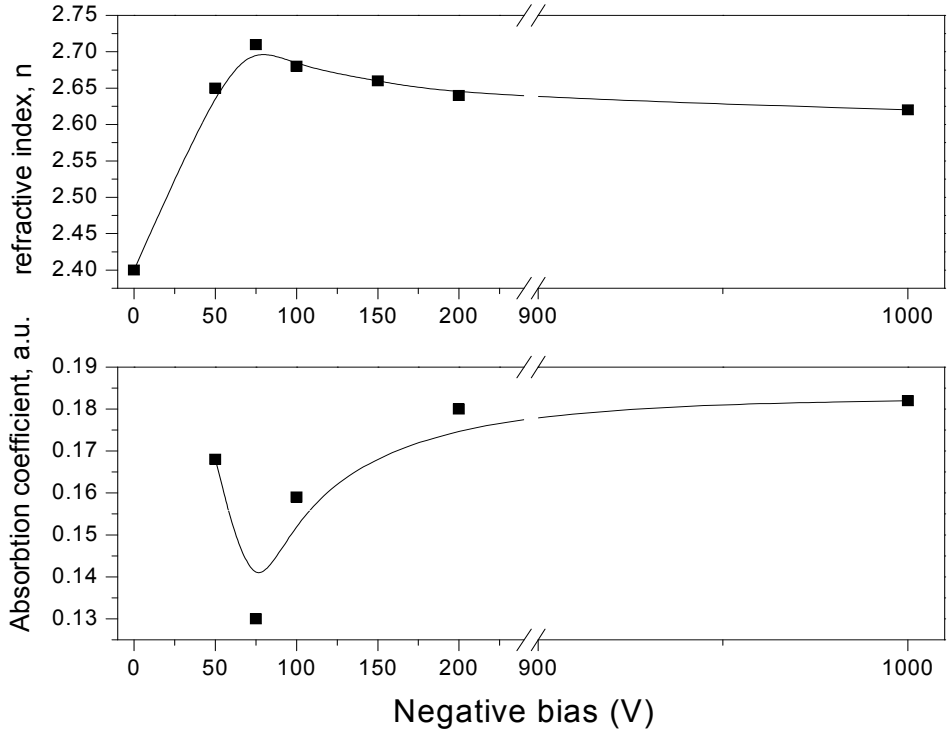
refractive index, n
Absorbtion coefficient, a.u.
Negative bias (V)

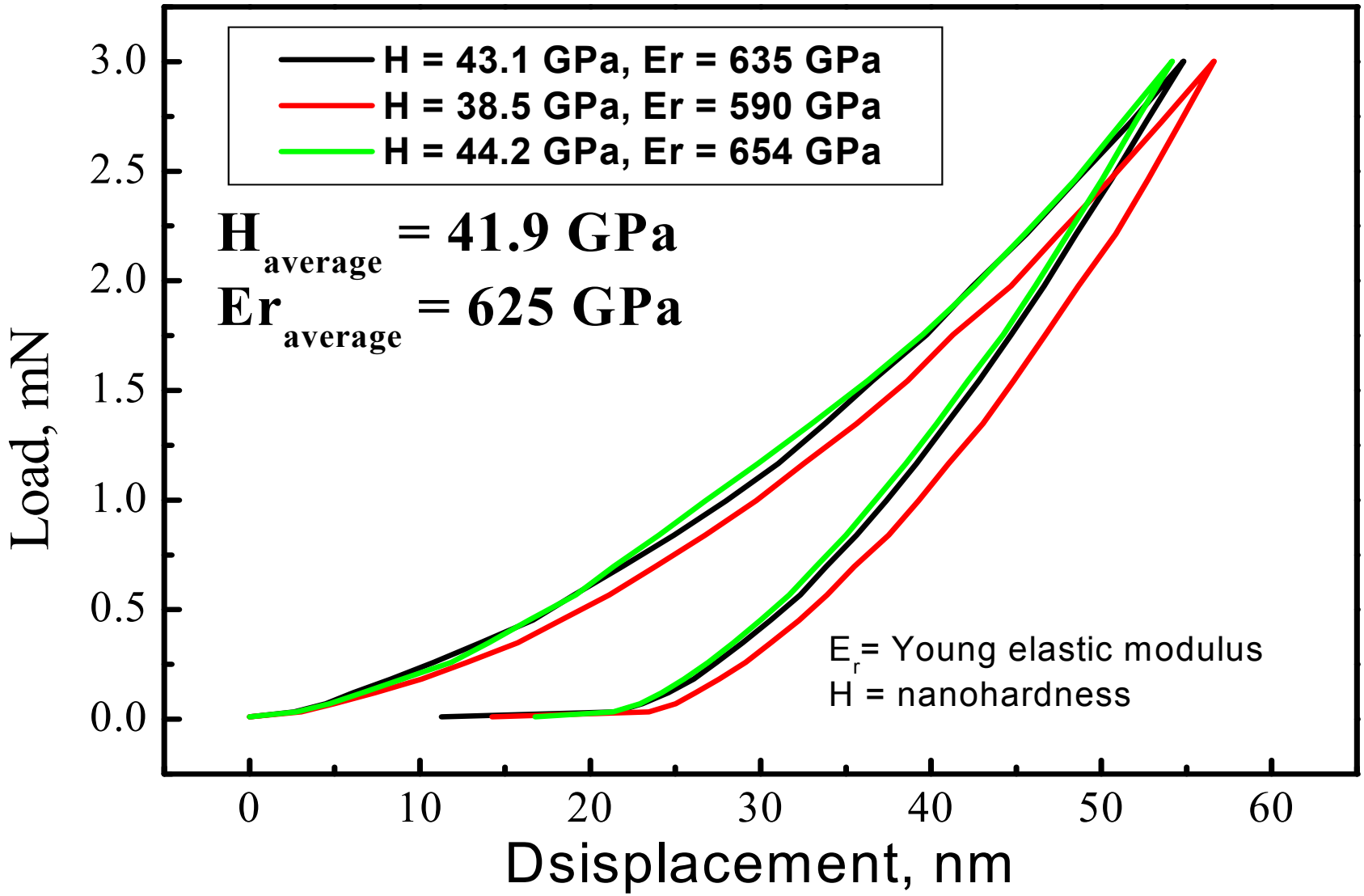
H = 43.1 GPa, Er = 635 GPa
H = 38.5 GPa, Er = 590 GPa
H = 44.2 GPa, Er = 654 GPa
H average = 41.9 GPa
Er average = 625 GPa
E r = Young elastic modulus
H = nanohardness
Load, mN
Dsisplacement, nm
0.0
0.5
1.0
1.5
2.0
2.5
3.0
0
10
20
30
40
50
60

• *Raman characterisation of the samples*

Micro-Raman-LABRAM HR 800 –Horiba Jobin Yvon on surfaces observed through the optical microscope

.

Laser sources: λ=633 nm, 514nm, 488nm
Power on sample: 2.5-13.2 mW
Range: 150-4000cm^{-1}

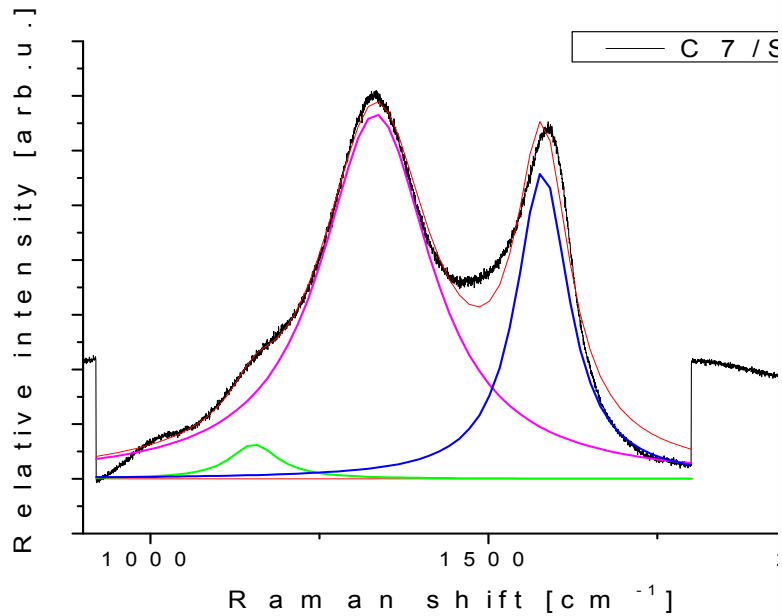

C/Si 200nm I_D/I_G=2.46

CNT on Si

The most important feature in the Raman spectrum of CNT's is the Radial Breathing Mode (RBM), which is often observed between 100 and 500 cm-1. The frequency of the RBM in cm-1 is directly linked to the reciprocal of the nanotube diameter (dt)

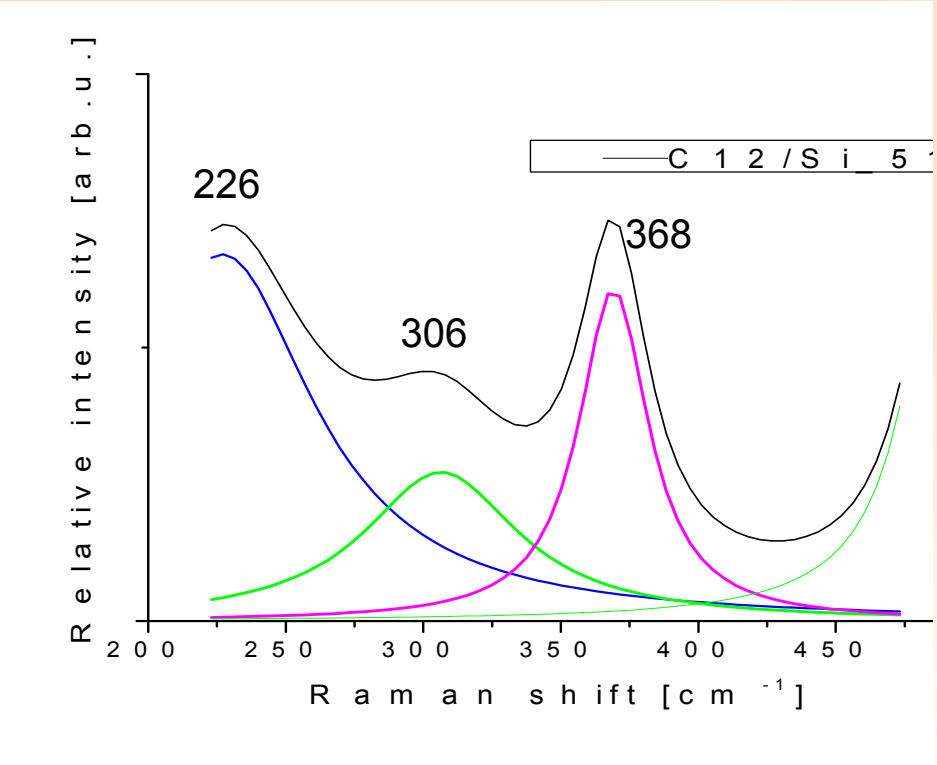

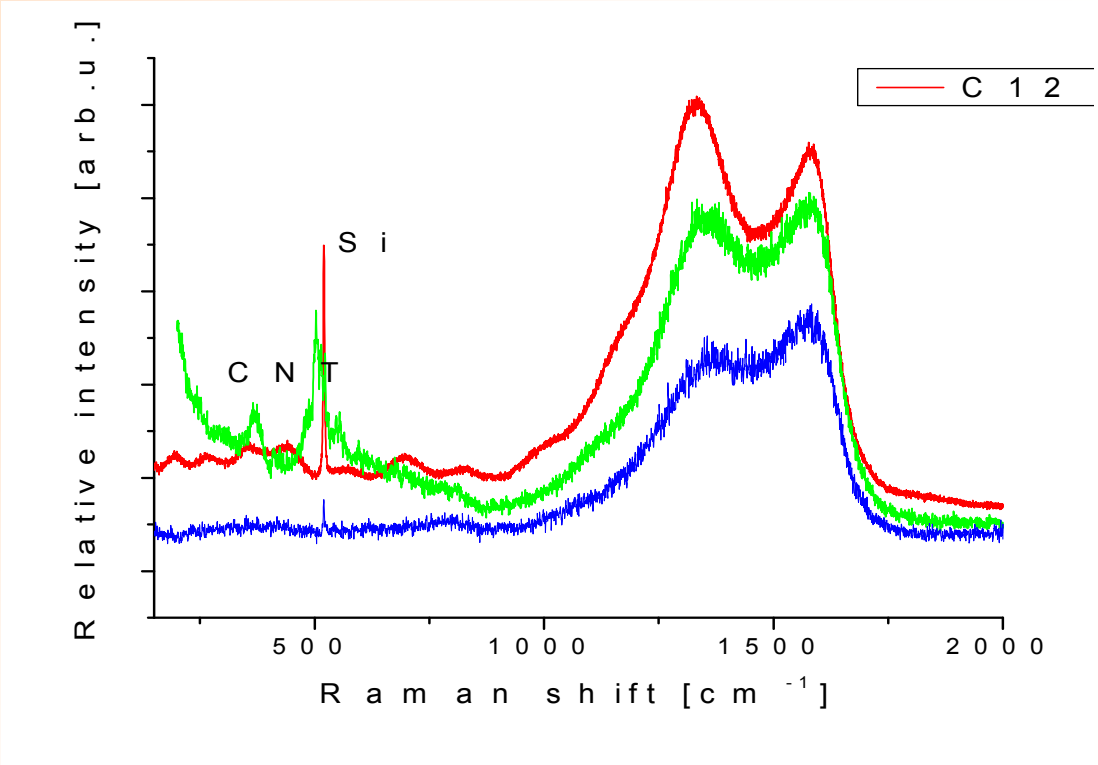

C/Si 100nm CNT bunch in the low frequency region

Non isolated SWNT's are subject to inter-tube interactions which increase the frequency of the RBM

- The characteristic D and G bands (C-C stretching in the graphite plane) modes of carbon were found in all samples, with the ratios of the integral intensities varying slightly with: *i*)deposition parameters; *ii)* thickness; *iii)* substrate material.
- In addition to the sp^2 and sp3 modes, a feeble Raman feature was observed in the low frequency range of the spectra of C/Si deposited at ion energies below 800 eV. This feature is specific to CNT-like structures and its characteristic frequency is related to the nano-dimension of the crystallites embedded in the disordered carbon phase.
- RBM (Radial Breathing Mode) frequency is subject of resonance effects


FILTRU
RG 715
BEAM SPLITTER
MARE
FILTRU
CRT
FILTRU
IR.

CONCLUSIONS

- The carbon-metal films were identified as a nanocrystals complex (5 nm average diameter) surrounded by amorphous structures with a strong graphitization tendency.

- The Raman spectra showed typically D and G-bands of the amorphous carbon. By XPS were identified C-C (sp^3 bonds) and C=C (sp^2 bonds) depending on process parameters and carbon-tungsten relative concentrations.

- The coefficients of friction of the prepared films were in the range of 0.15-0.25, for C-Ag, 0.15-0.25 for C-Ni and 0.4 –0.45 in the stable phase for C-W, three to five times lower than the uncoated substrates.

GMR

- Giant Magnet-Resistive films
- GMR factor: $(R_H - R_0)/R_0$
- Or: $\Delta R/R$

The GMR effect, discovered in 1986-1988, means the very large change in resistance (due to the spin-dependent scattering of electrons) in a magnetic ultra-thin multilayer film.

Physical properties of the magnetic super lattices

Very small thickness of the layer (nm range)

- **change of the magnetic moment**
- **surface or interface anisotropy**
- **low-dimensional effects**

Multilayer effects

- **interlayer coupling**
- **exchange interaction**

Technological applications:

Magnetic sensors

- **high sensitivity for low fields**

Magnetic read heads

- **high linear voltage versus field**

The GMR is a spin determined electrical phenomenon:

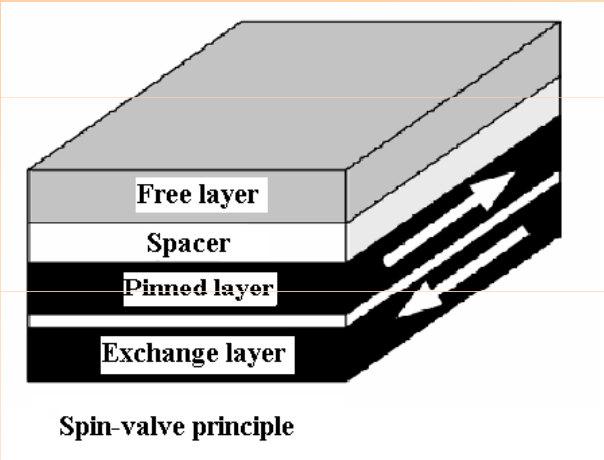

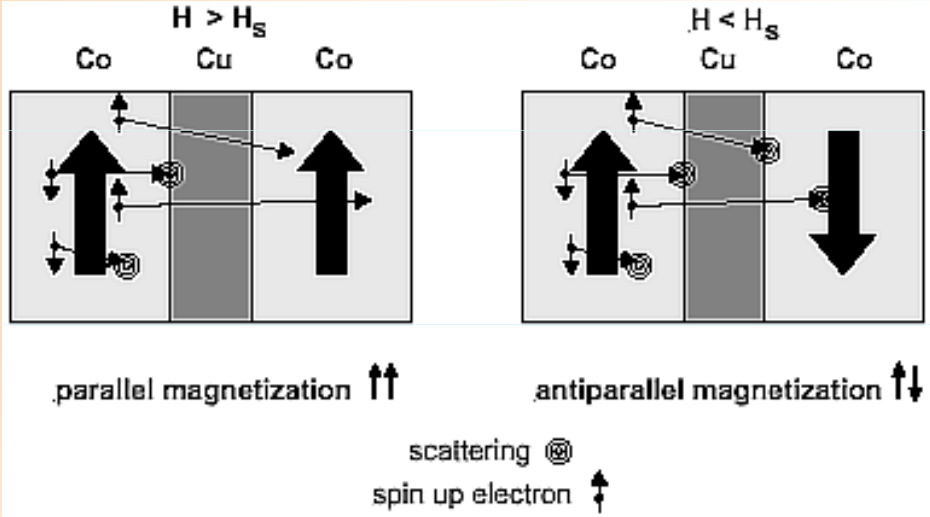

Consider two electron collision in metals.

There are two cases:

A. Parallel spin case= symmetric spin function → anti-symmetric scatter amplitude:

$$f(\theta,\varphi)_{s\text{-}a} = C[f(\theta,\varphi) - f(\pi-\theta,\varphi+\pi)] \rightarrow \text{collision cross section:}$$

$$\sigma_a = |f(\theta) - f(\pi-\theta)|^2 \quad (1)$$

B. Anti-parallel spin case → symmetric scatter amplitude:

$$f(\theta,\varphi)_{s\text{-}a} = C[f(\theta,\varphi) + f(\pi-\theta,\varphi+\pi)] \rightarrow \text{collision cross section}$$

$$\sigma s = |f(\theta) + f(\pi-\theta)|^2 \quad (2)$$

Conclusion: $\sigma s > \sigma a$ (3)

GRANULAR STRUCTURES

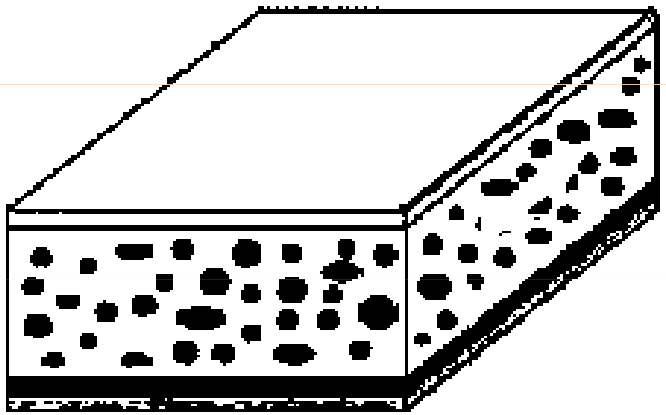

GMR structure: granular film

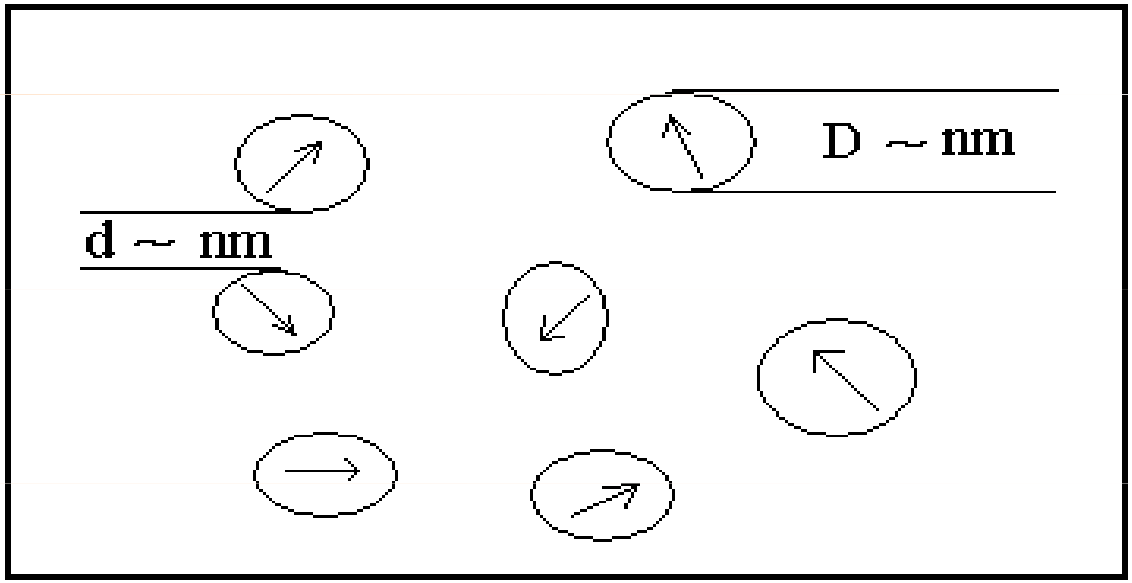

The magnetic domains are introduced into a conducting (or insulator) material network.

Critical parameters:

- the cluster dimensions
- the distance between the clusters

- the magneto-resistance effect is lower as in the multi-layer case
- the initial domain orientation can no be made purely anti parallel –at least it is randomly oriented.
- when the domains are of the same dimensions the GMR dependence against the external magnetic field is expected to be square-like.

Giant and tunneling magnetoresistive (GMR, TMR) films

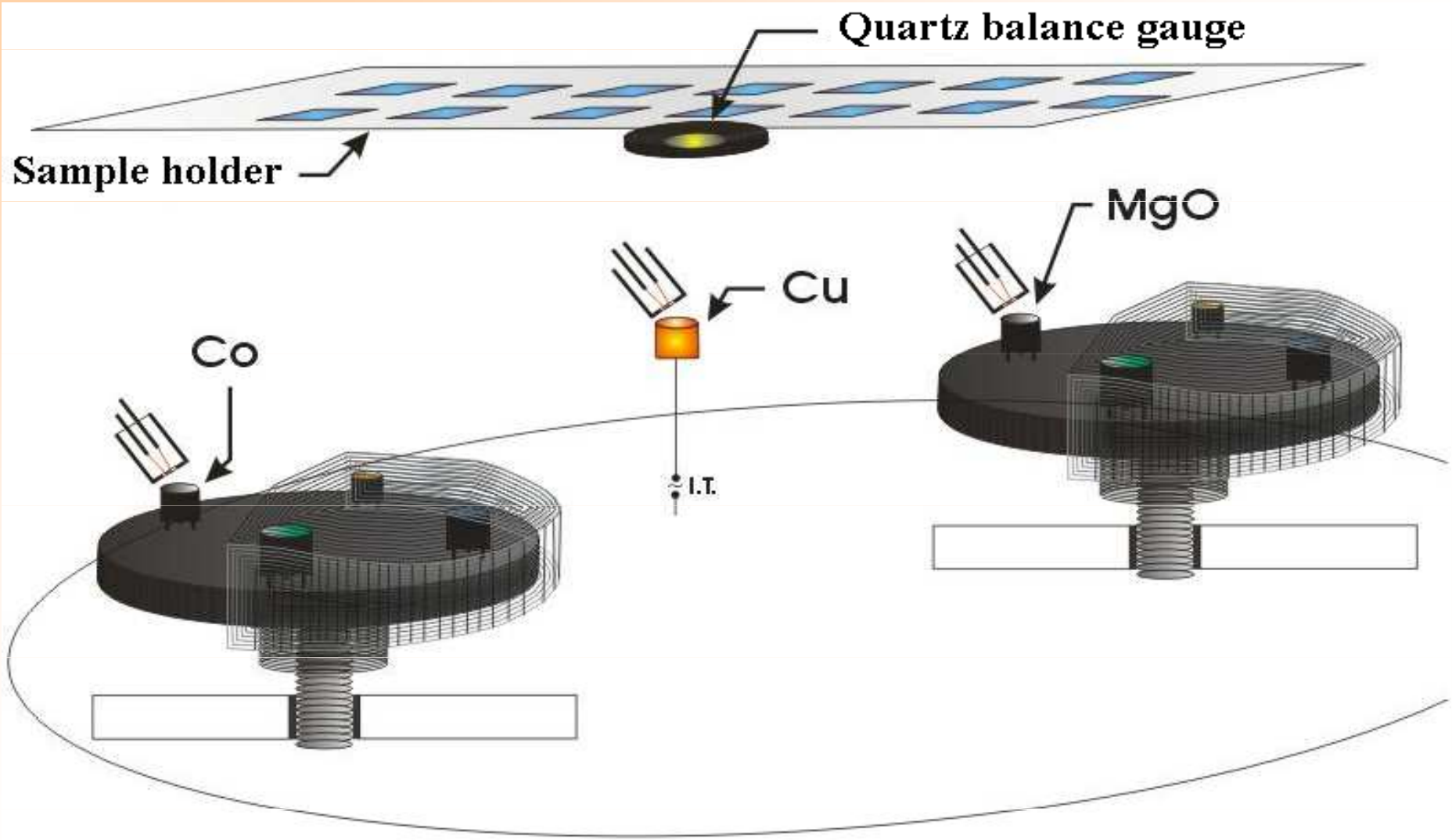

Multi elements deposition system

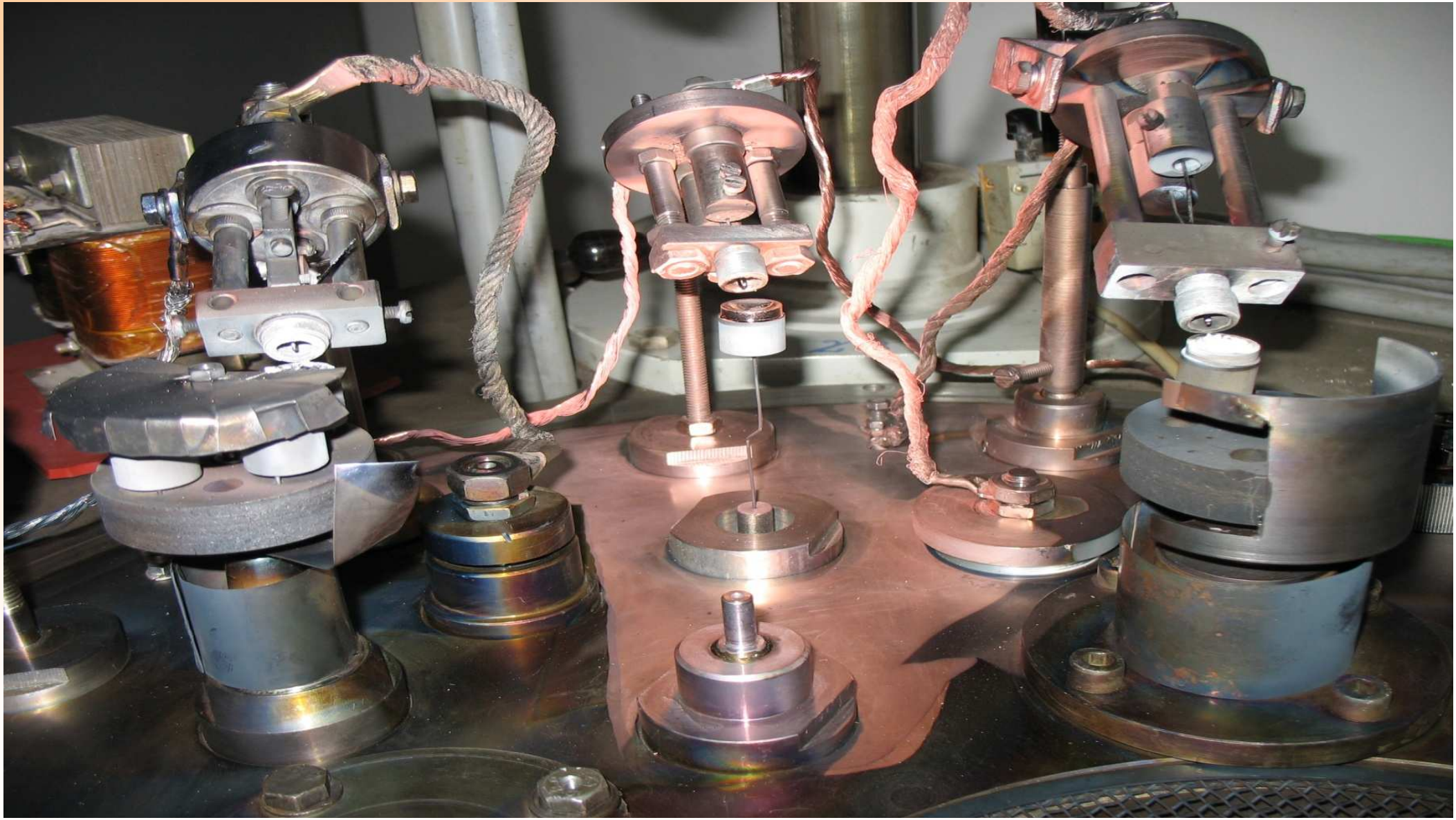

Composite and multilayer coatings

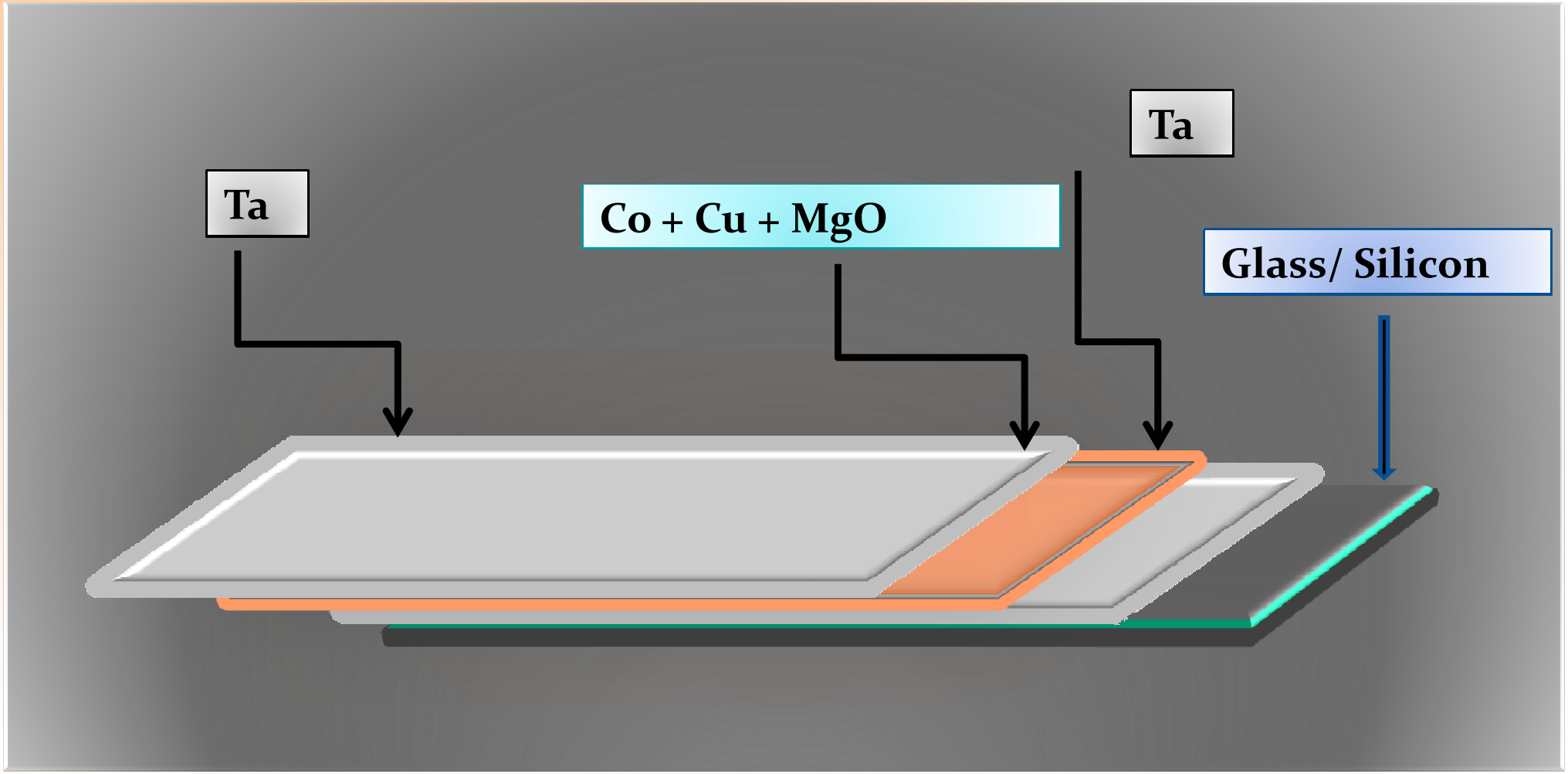

GRANULAR, MAGNETOREZISITIVE FILMS

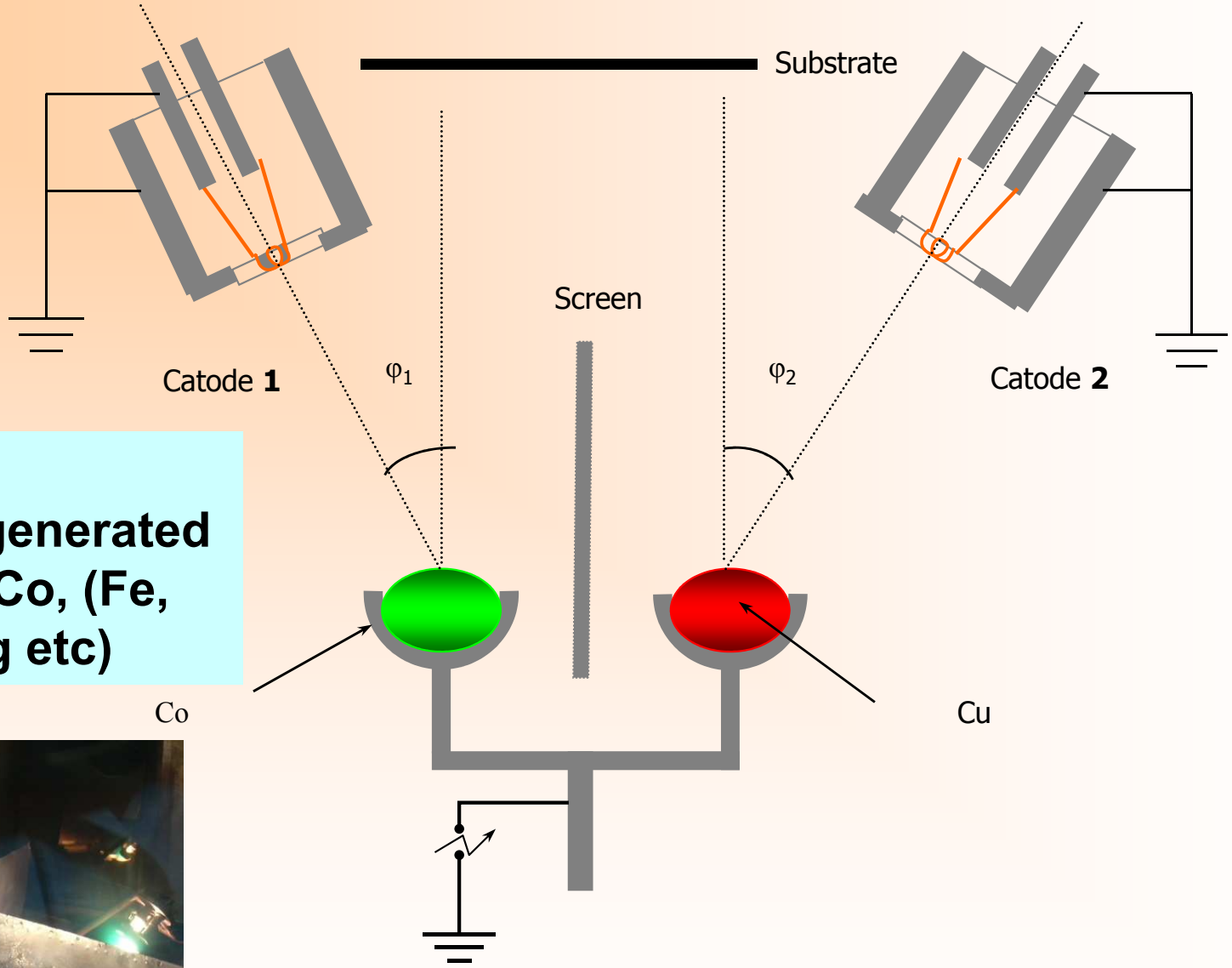

-two (or three) independent generated plasmas : for Co, (Fe, Ni) and Cu (Ag etc)

- **Two (three) independents TVA guns**
- **Every gun: independent filament and dc supply**
- **A metallic screen separates TVA discharges.**

Plasma appearance in Fe-Mn vapors

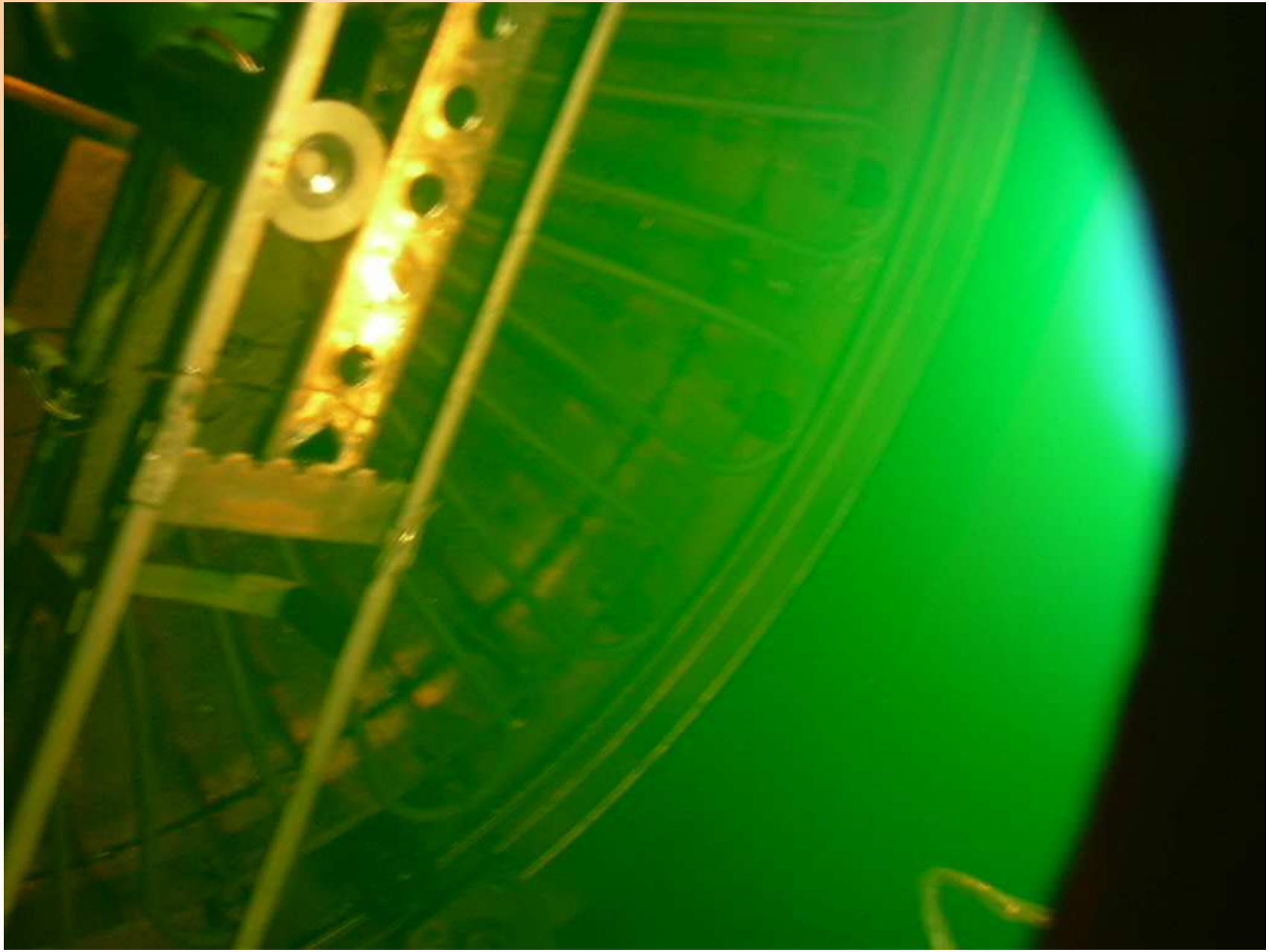

Fe concentration in Cu matrix

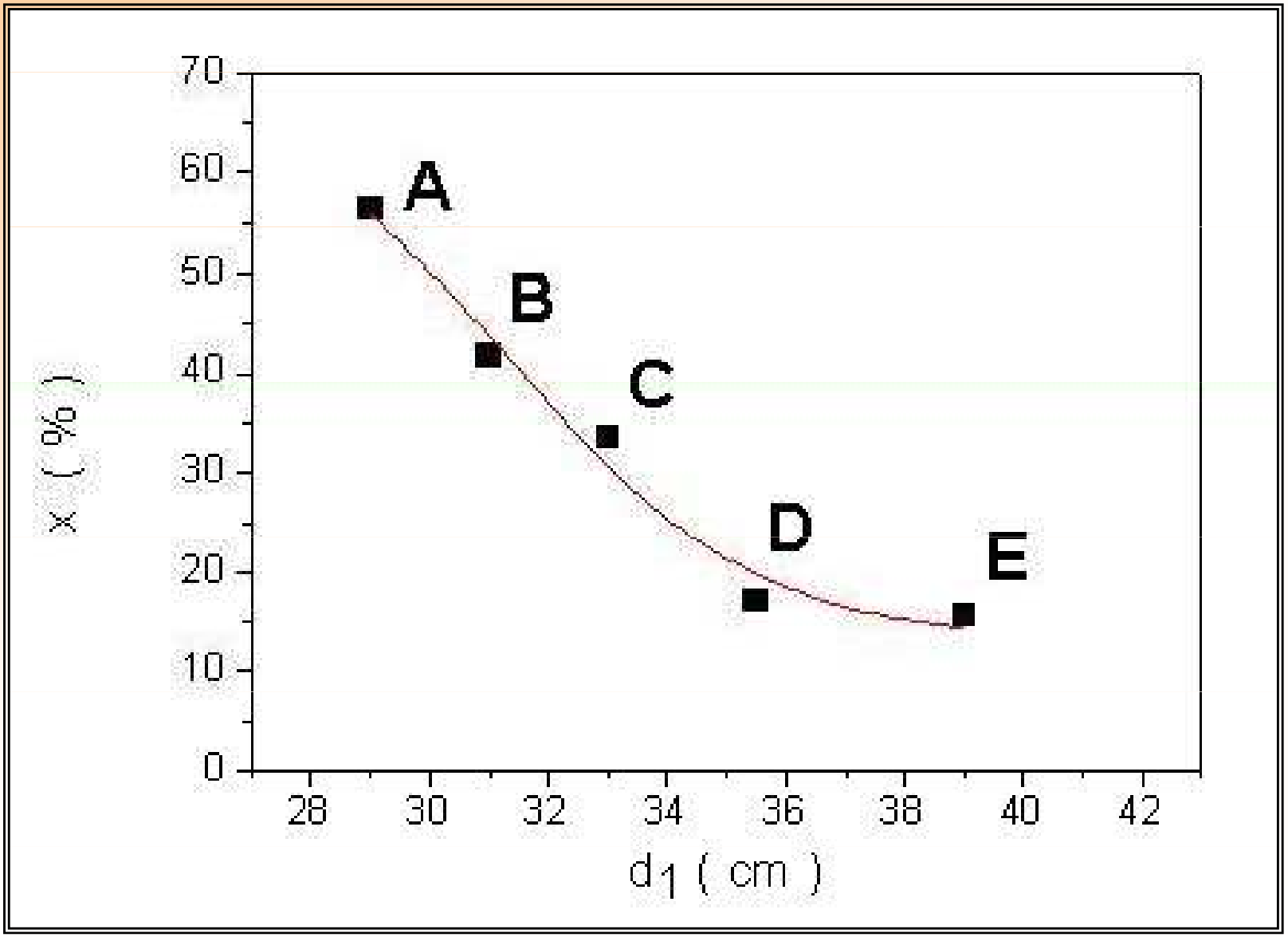

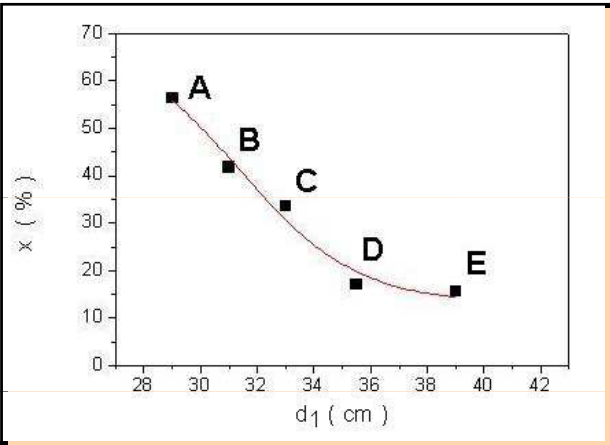

XRD of Fe-Cu films

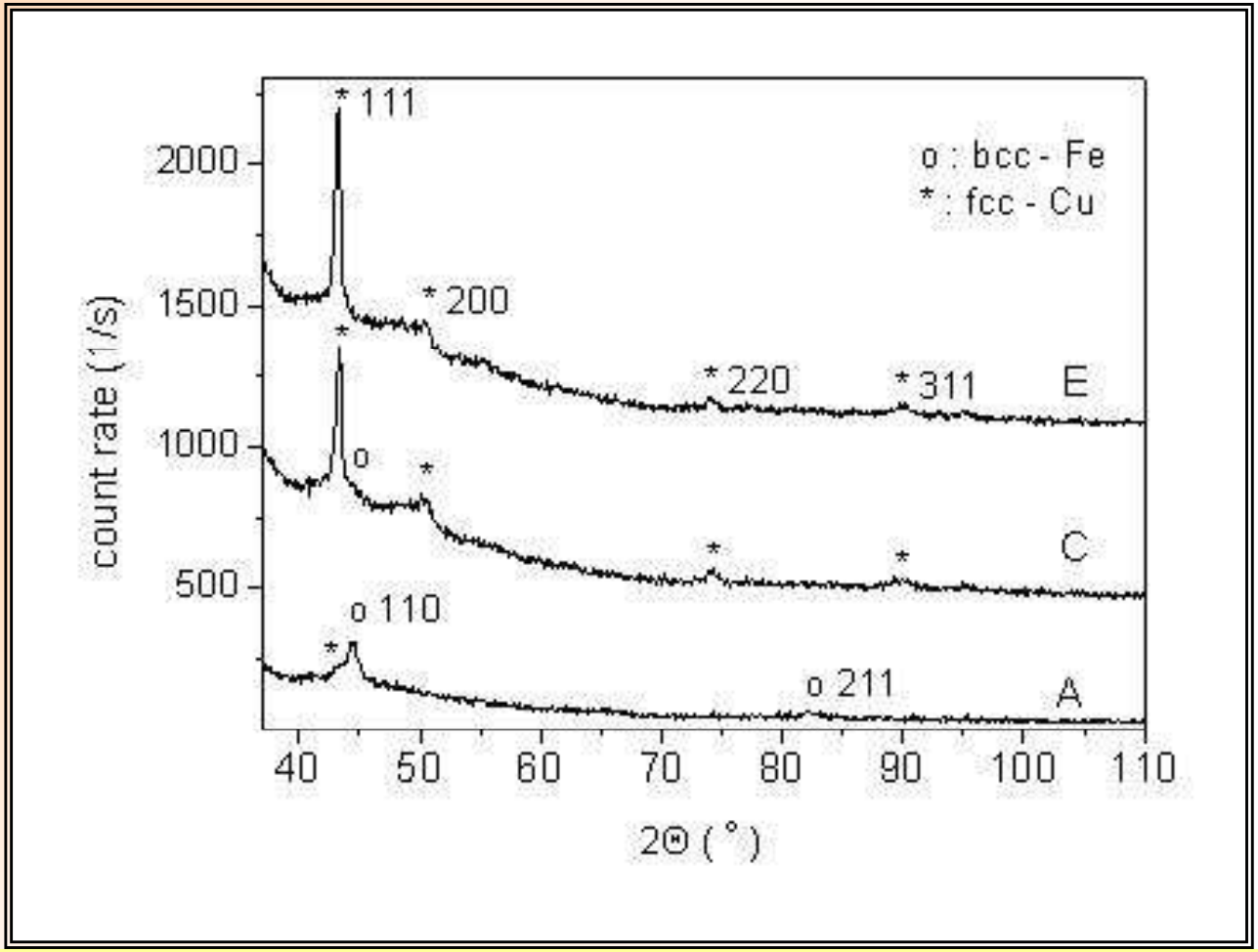

- **A to E: Face centered cubic (fcc) Cu phase and the body centered cubic (bcc) α-Fe phase. High Fe content (A) => lattice defects or fine particles.**
- **The main peak 111 of the fcc-Cu phase only appears as a weak shoulder of the Fe-110 peak at high Fe concentration (A)**
- **Increasing the relative copper content (C and E), the fcc-Cu phase become more evident.**

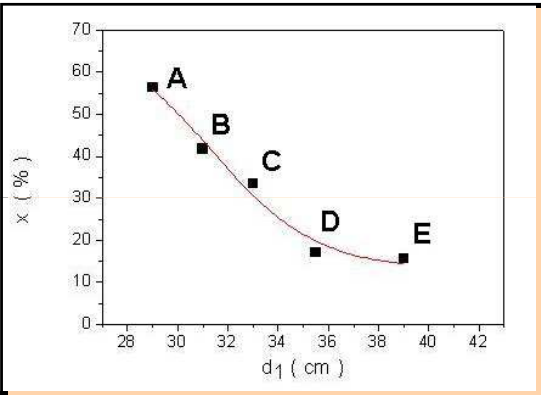

Mössbauer analysis

^{57}Fe Mössbauer spectra were collected at room temperature in transmission geometry, by using a constant acceleration spectrometer and a ^{57}Co(Rh) matrix.

The spectra of samples A and B give evidence for the presence of two magnetic nonequivalent Fe positions (bulk and interfacial) of the α-Fe phase.

A third paramagnetic component (a central singlet), with an isomer shift close to zero, was assigned to superparamagnetic bcc-Fe clusters.

The Mössbauer spectrum of sample C (with a lower amount of Fe) at RT reveals only superparamagnetic bcc-Fe clusters. Clearly, samples A to E present different magnetic interactions

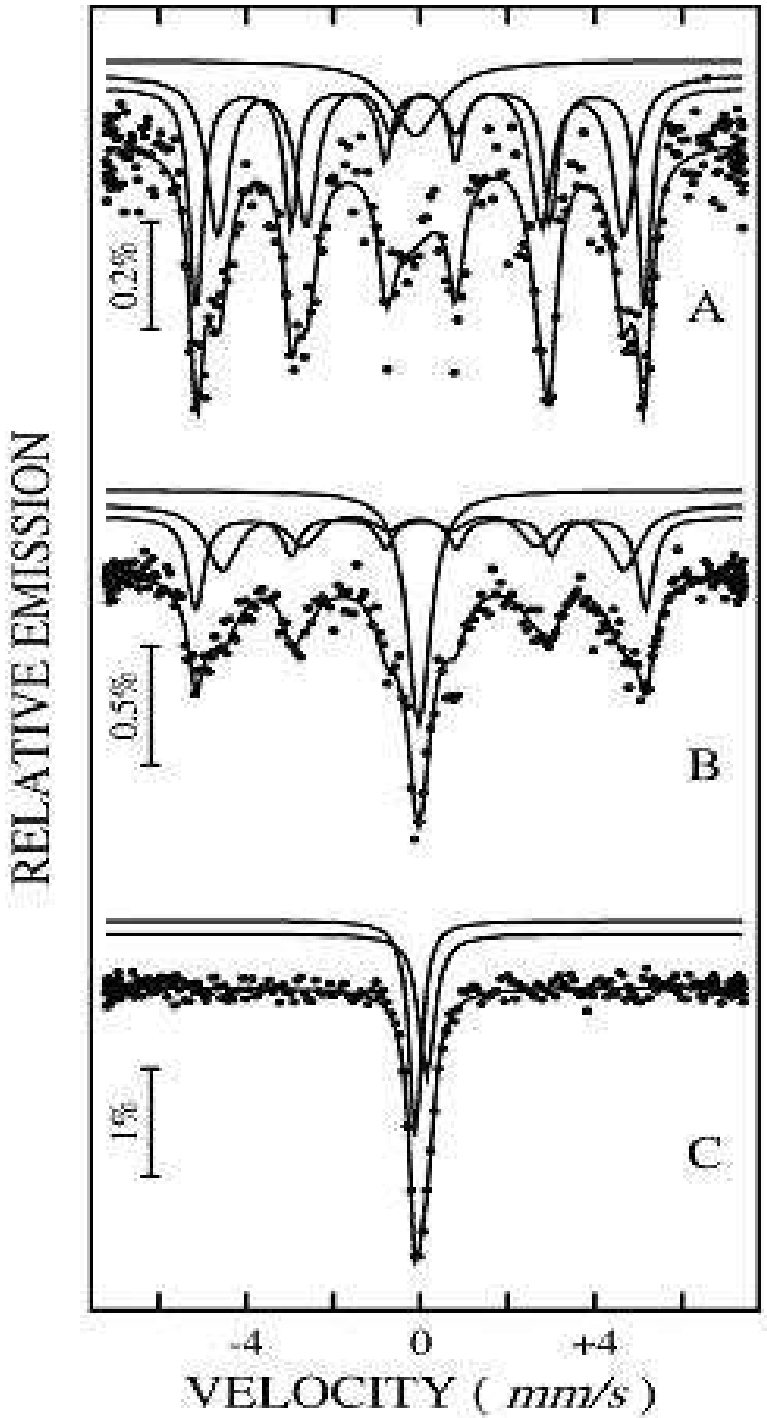

MFM microscopy of Fe-Cu films

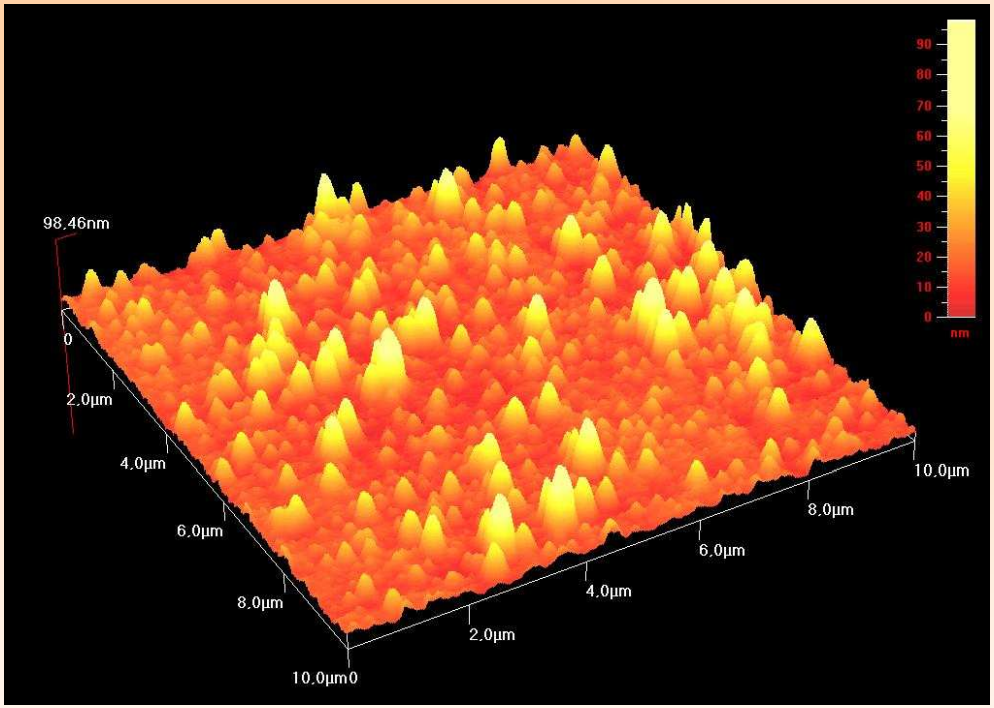

Topographic AFM image of a Fe-Cu film (B)

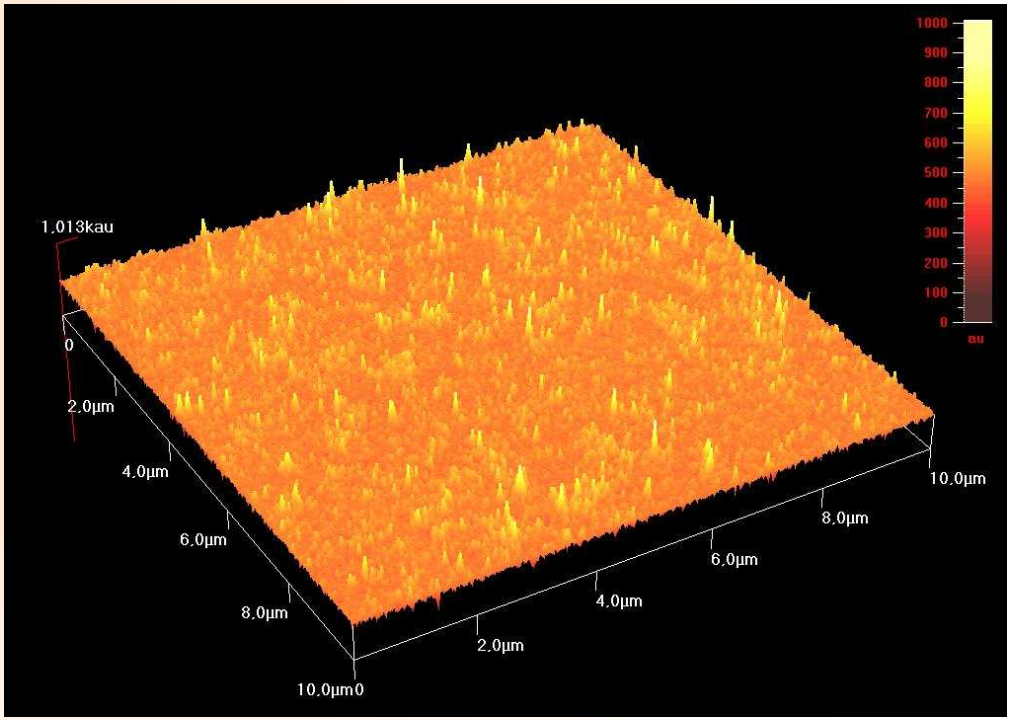

Magnetic domain distribution in a Fe-Cu film (B)

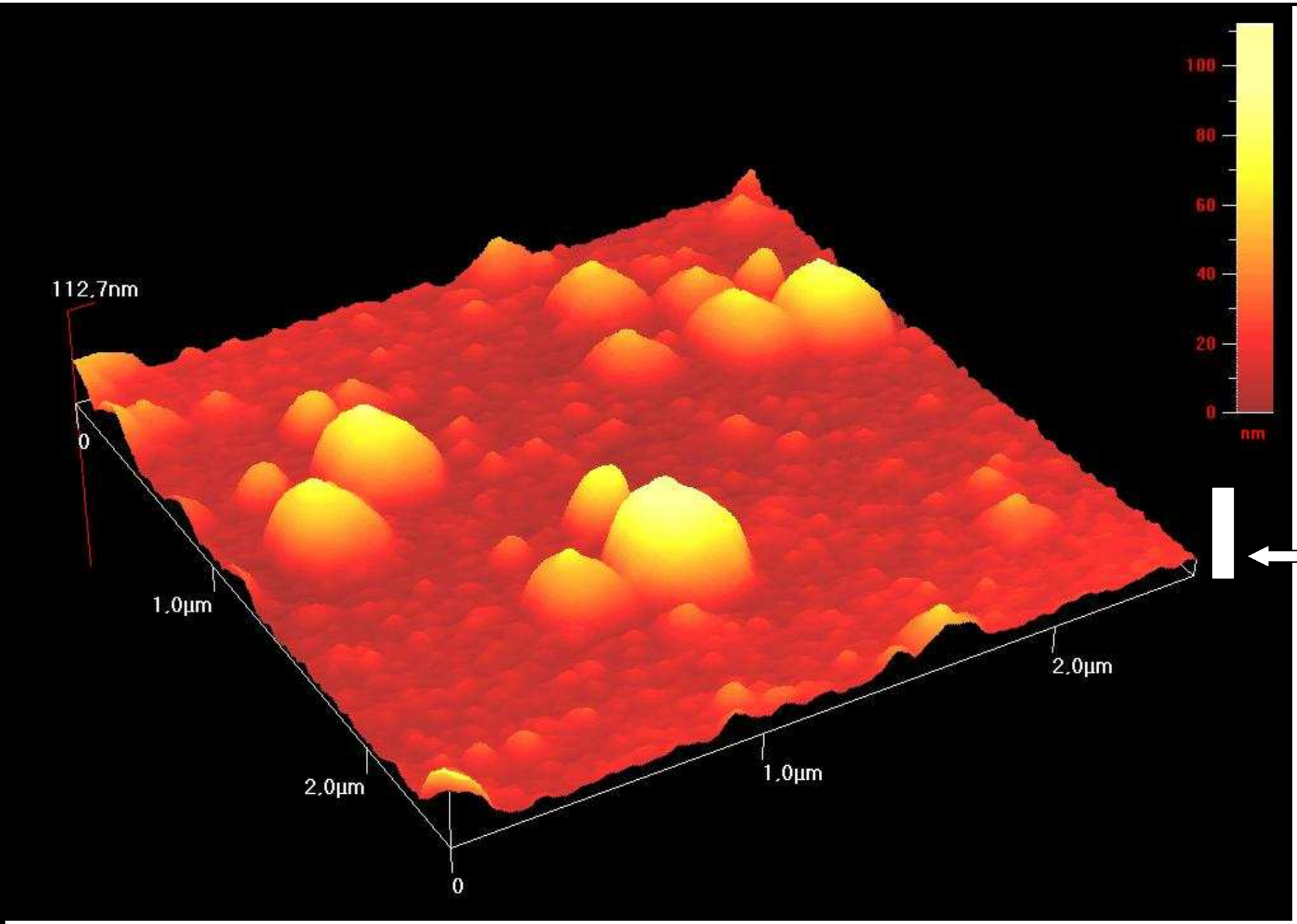

100 nm

Topographic MFM image

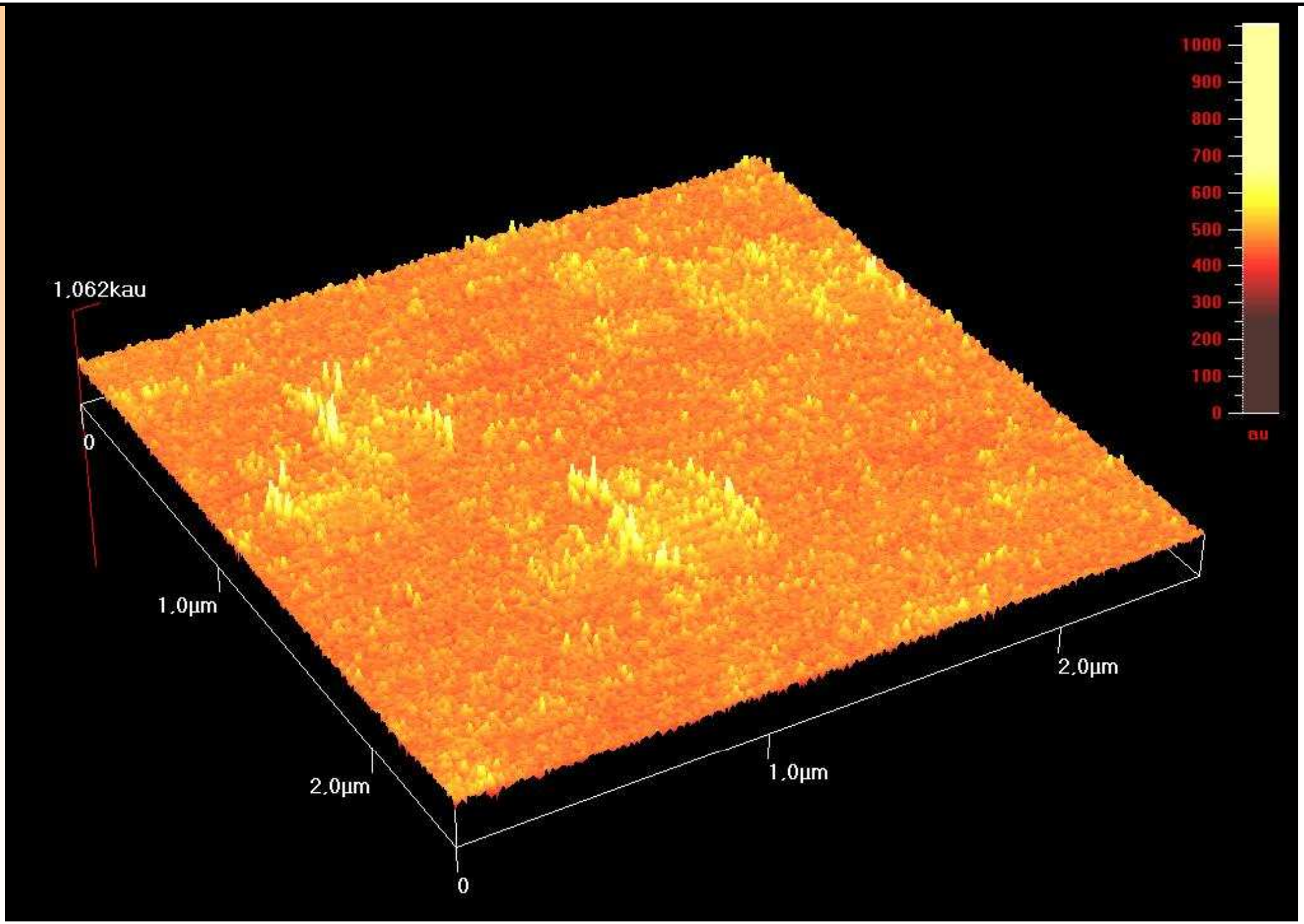

Magnetic domains distribution of a Fe-Cu film

GMR of Fe-Cu films

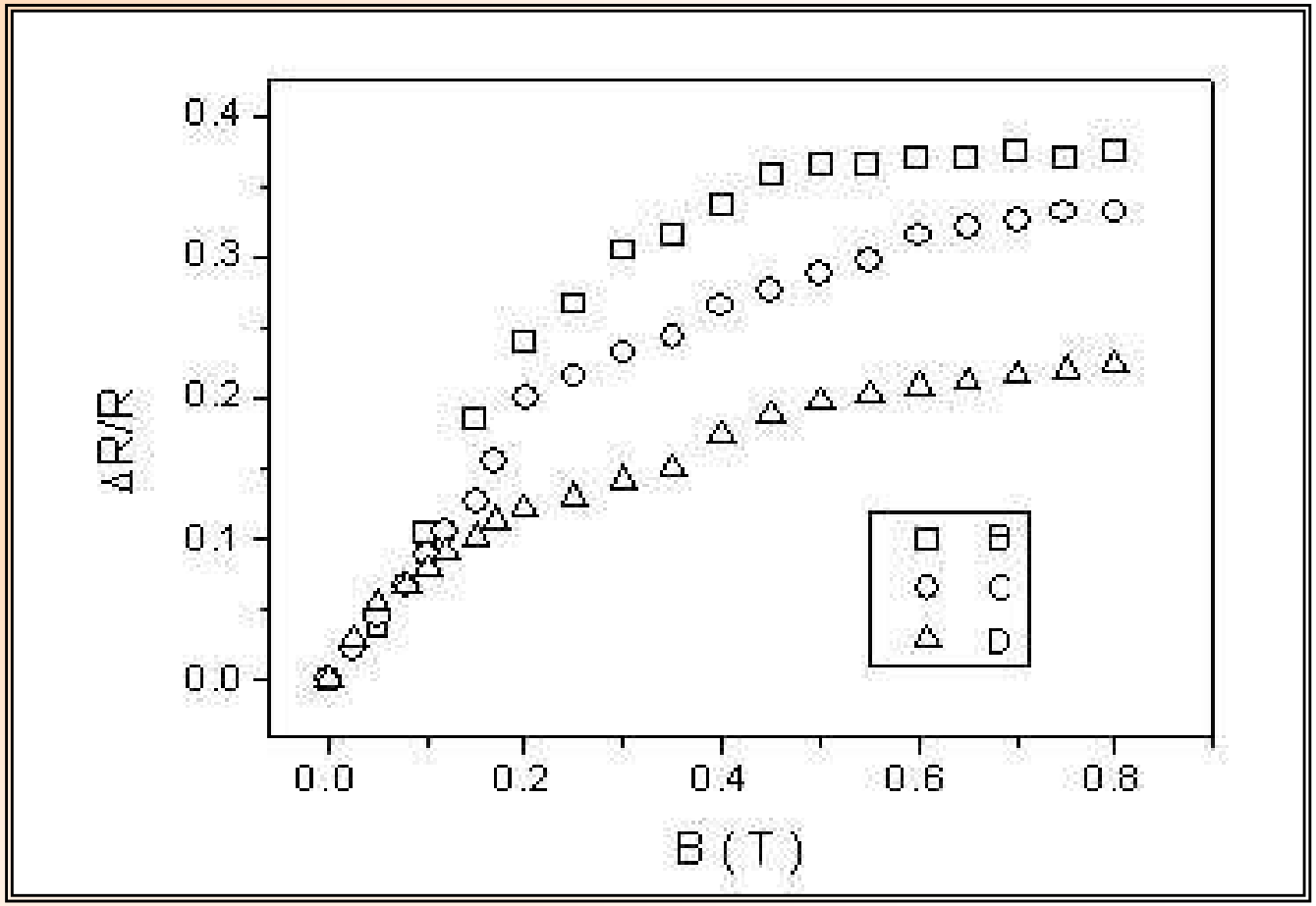

- Positive MR-effects of about 38% at saturating fields close to 0.8 T are definitely observed for sample B.
- Lower Fe content decreases significantly the observed effect, down to about 20% in sample D.
- However, for sample A, with the maximum Fe content, an effect of only 3% was observed and is most probably due to the lack of RT superparamagnetic bcc-Fe clusters in this film.

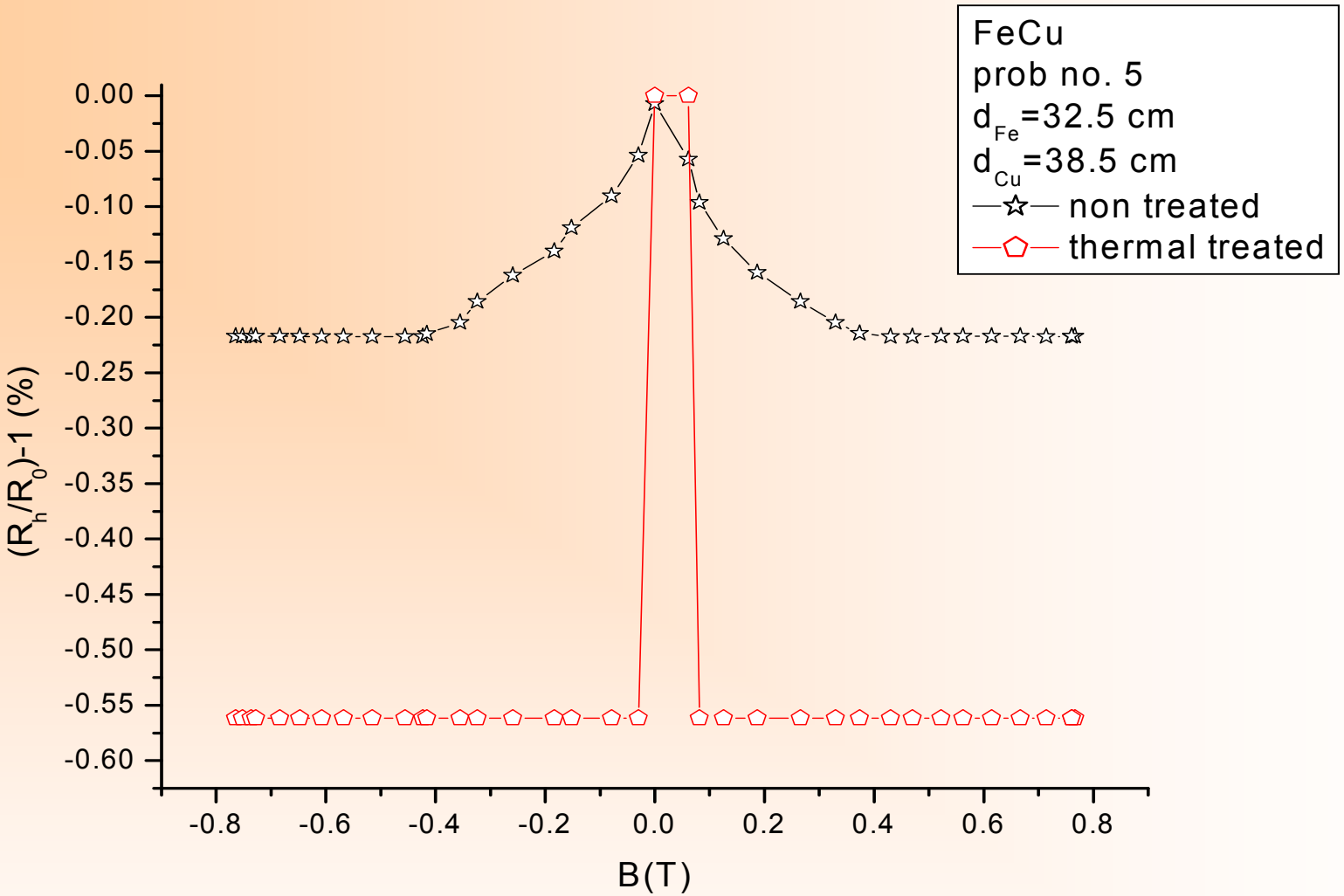

GMR in Fe-Cu thermally treated and as deposited= high abrupt variation=uniform dimensional distribution of formed domains

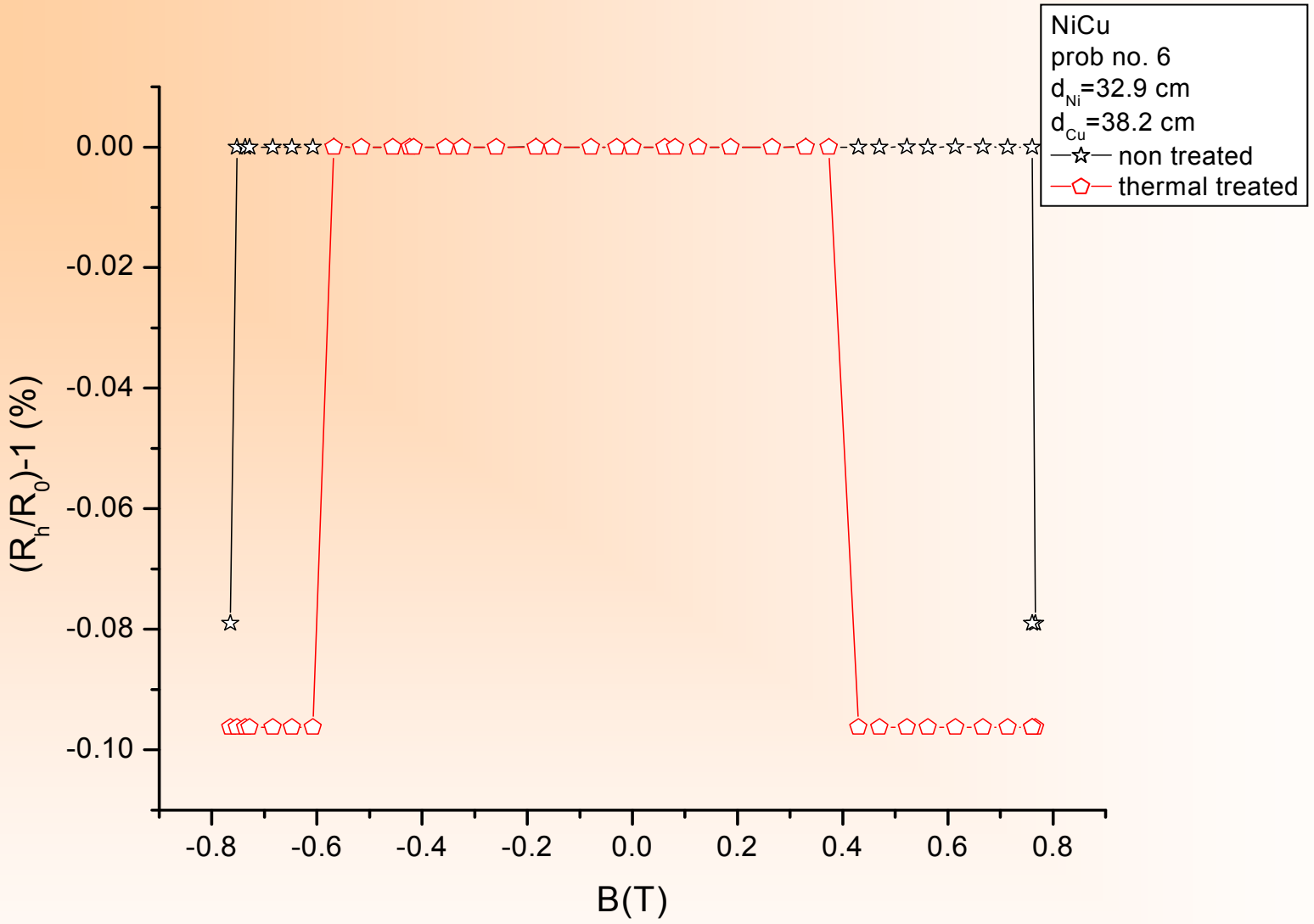

GMR in Ni-Cu composite layer

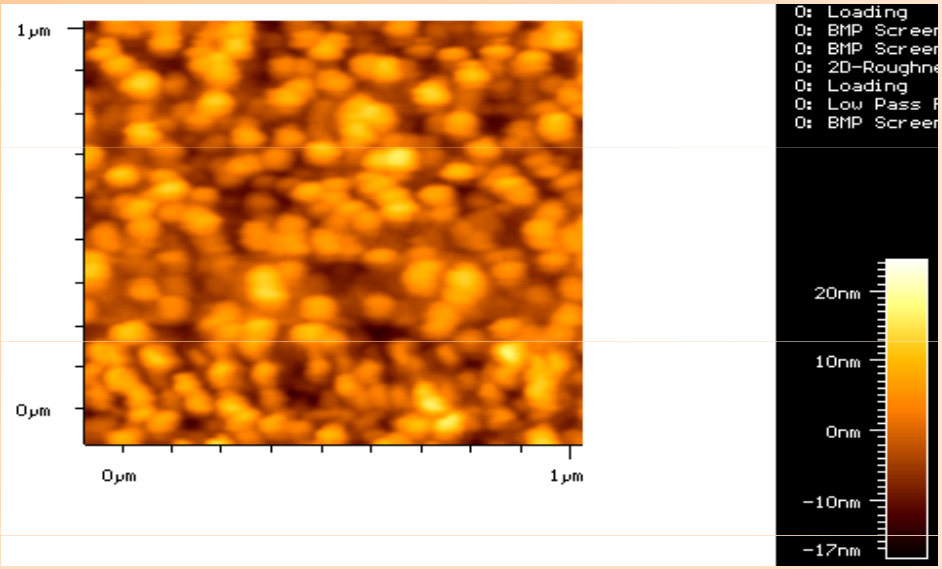

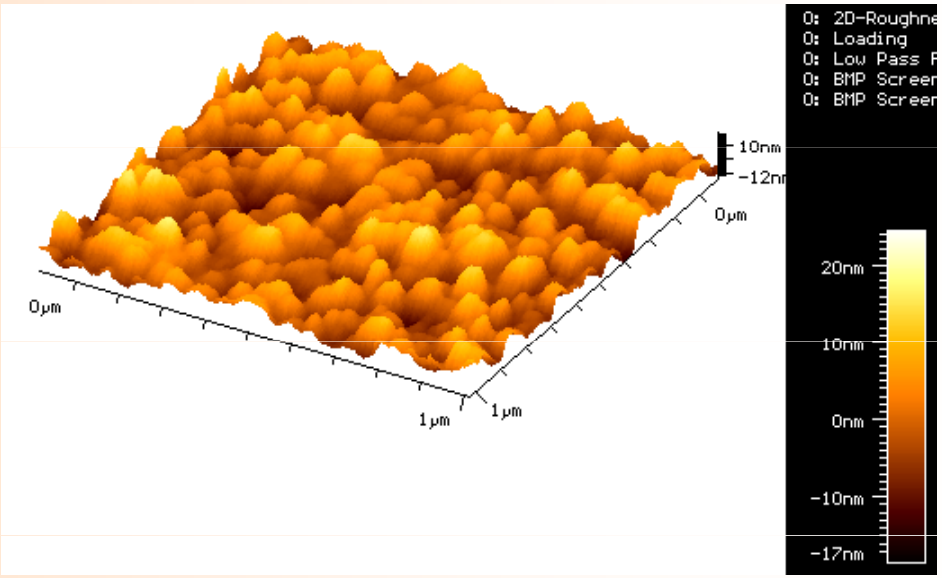

AFM images of the Co-Cu films

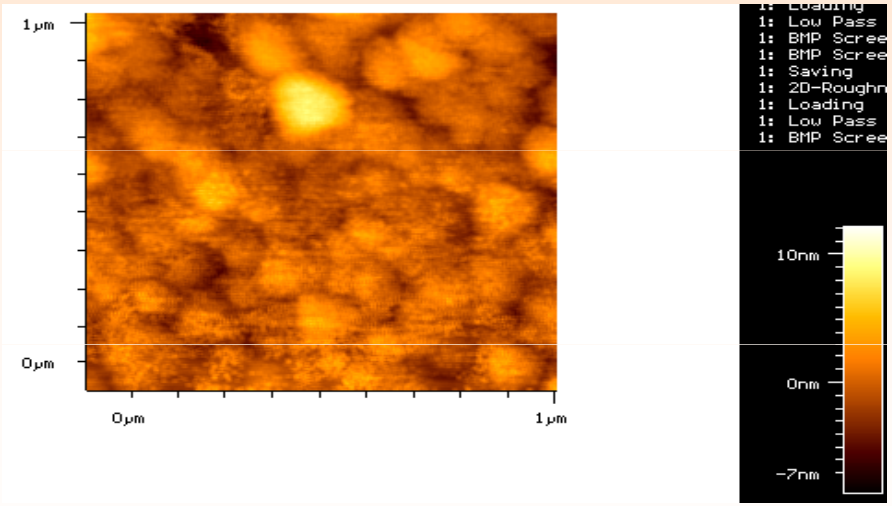

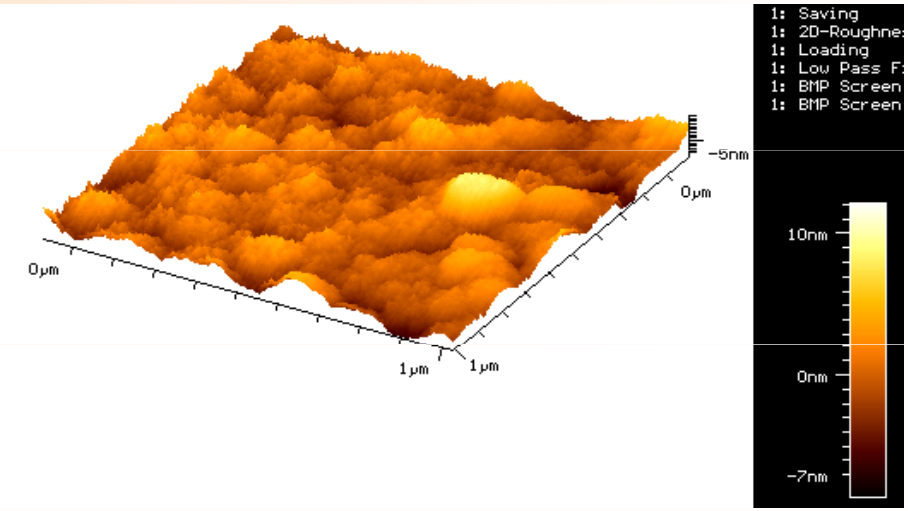

AFM images of the Fe-Cu films

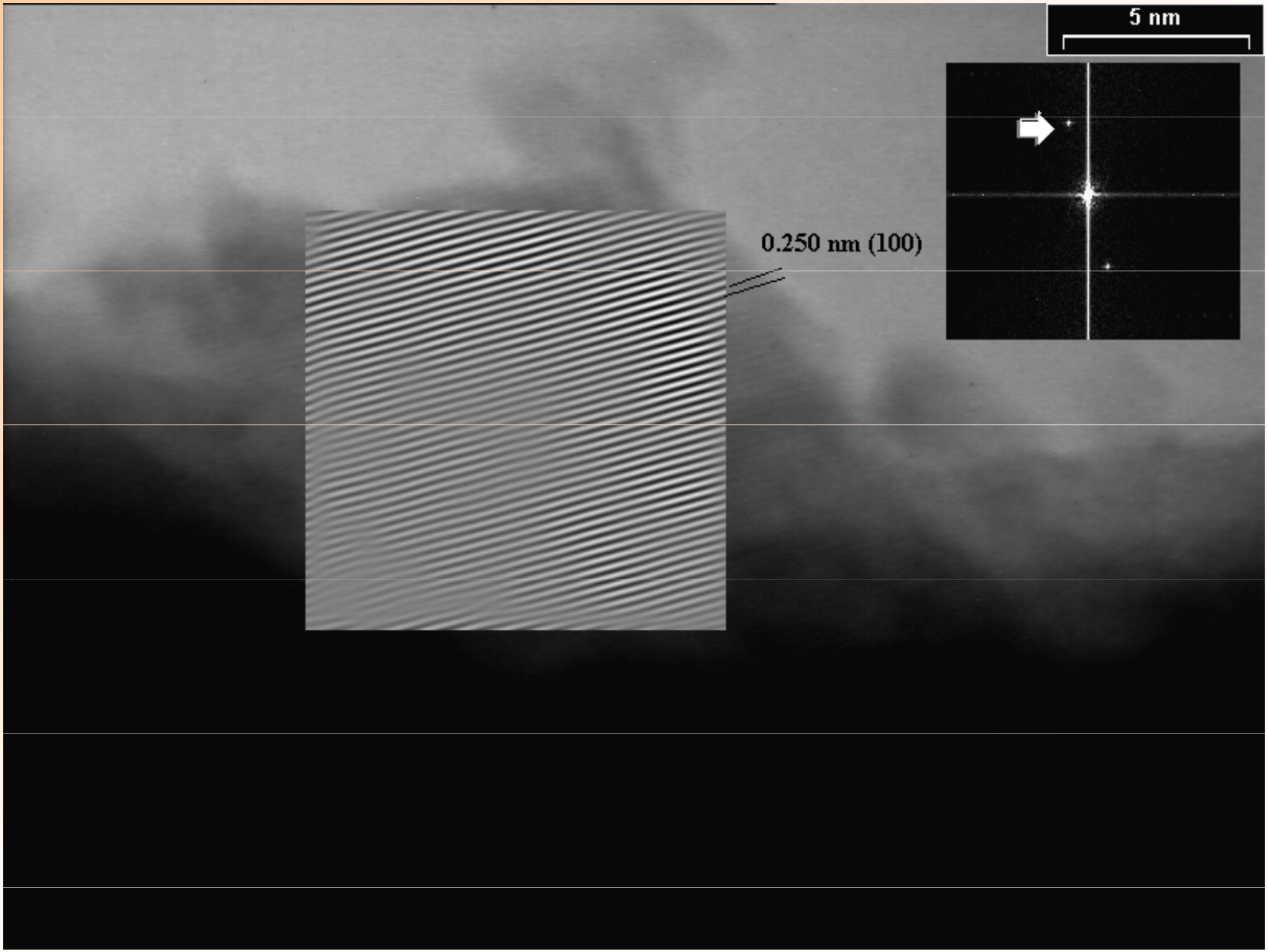
5 nm
0.250 nm (100)

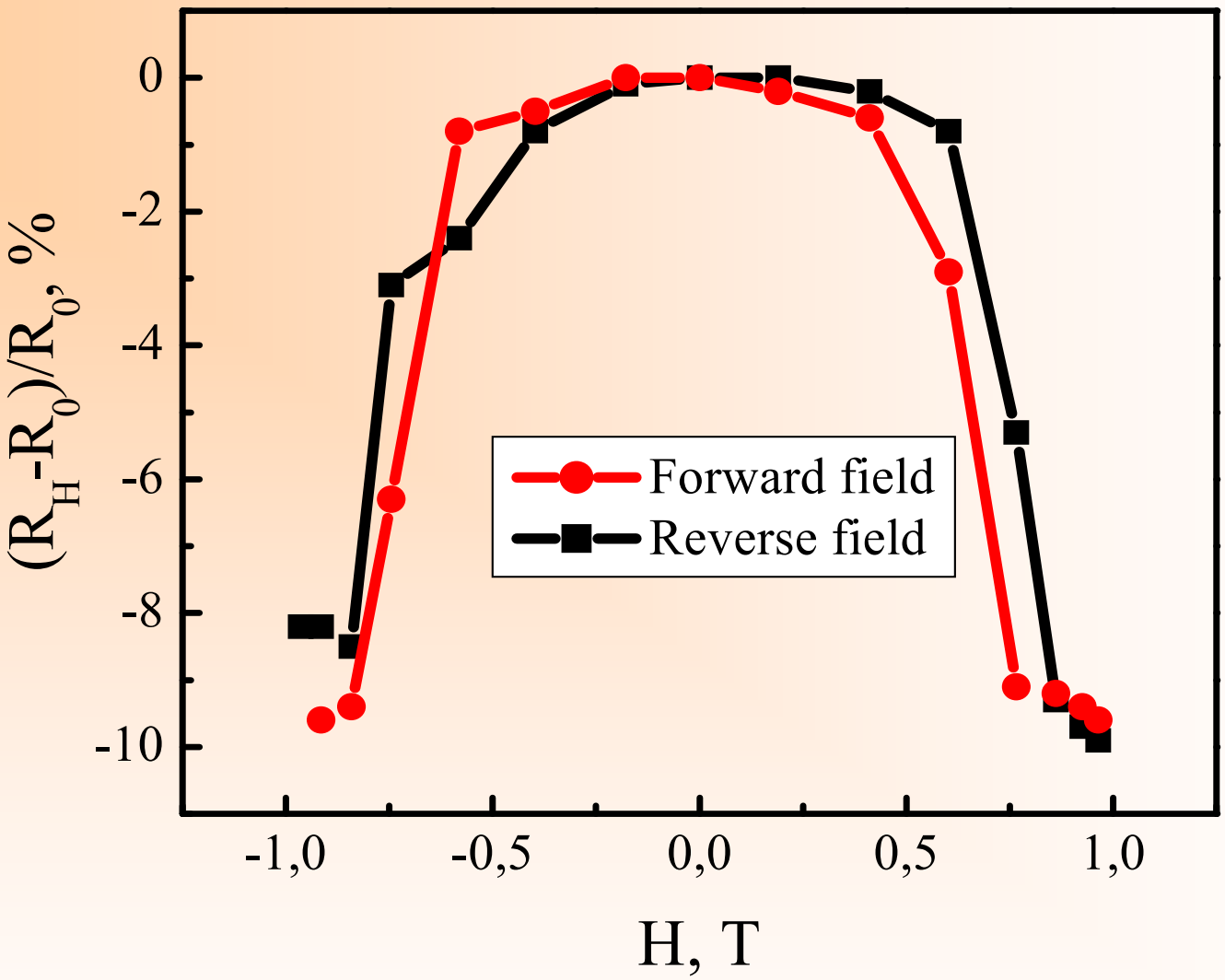

GMR in Co-Cu layers – high step variation

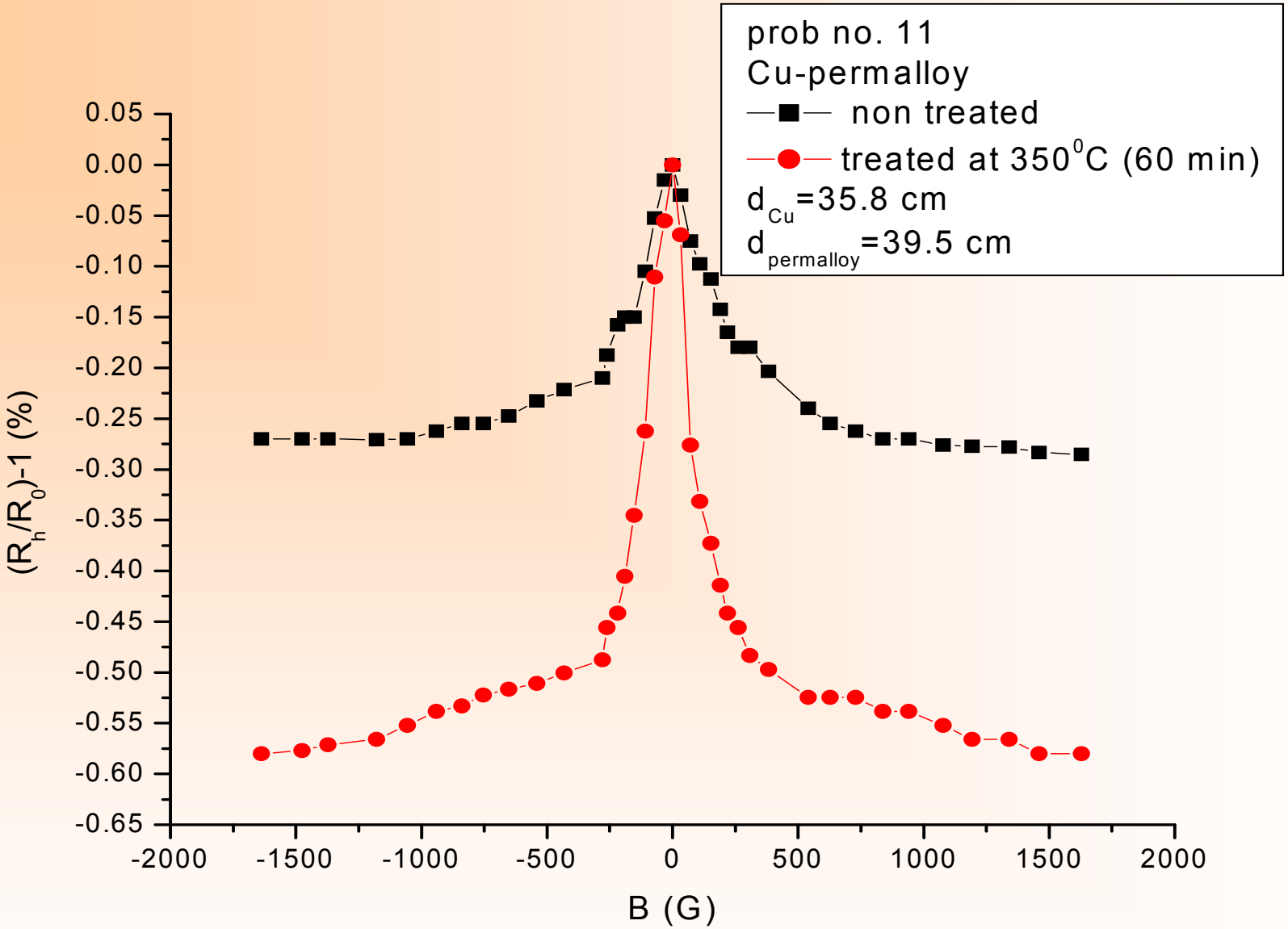

GMR in Cu-permalloy layers; no high steps present

-co-deposited gadolinium or holmium in combination with fullerene (C_{60})

-gadolinium or holmium were deposited from their plasma using the following conditions:

-filament heating current – 40 A

-current discharge – 300 mA (Gd) and 400 mA (Ho)

-the fullerene was evaporated from ceramic oven using 9A electrical current flowing through the surrounding copper conductor

-the Gd – C_{60} combination can furnish interesting magneto-electrical behavior, gadolinium being a rare earth magnetic element

-the Ho – C_{60} combination can furnish interesting conductor/semiconductor behavior

-the deposition geometry was similar with the one used for two metals co-deposition

-probes with different metal – fullerene relative concentrations were obtained

CONCLUSIONS (GMR section)

- Composite thin films were prepared by TVA technology
- One of the fim consisting of α-Fe nanoparticles embedded in the Cu matrix.
- The size of the Fe nanoparticles and their dispersion, to the purity of the Cu matrix, were analyzed starting from the Mössbauer spectra and finally correlated with the magnetoresistance effects, AFM and XRD measurements.
- The greatest GMR effect appear in the case of Co-Cu structure and for Fe-Cu and Ni-Cu cases, very special kind (quadratic) of GMR dependence appear.
- This could suggest a very narrow distribution of the cluster dimensions within the copper structure that can be explained by the special conditions of deposition in TVA technology.

High temperature oxidation resistant composites:

Re, Re-Ni-Cr, Ni-Al multilayers

- Plasma ignition in pure Re vapours: thoriated tungsten filament heated by a 90-100 A a.c. current.
- The emitted electrons: were focused on the Re anode by a Mo Whenelt cylinder.
- The anode: Re rod of 8-10 mm in diameter and supported by a Mo flange.
- The distance between the thermoemissive filament and the Re anode: 3-4 mm
- The angle between the electron beam and the vertical line: 60^0.

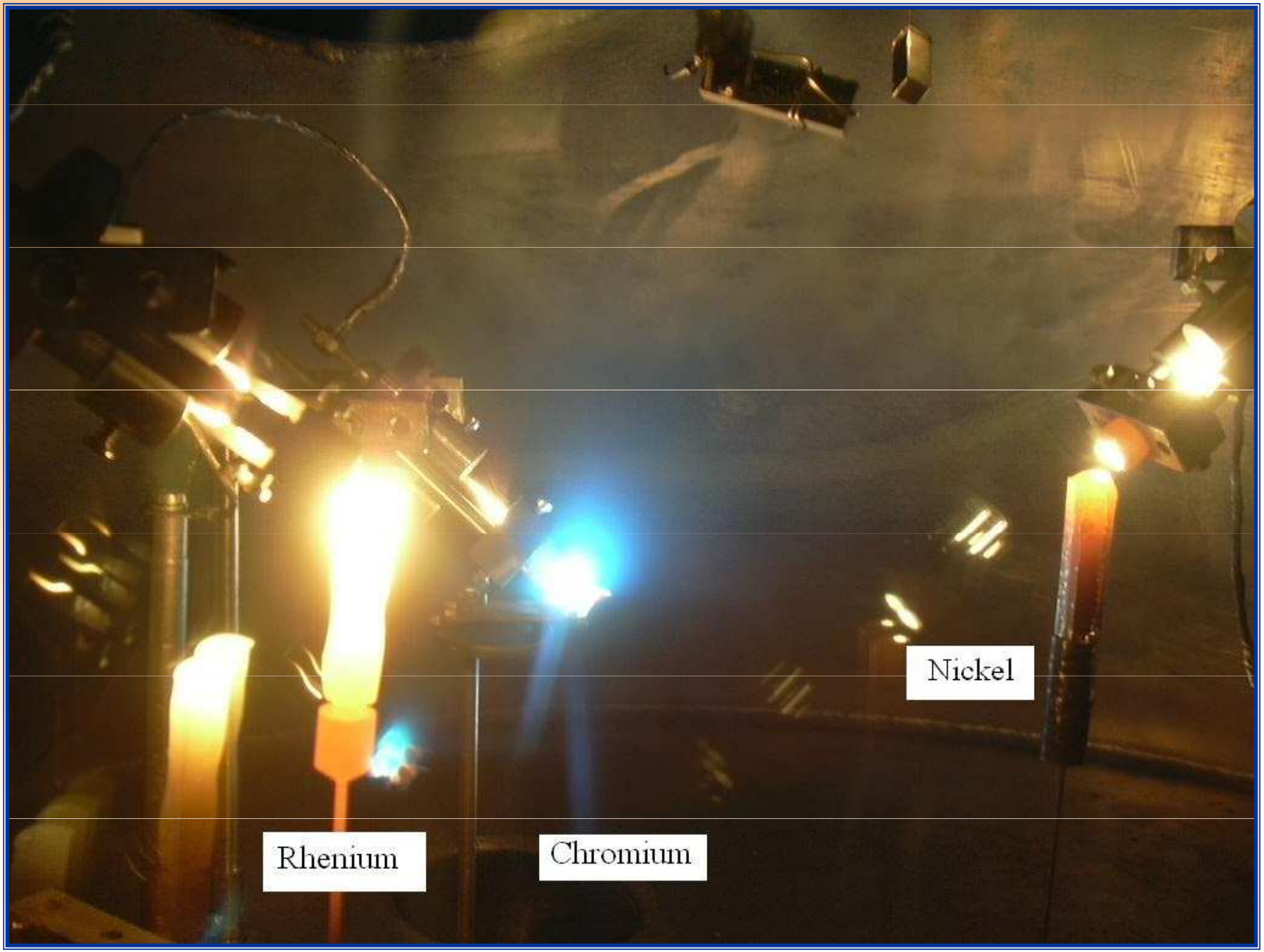

Experimental set-up used for simultaneously depositions of Re, Ni and Cr

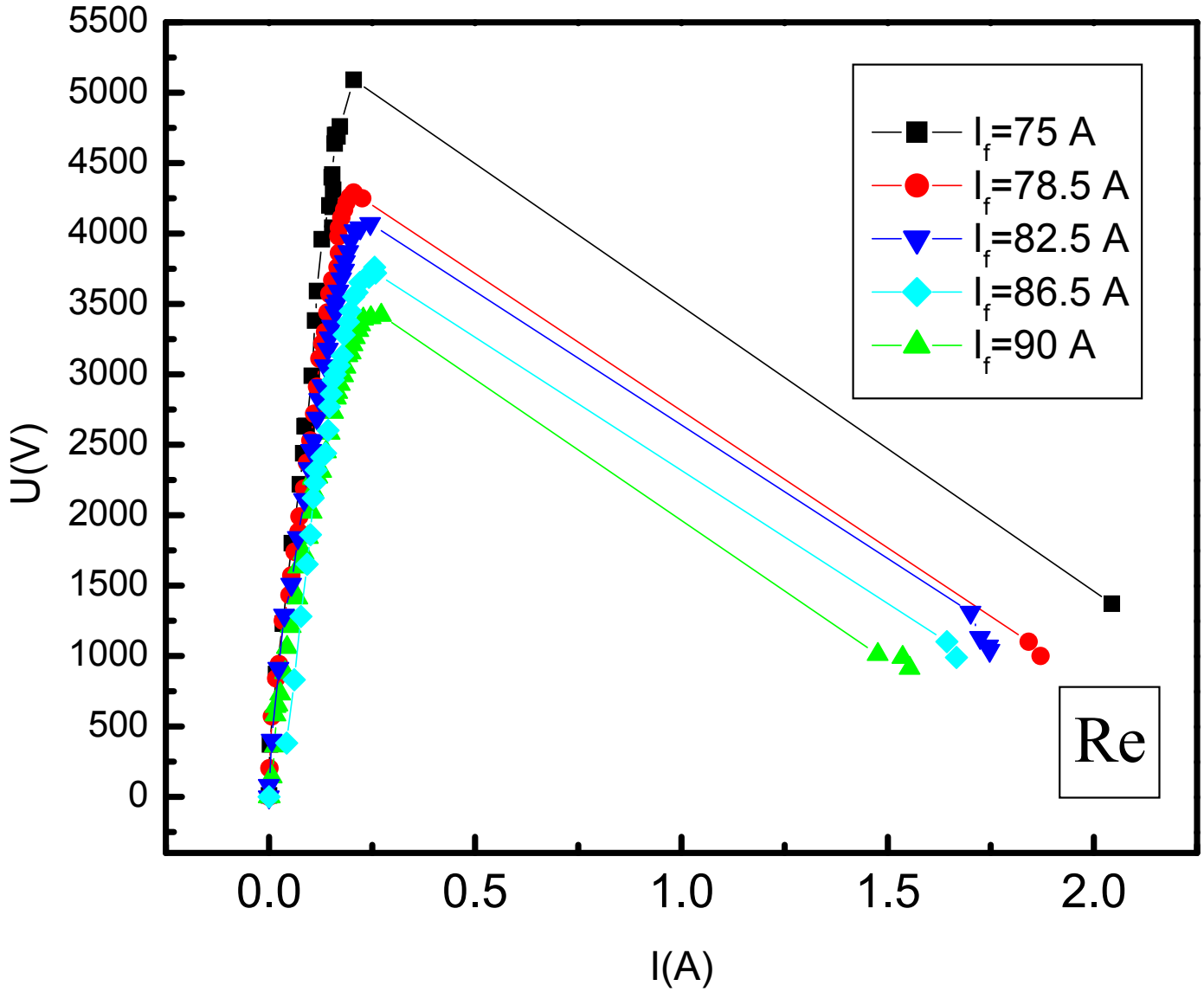

I-V charateristics of Re plasma as function of the filament current

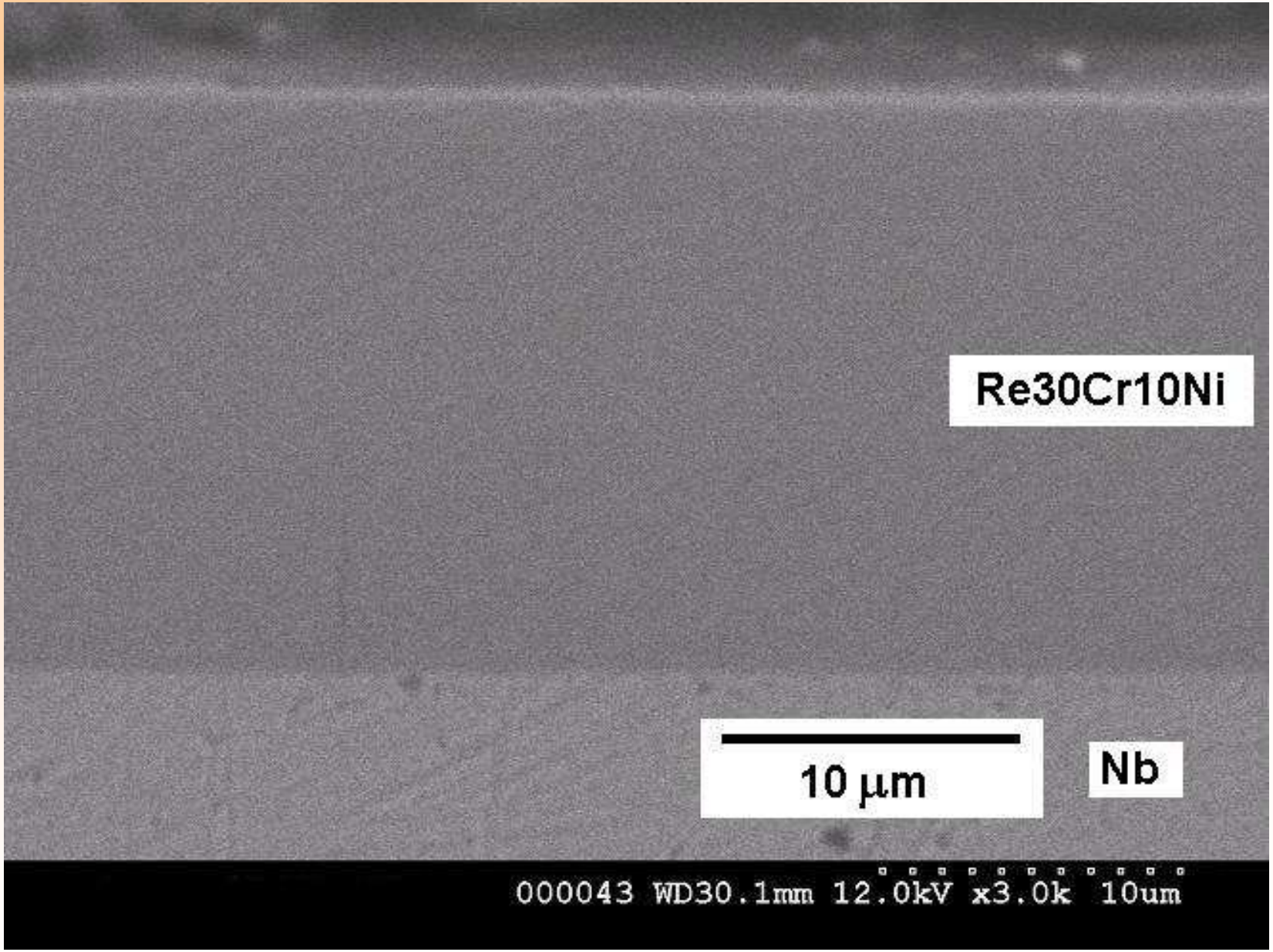
Re30Cr10Ni
10 μm
Nb
000043 WD30.1mm 12.0kV x3.0k 10um

Mixed layer formation –low friction composites

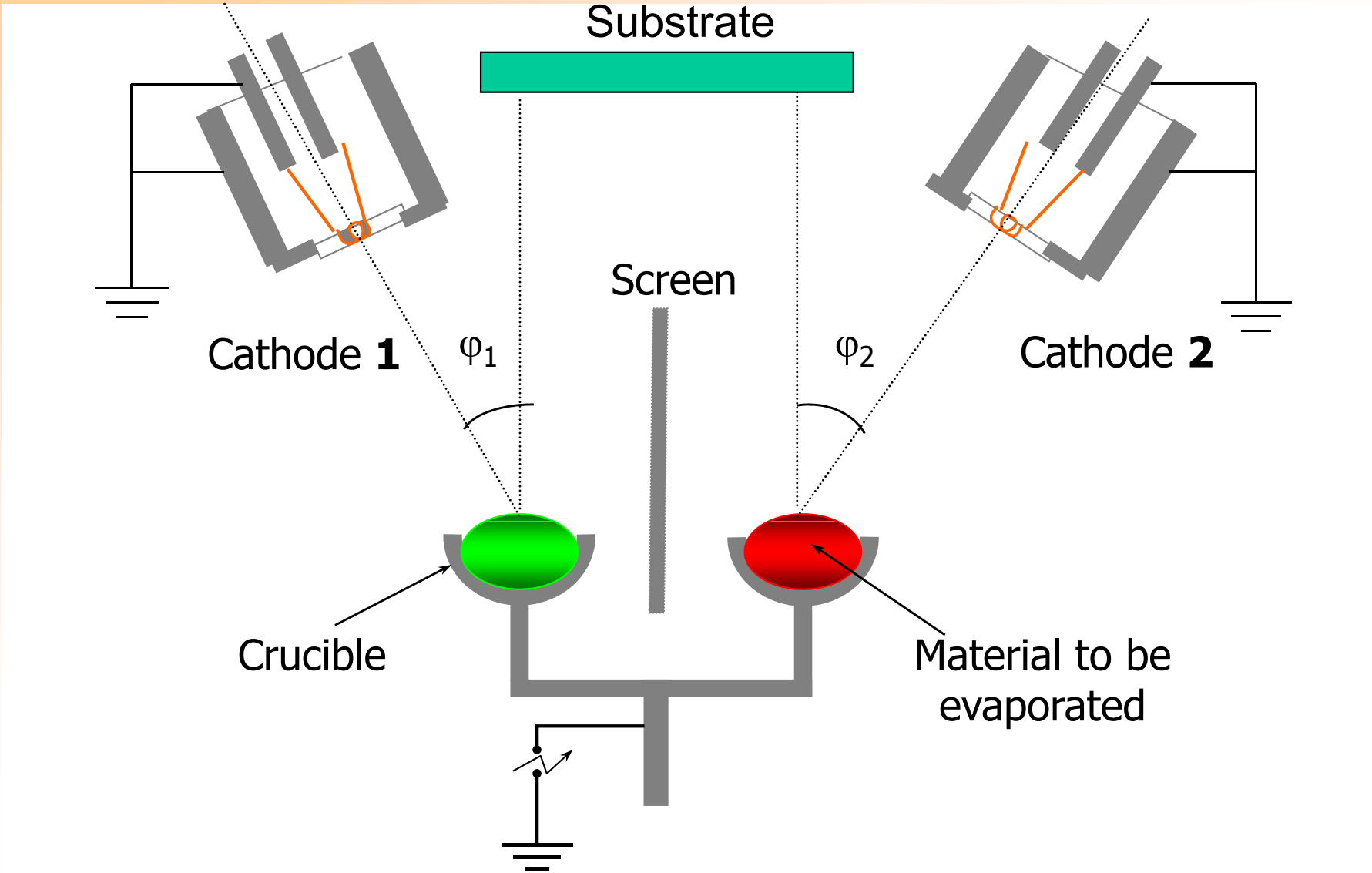

HRTEM of Ni-C layer

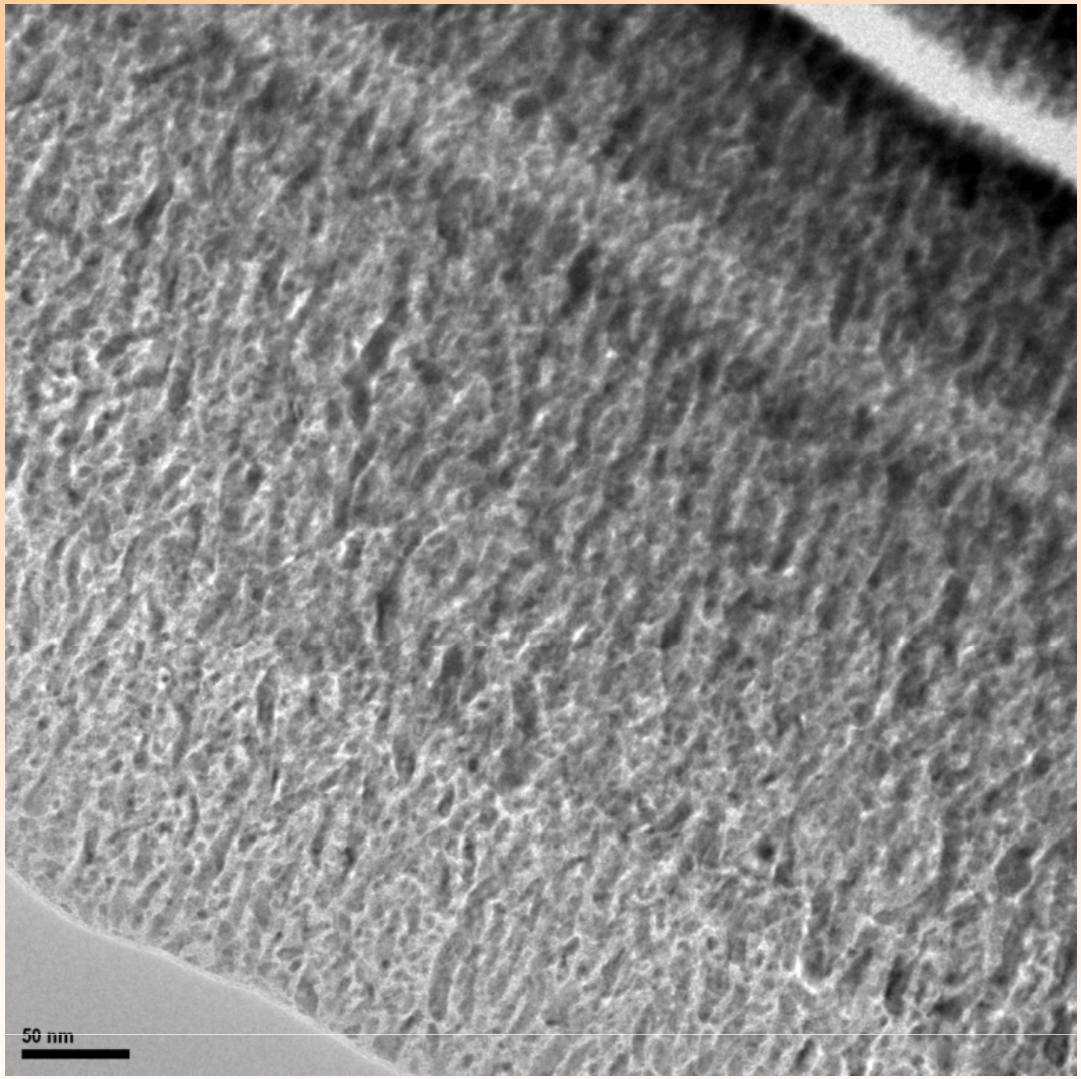

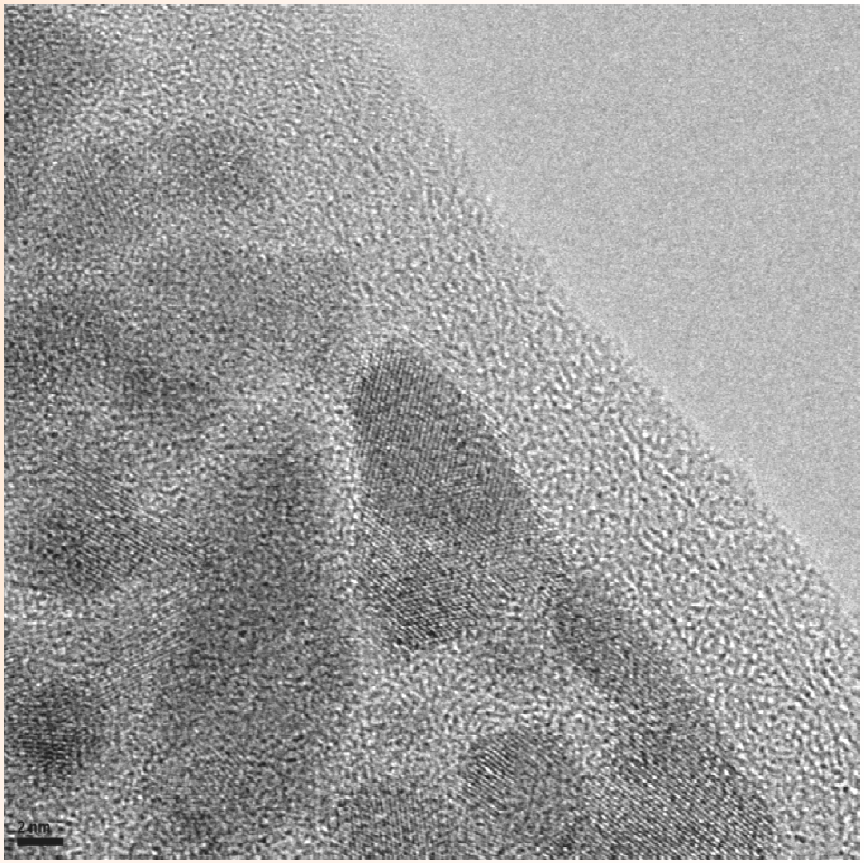

2 nm

Images of the structure of the upper layer: tubular features with about 10 nm width and 50-100 nm length appear together with small grains with a lateral size of about 5 nm. The mentioned features are surrounded by a brighter carbon matrix.

Coefficient of friction of C-Ni composite

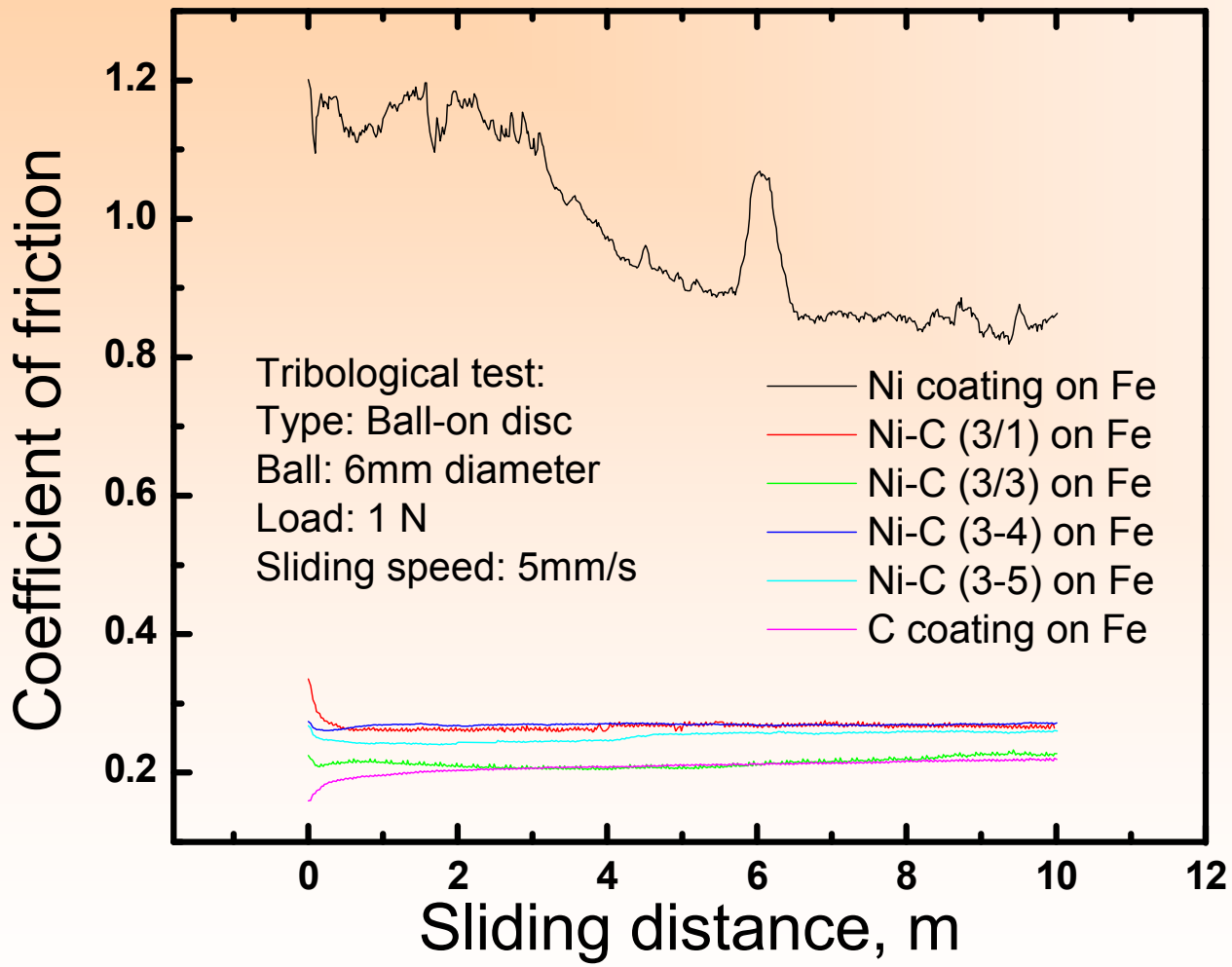

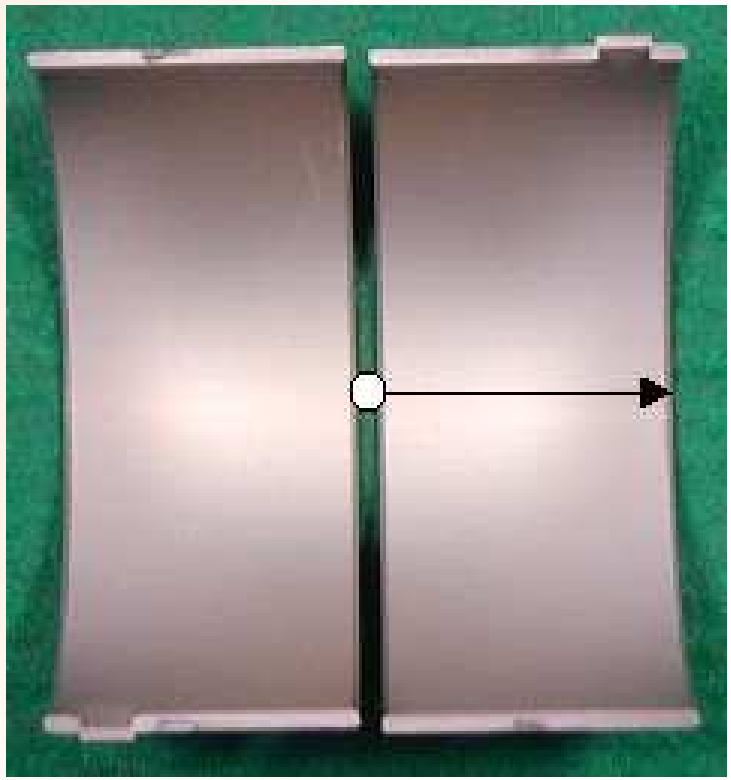

Plain bearings for automotive applications

CONCLUSIONS

Using TVA method were obtained nanostructured films with applications in:
Electronics (magnetoresistive films0
Mechanics (solid lubricants)
Nuclear technology (compact films for First Wall coatings)

Be-W composite preparation

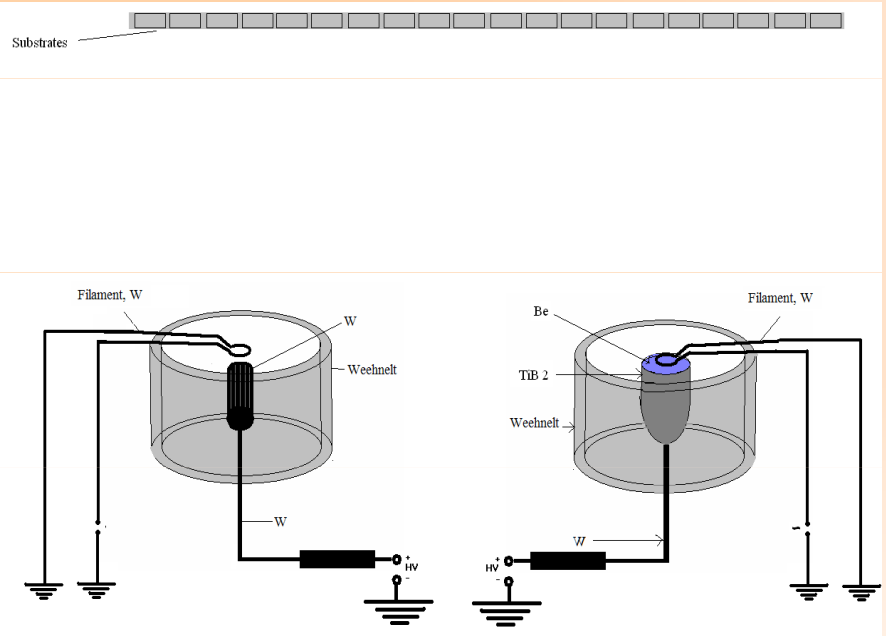

Deposition set-up

Distance between anodes: 20cm
Sample holder-anodes dist.: 25 cm.

W anode

Concentration variation

- The relative concentration for each of the material of a certain sample depends on the incident particle flux and on the incident angle:

$$c \approx \frac{1}{d^2} \cos \theta$$

- d is the distance from the source (anode) to the sample and θ is the particle incident angle of the substrates

Theoretical estimation of the relative concentration

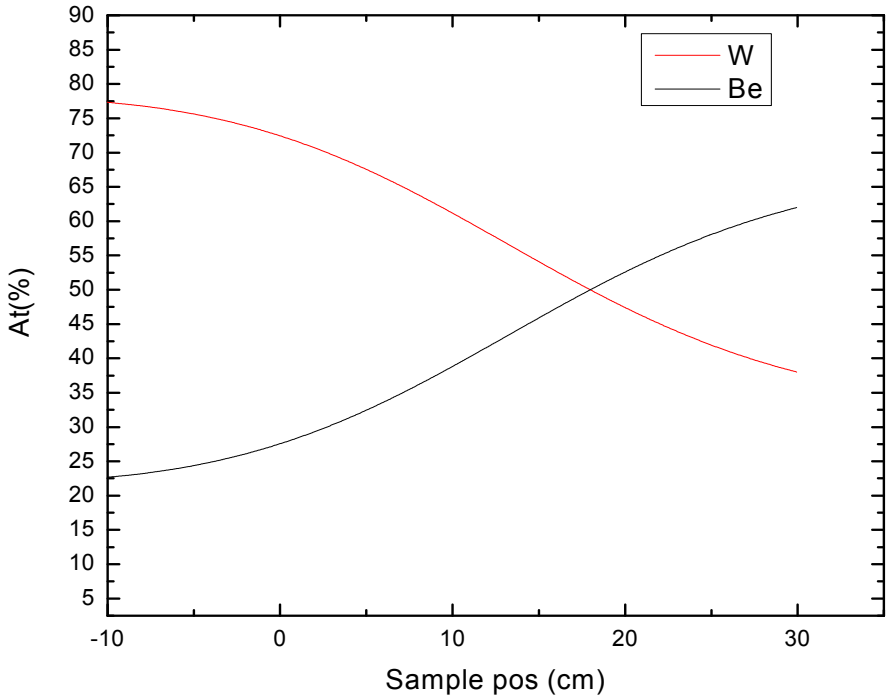

Relative concentration based on EDS measurements

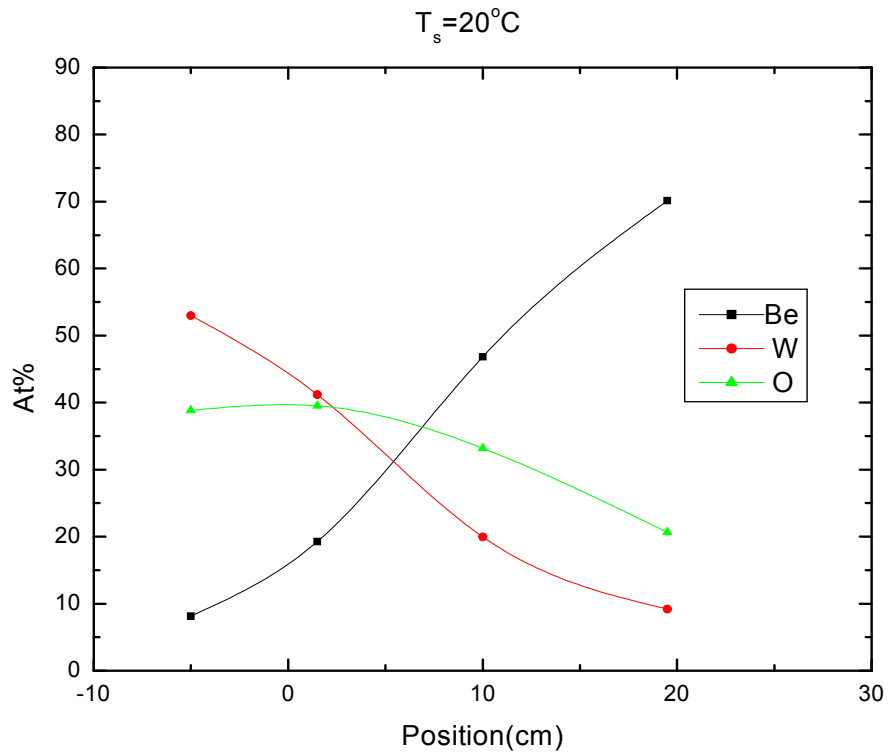

Be+W on graphite at R.T.

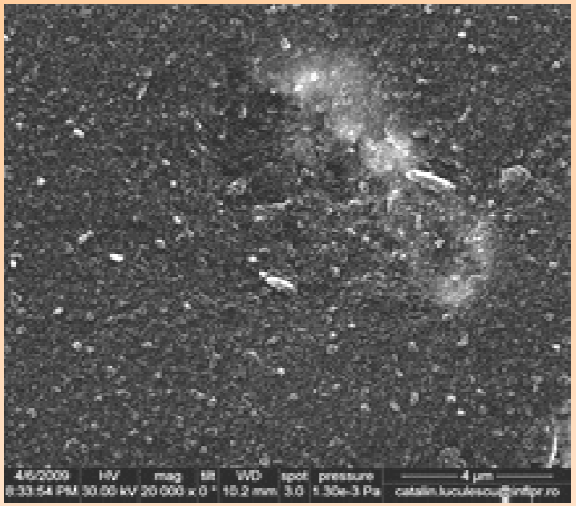

Be - 52.36 %
O - 38.81 %
W - 8.83 %

Be+W on Si at 350°C

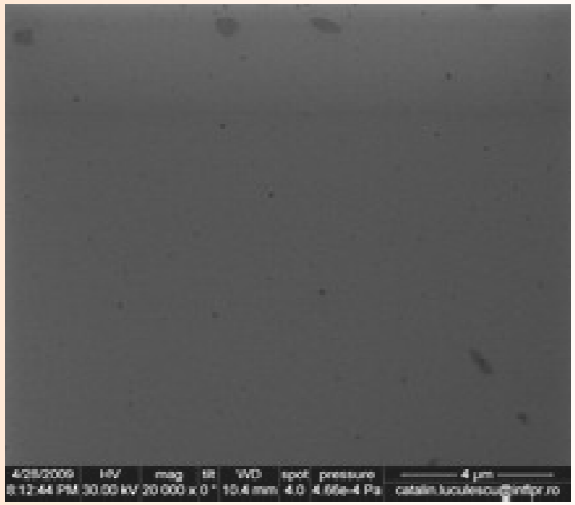

Be- 12.52 %
O - 22.98 %
W – 64.48 %

Be+W on Si at R.T.

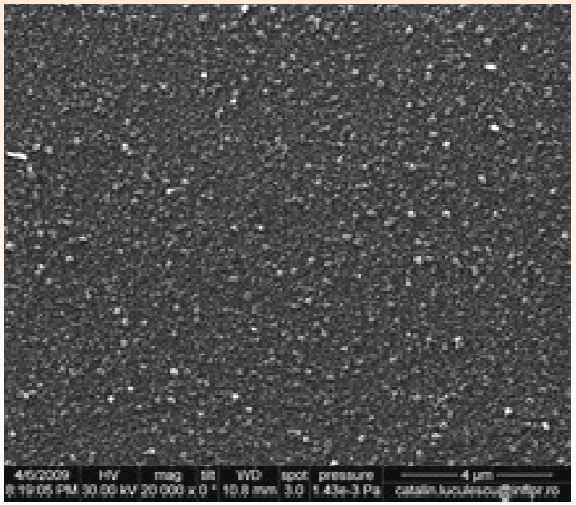

Be - 60.55 %
O - 36.21 %
W - 3.25 %

Be+W on Si at 500°C

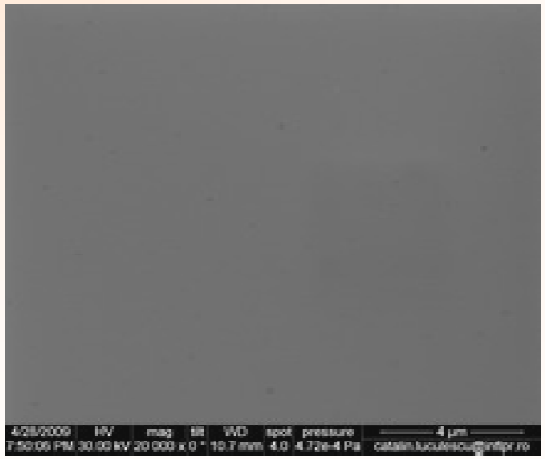

Be- 11.83 %
O – 18.09 %
W – 70.06 %

Rough surface morphology of the RT prepared samples.

Smooth surfaces on the heated substrates samples:> higher atom's mobility

RBS experimental and SIMNRA code simulated spectra of the Be-W film deposited on graphite substrate at room temperature and 500°C

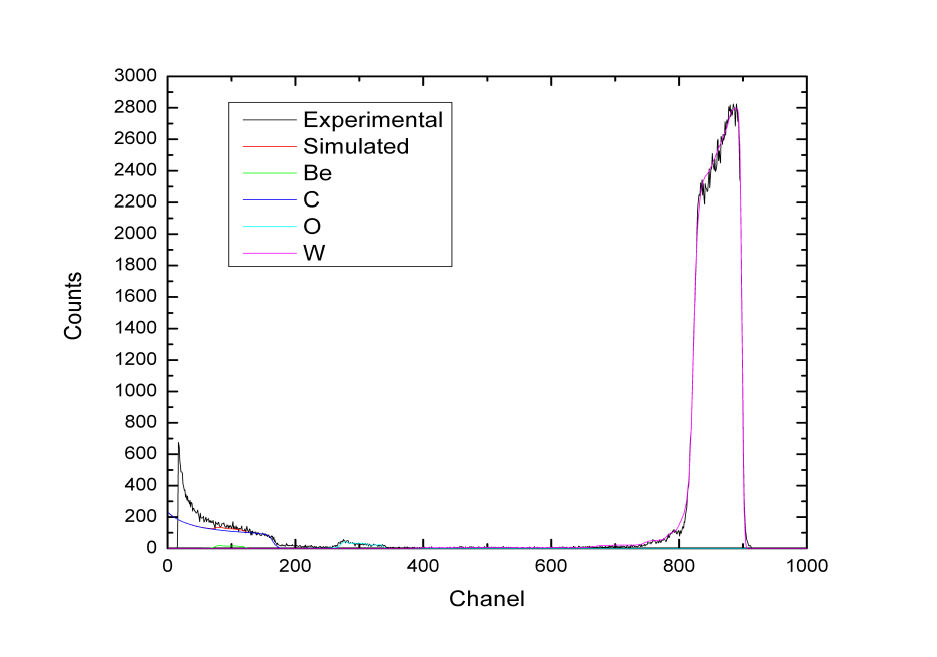

Be-W film prepared at RT

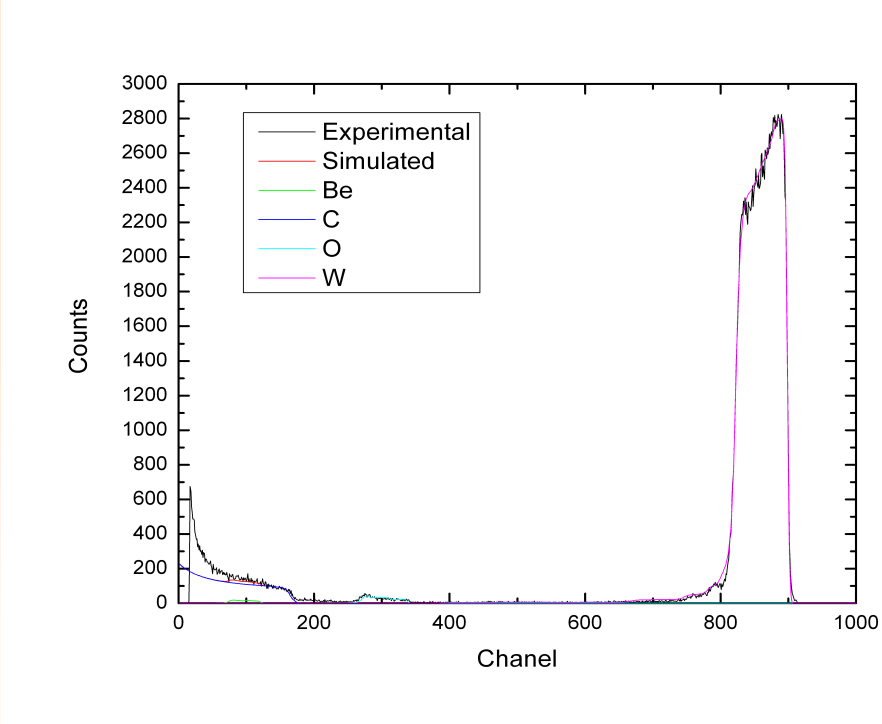

Be-W film prepared at 500°C

The depth profile of the Be-W film deposited on graphite substrate at RT.

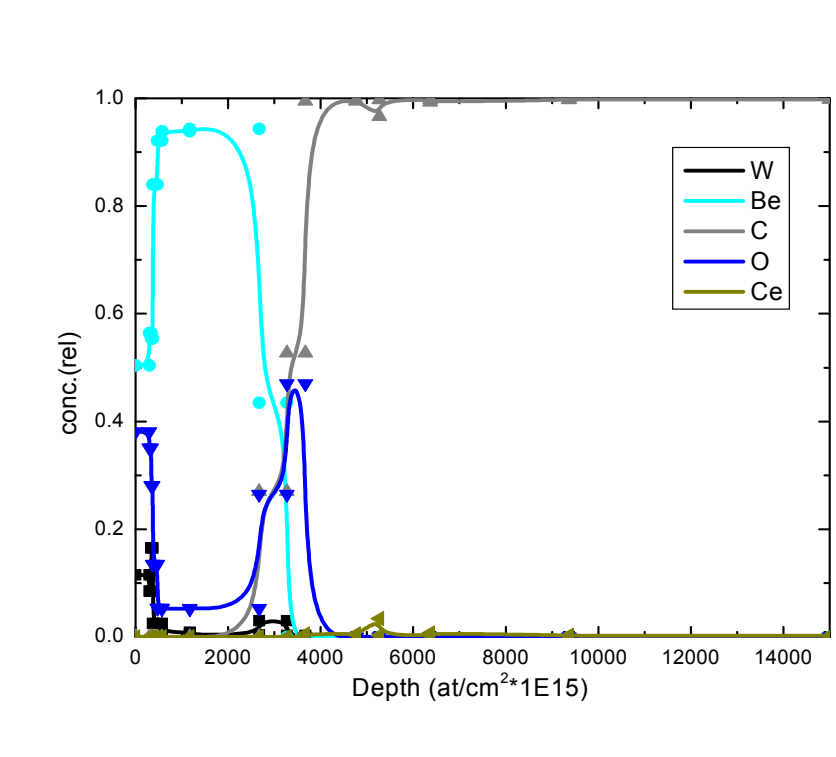

At RTsubstrates the Be-W film was oxidized only at the surface and at the interface

For the heated substrates the oxygen was present at the surface, and diffuses into the material, oxidizing the beryllium and the tungsten in the whole film.

Oxygen present at the interface begins to migrate into the substrate as the temperature increased.

The depth profile of the Be-W film deposited on graphite substrate at 500°C

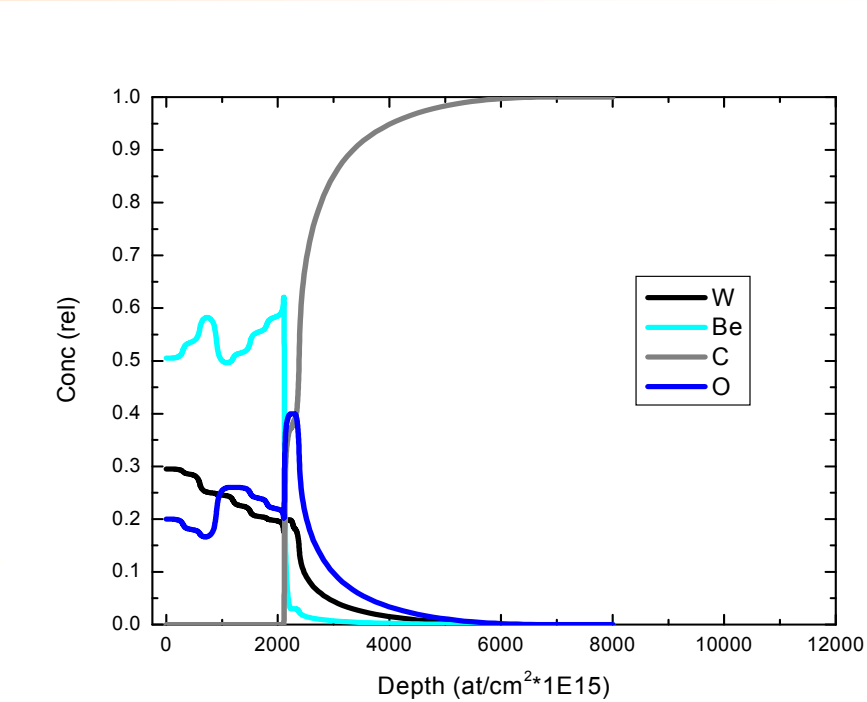

XPS survey spectra at the interface of Be-W film

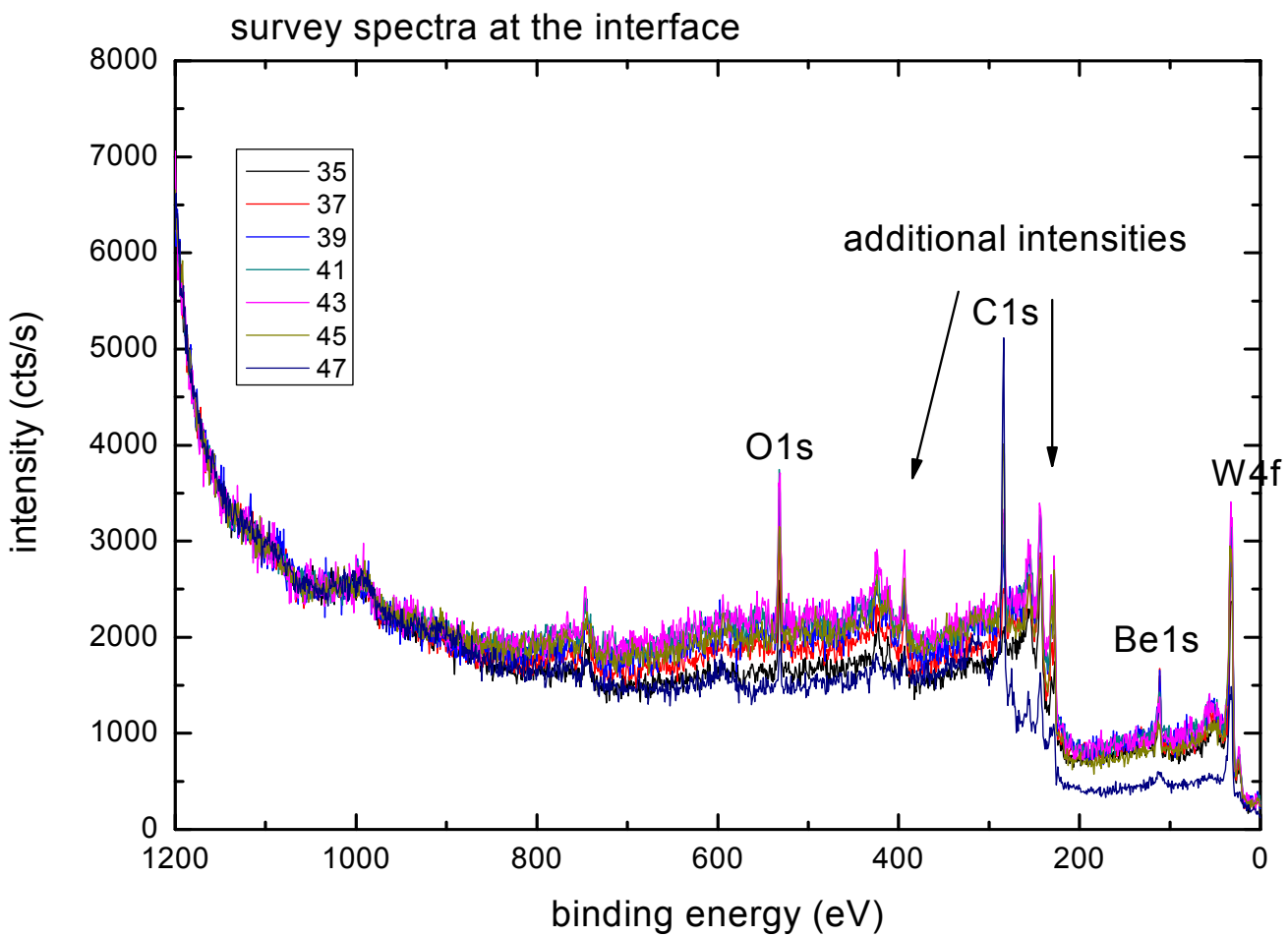

XPS core spectra

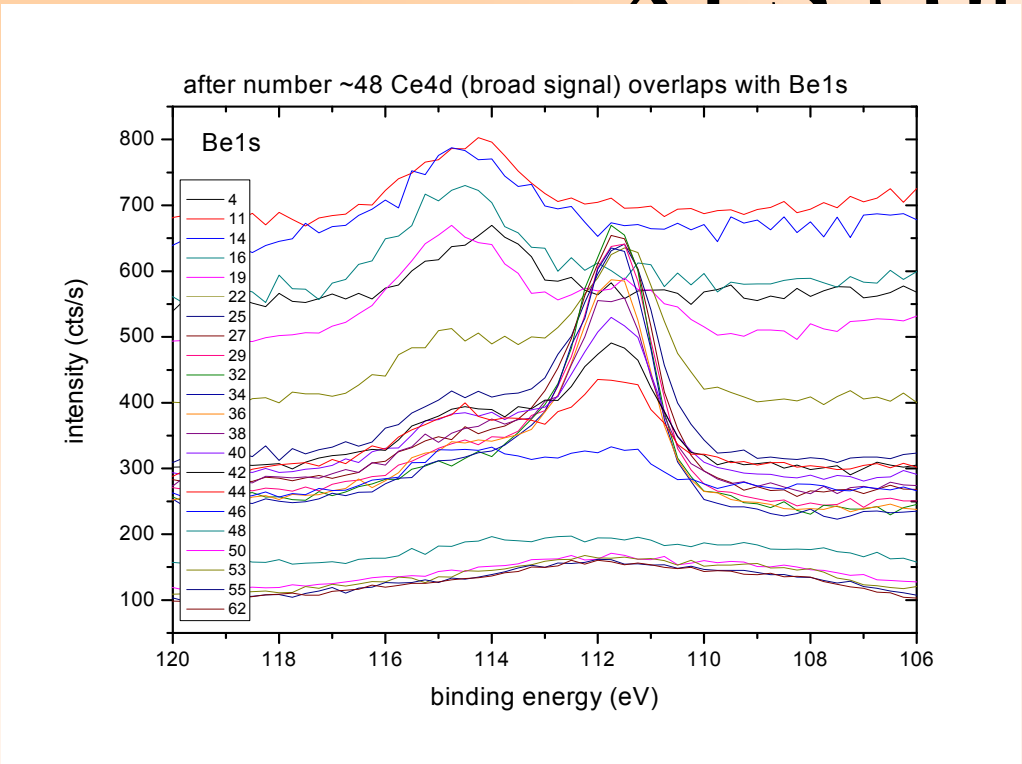

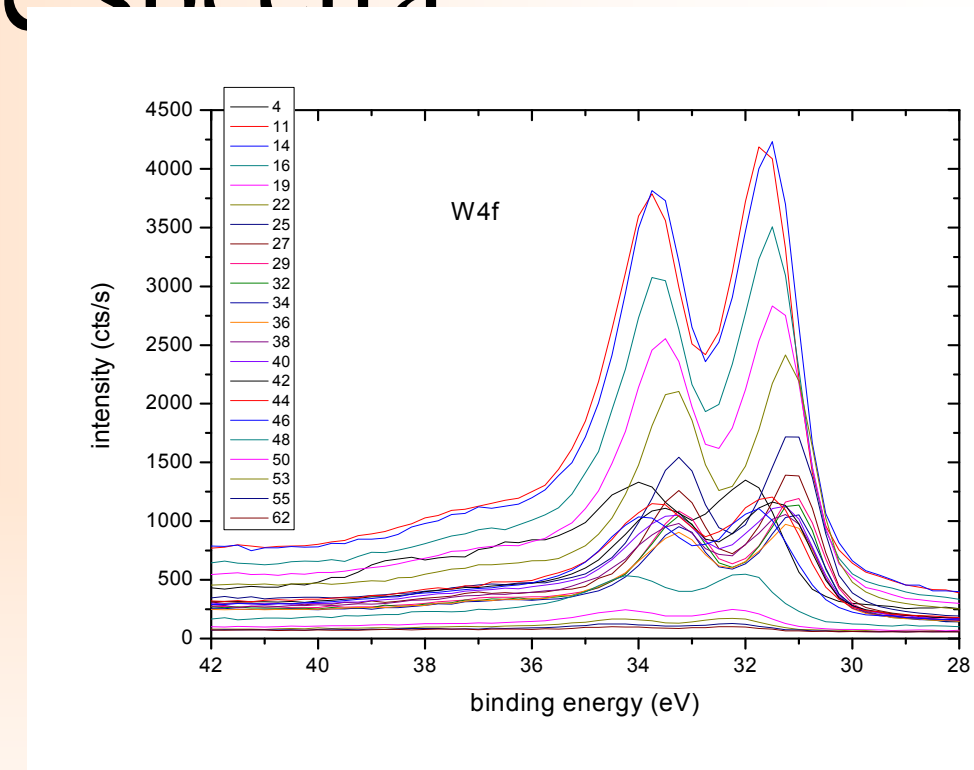

Be1s peak of the Be-W film

W4f pattern

Be-C formation

Be film depositions on graphite substrate

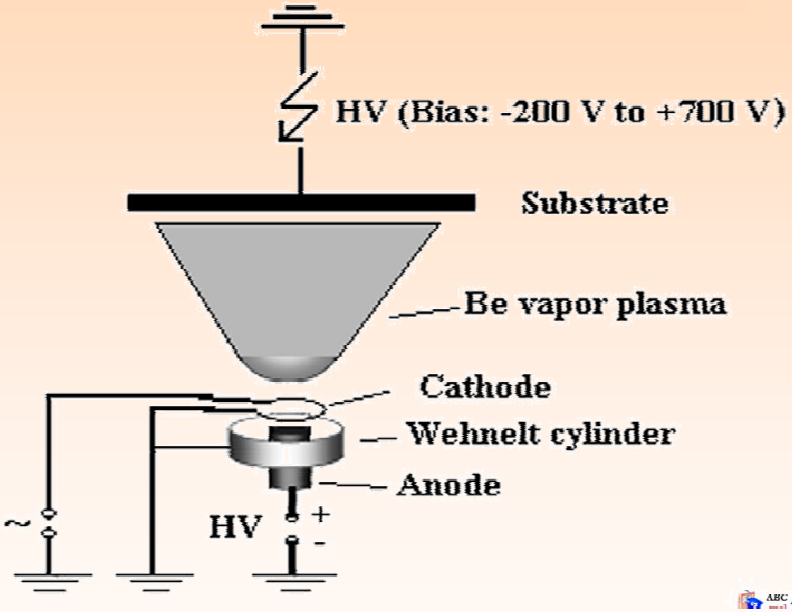

Discharge parameters (Be deposition on graphite)

I_{fil}= 50 A
$I_{discharge}$= 1.5 A
$U_{discharge}$= 600 V

Be fim morphology and structure

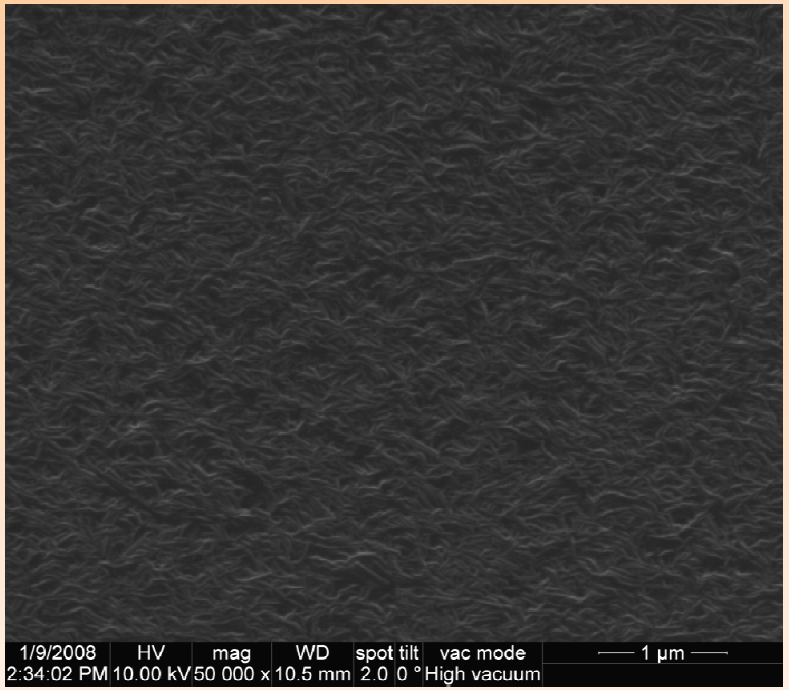

Si substrate

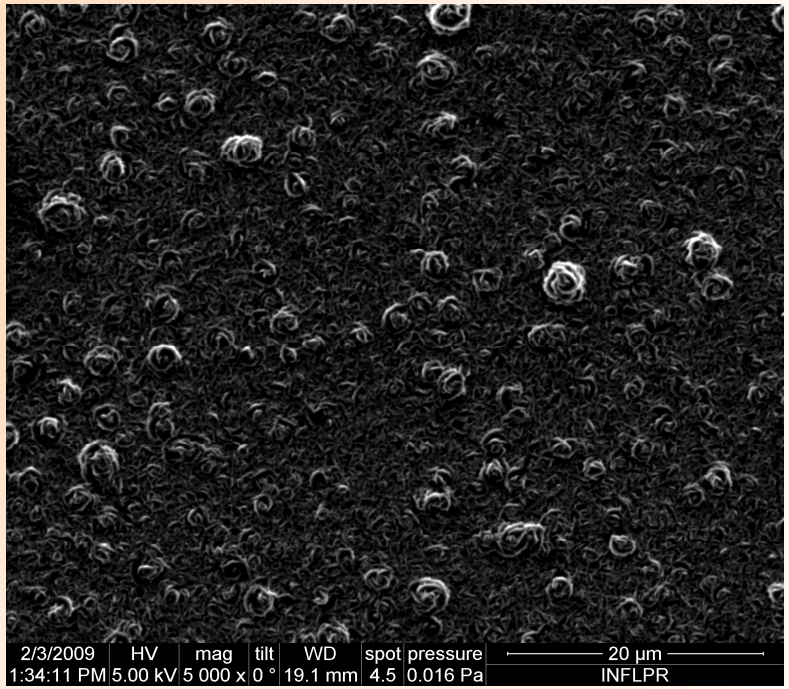

Graphite substrate

Polycrystalline Be

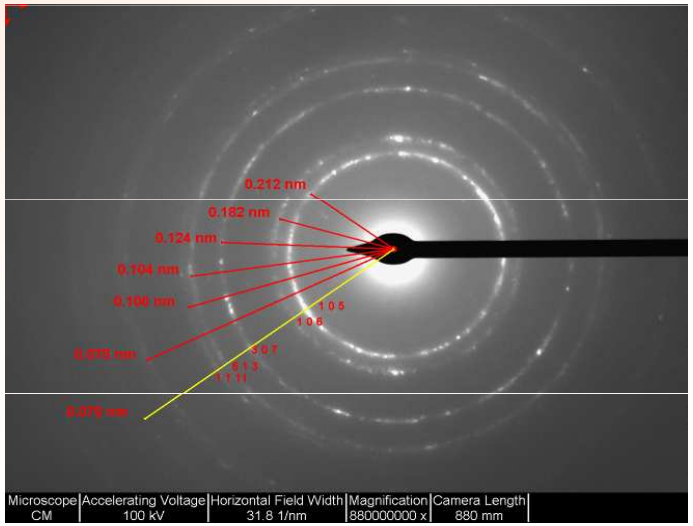

SEM images

Before (left side) and after (right side) annealing Be film on graphite at 750 ºC

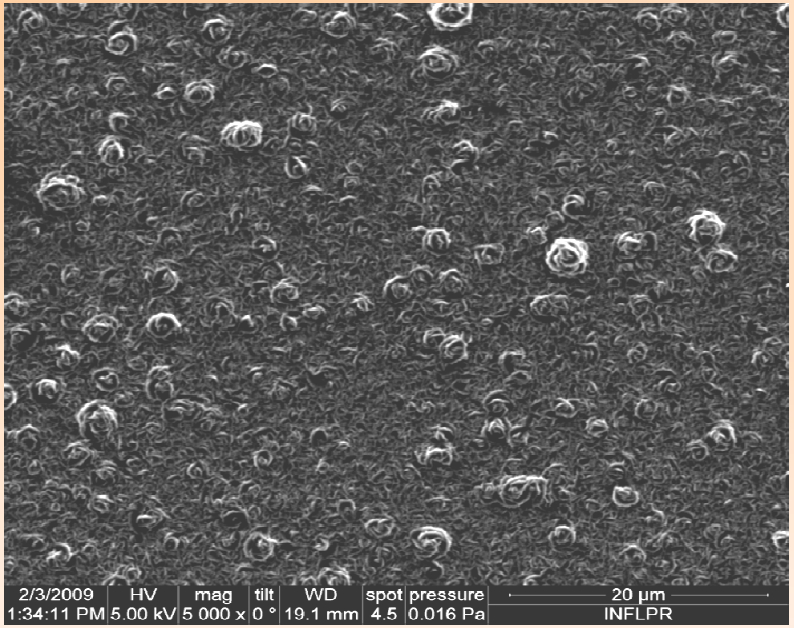

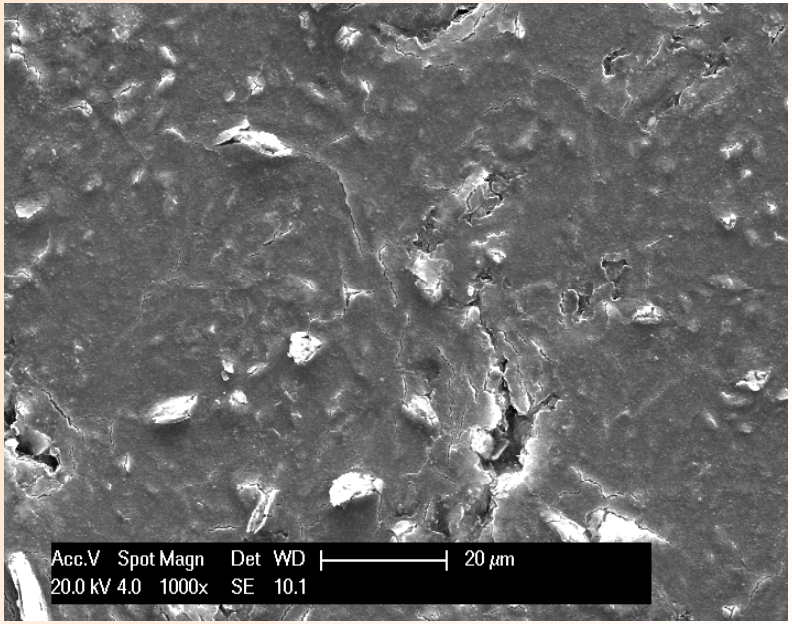

After annealing at 750 ºC:

- **re-crystallization**
- **surface cracks/holes**
- **the film remains stable**

TT 350°C

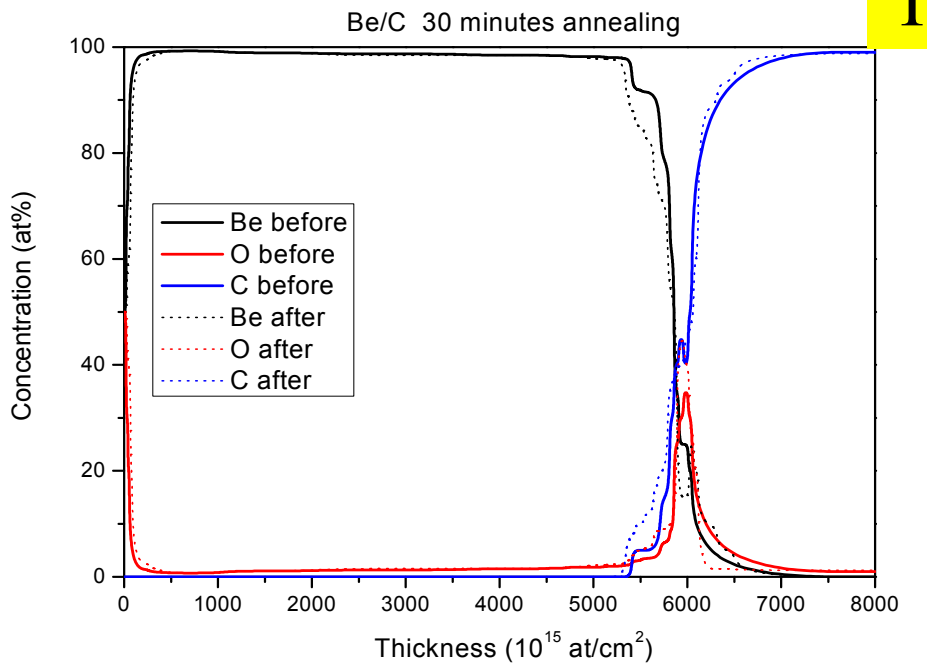

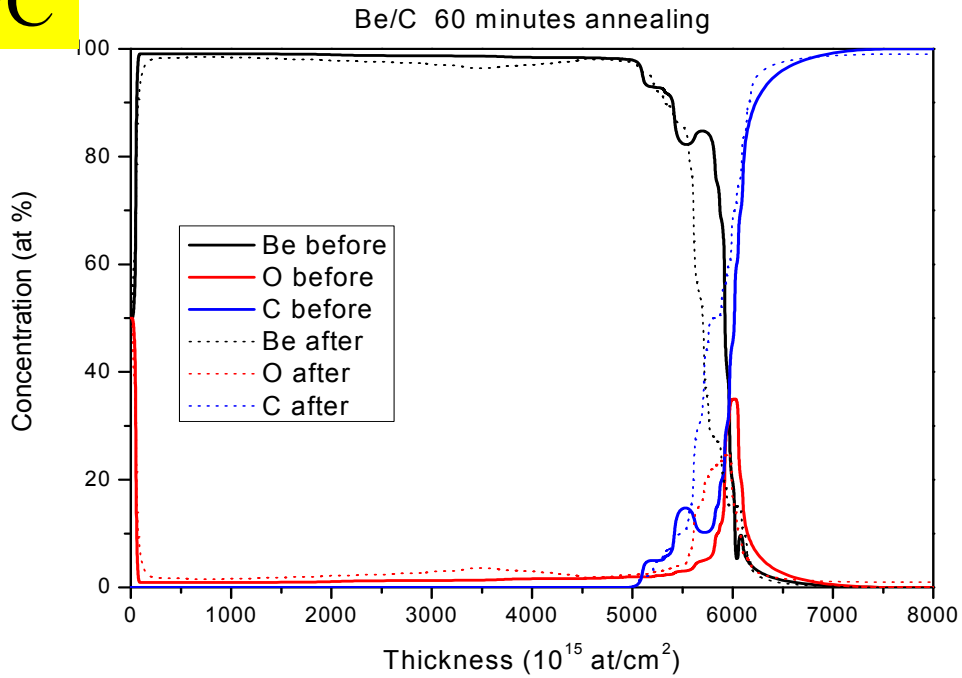

As deposited (Be on graphite) samples:

- oxidized surface (due to air exposure after deposition)
- oxygen present at the interface (porous graphite surface/residual oxygen in the deposition chamber)

Annealed samples:

- oxidized surface
- oxygen from the interface migrates into the film
- mixed material formation occurs at the interface

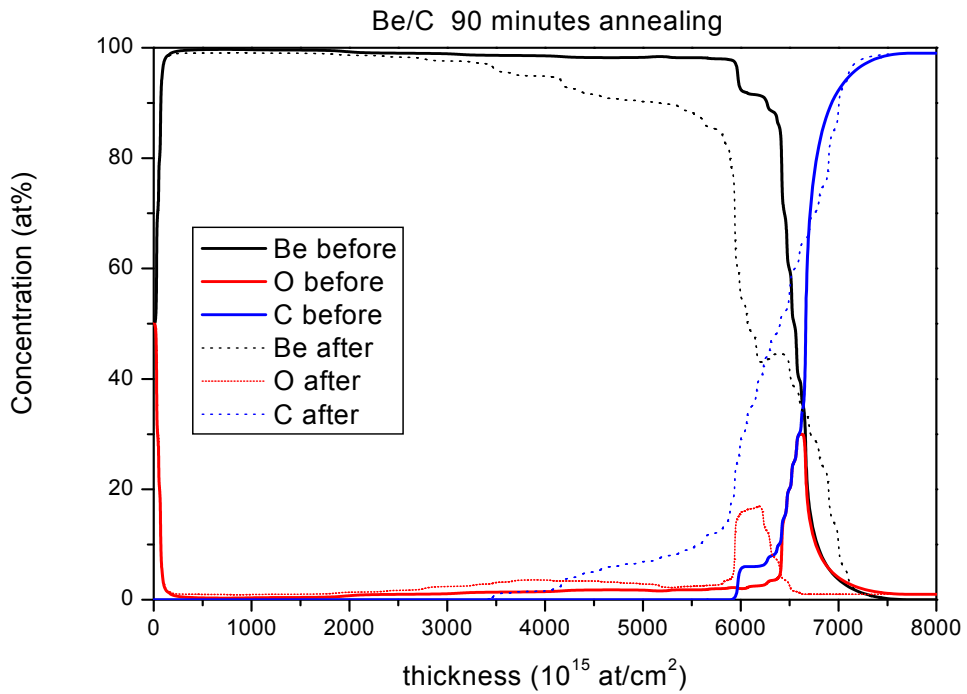

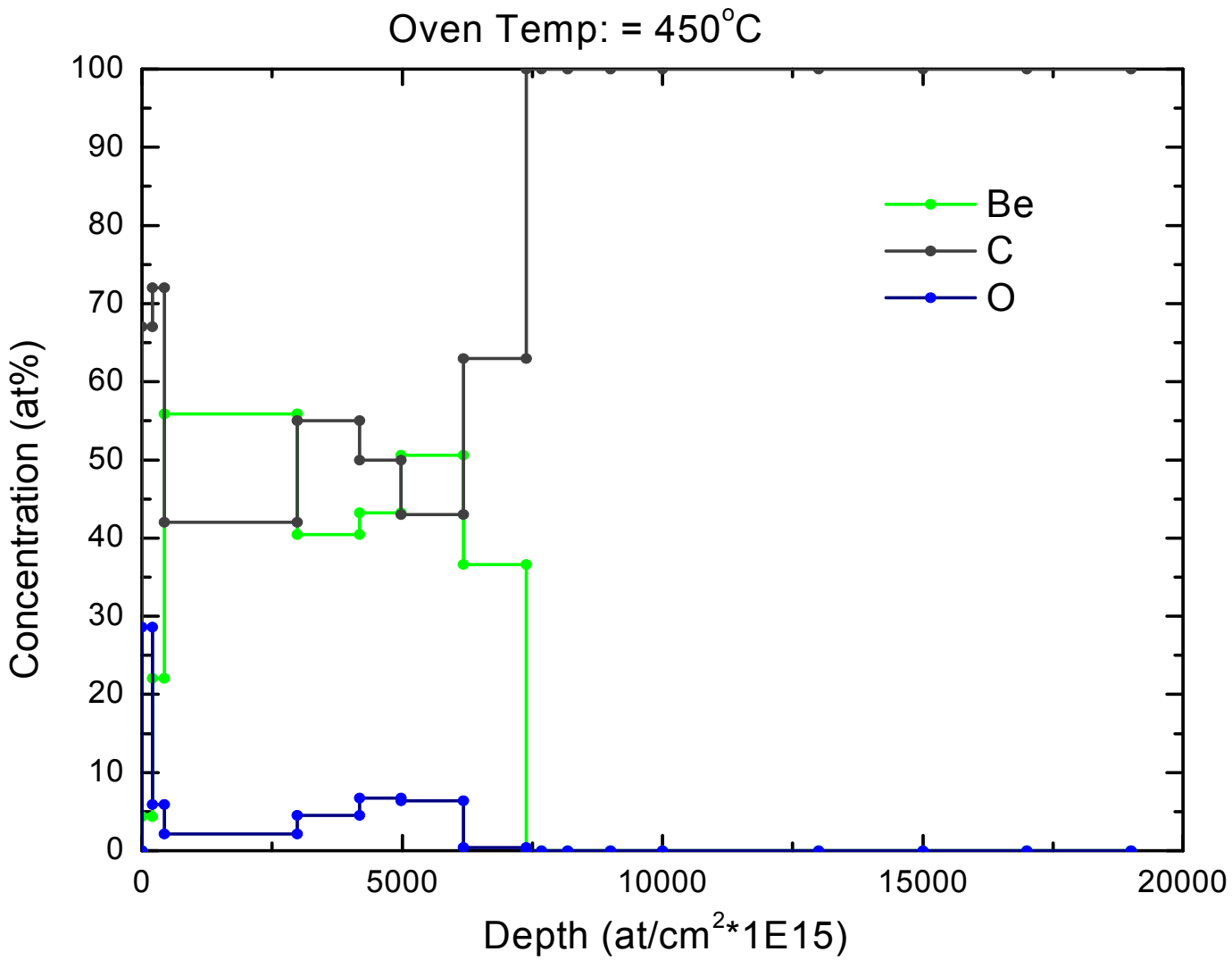
Oven Temp: = 450°C
Concentration (at%)
Depth (at/cm2*1E15)
Be
C
O
0
10
20
30
40
50
60
70
80
90
100
0
5000
10000
15000
20000

RBS Measurements

Thermal treatment at 750 ºC of the Be film coated on graphite

Heating the sample to 750 ºC it was observed from the RBS spectra that the carbon from the substrate diffused into the beryllium film forming a mixed layer. Also, the oxygen present at the Be – C interface diffused to the surface.

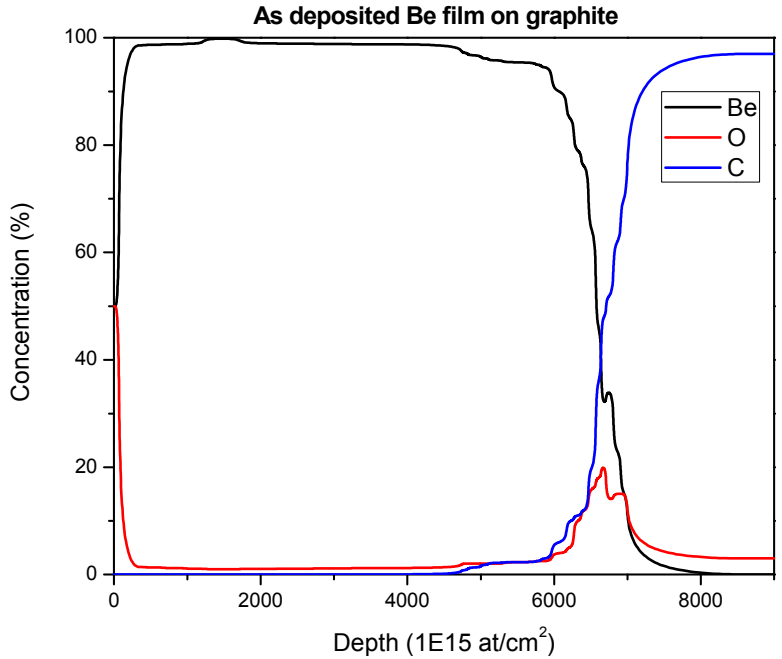

RT

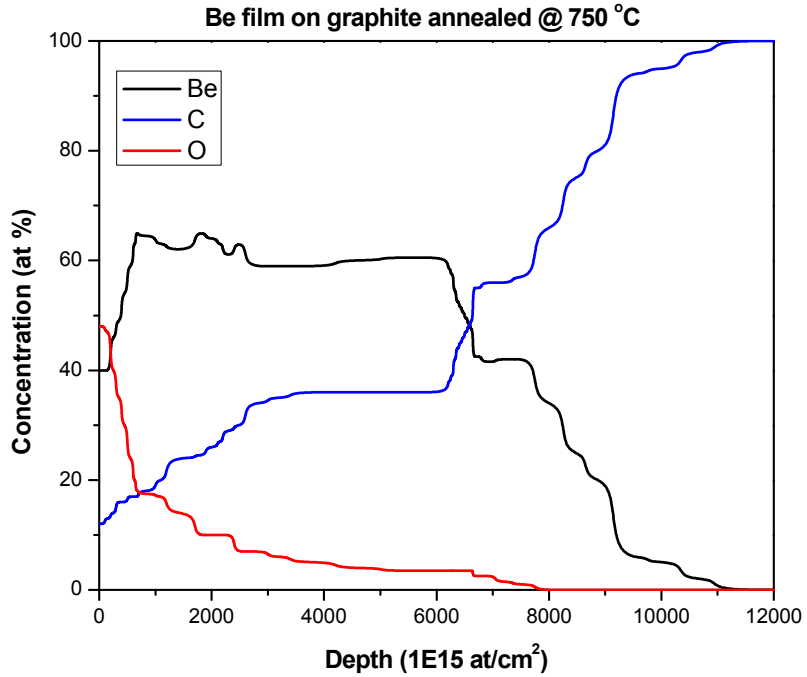

750ºC

XPS measurements

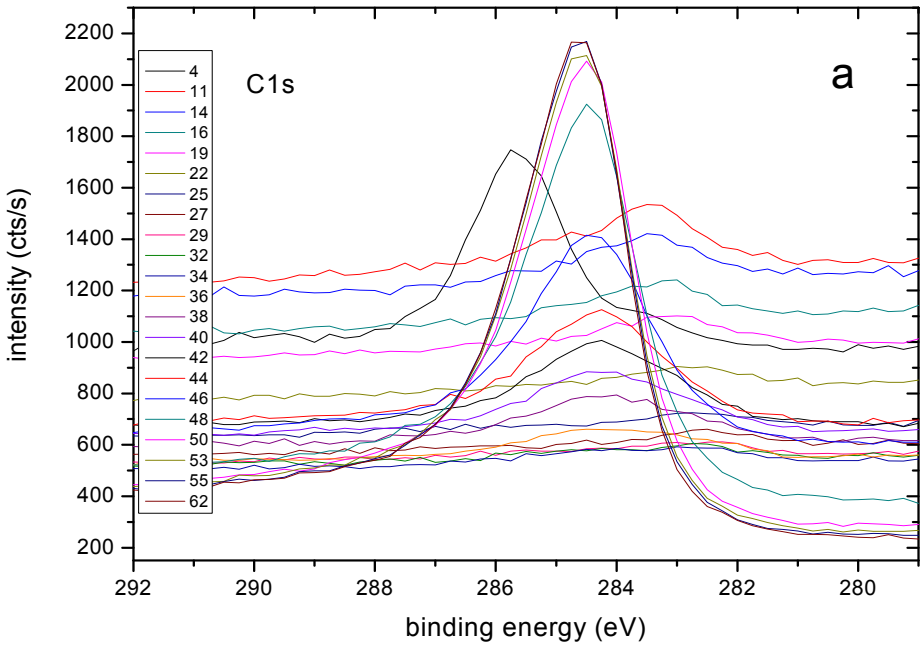

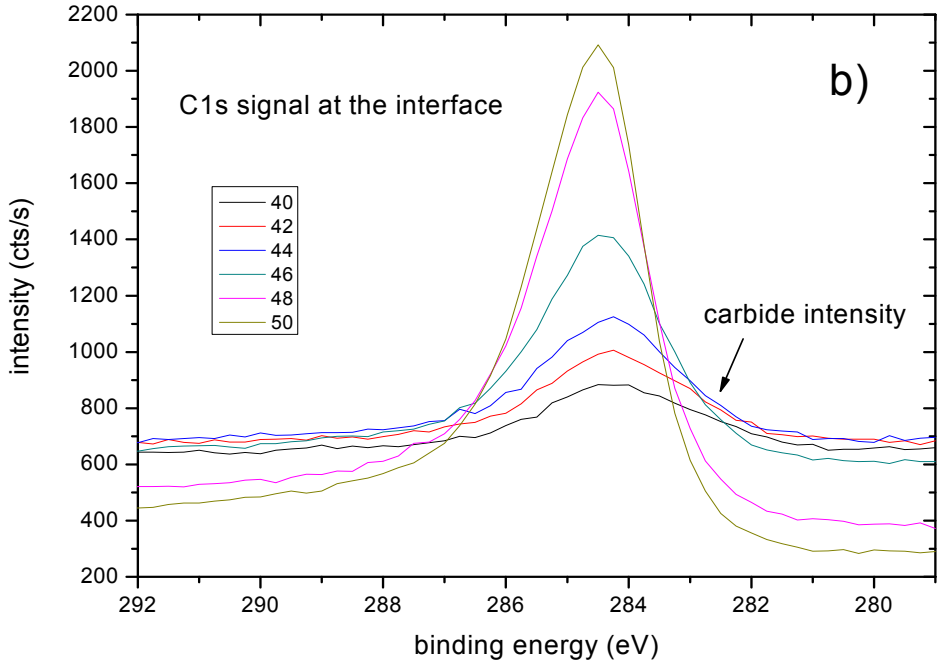

C1s peak in depth

C1s peak at the interface

Be_2C formation:

Be reactivity; Ion bombardment

XPS measurements

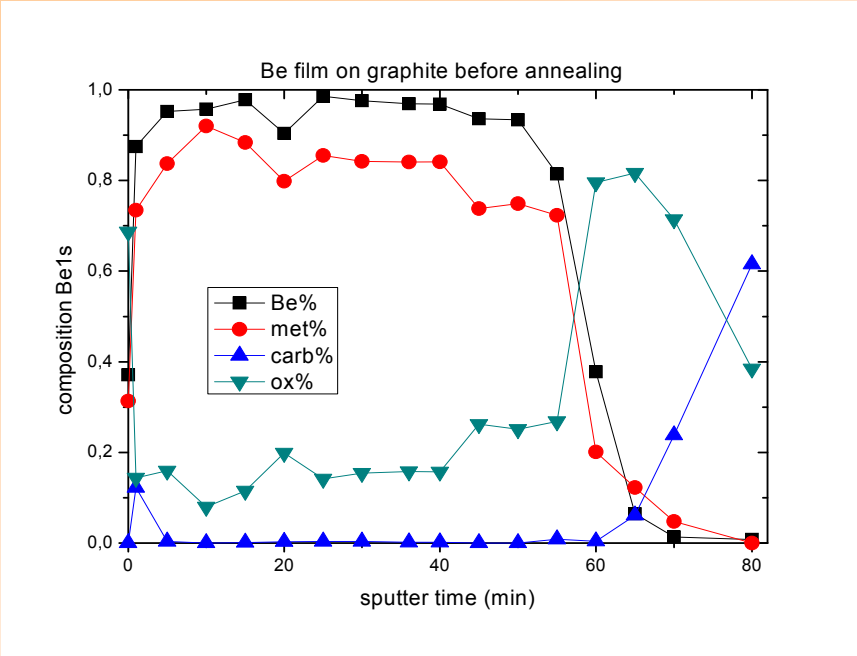

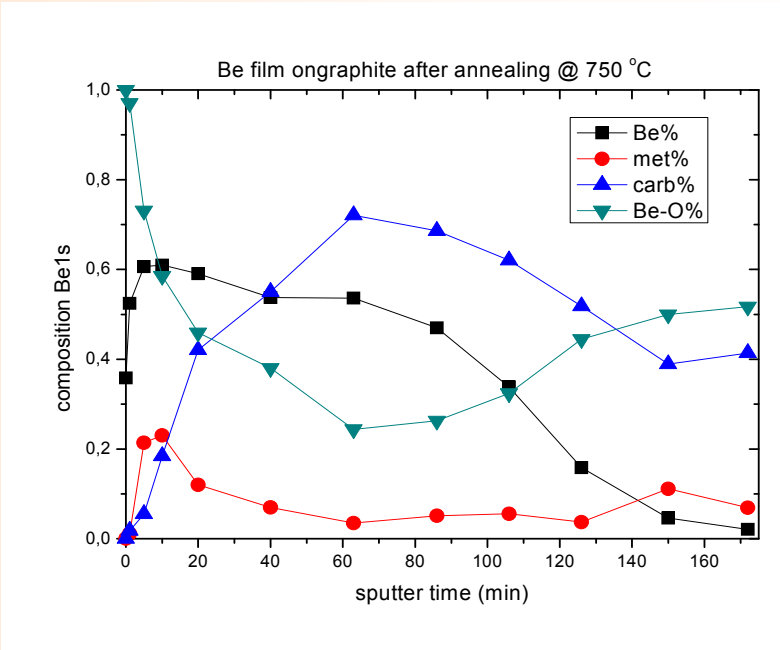

XPS measurements before (left side) and after (right side) thermal treatment are in good agreement with the results obtained by RBS

- Be_2C alloy is present in the whole film
- strong oxidation of the film
- less than 20 % of the beryllium remains in pure metallic form
- the film remains stable

Be-C-W films preparation

Be - C: TVA evaporation anode

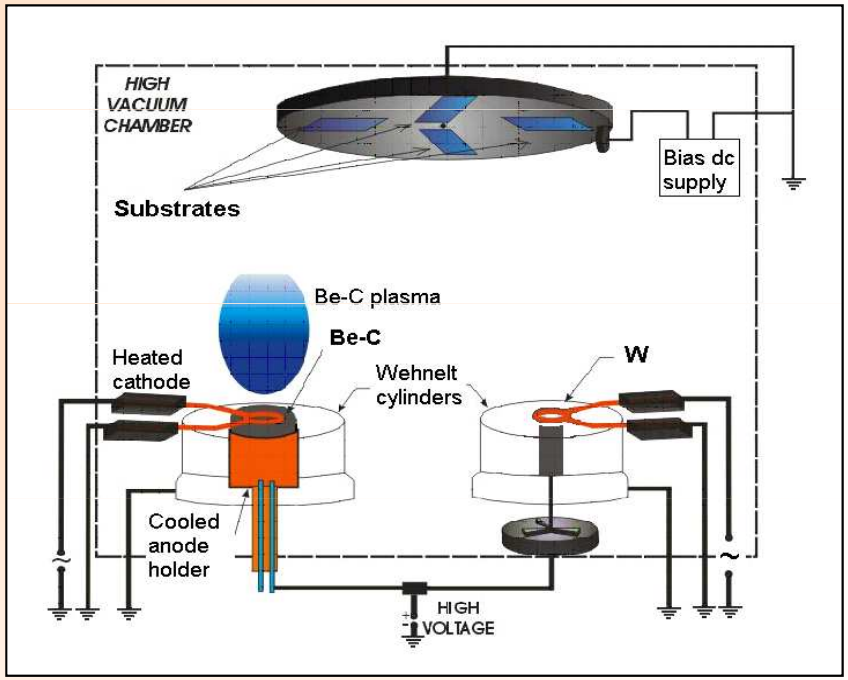

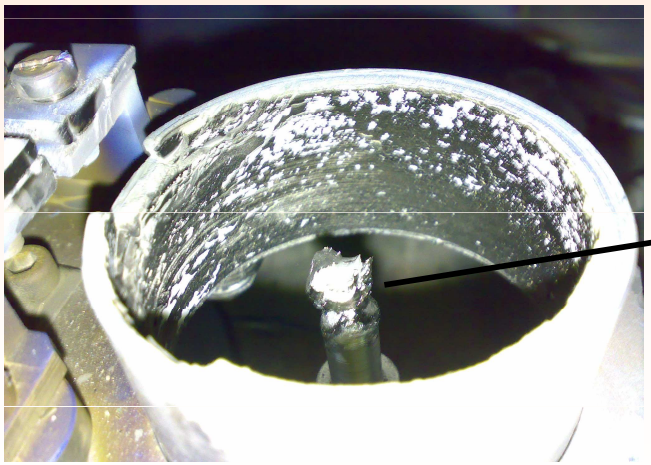

W: TVA evaporation anode

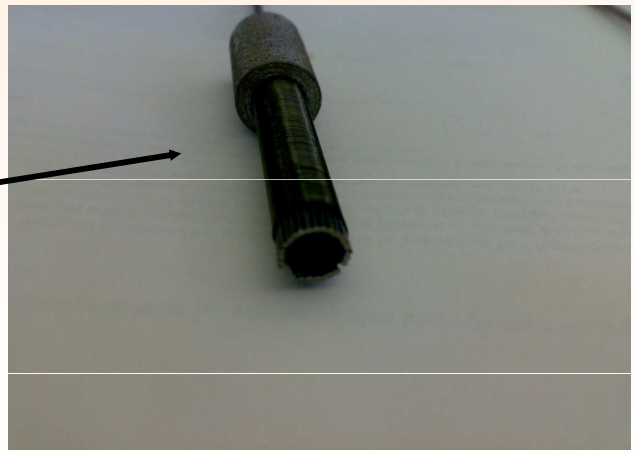

W rod

Morphology of Be-C-W films

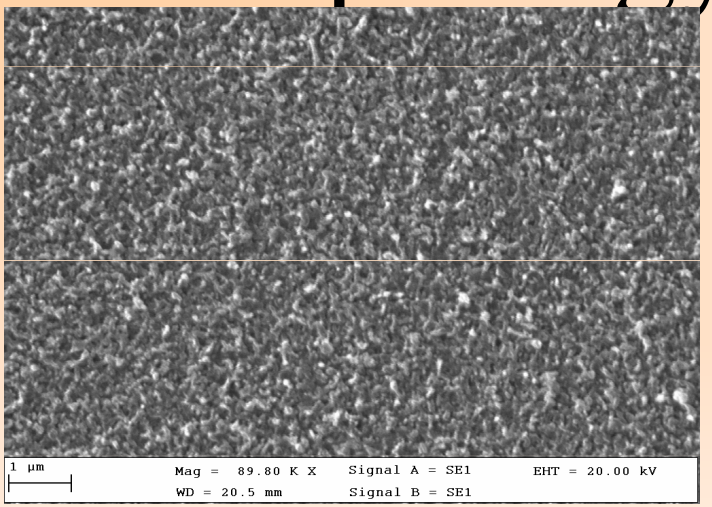

Be-CW22

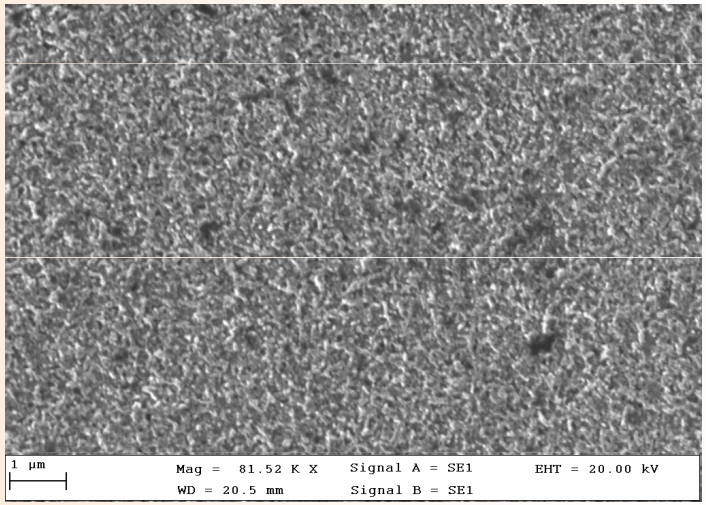

Be-CW23

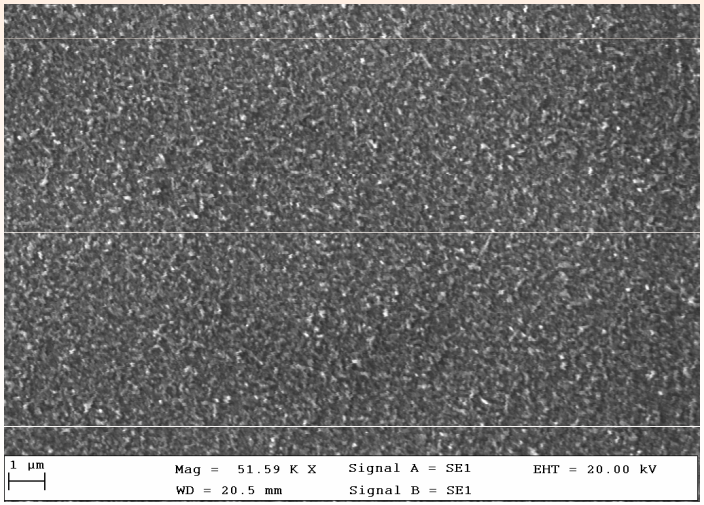

Be-CW24

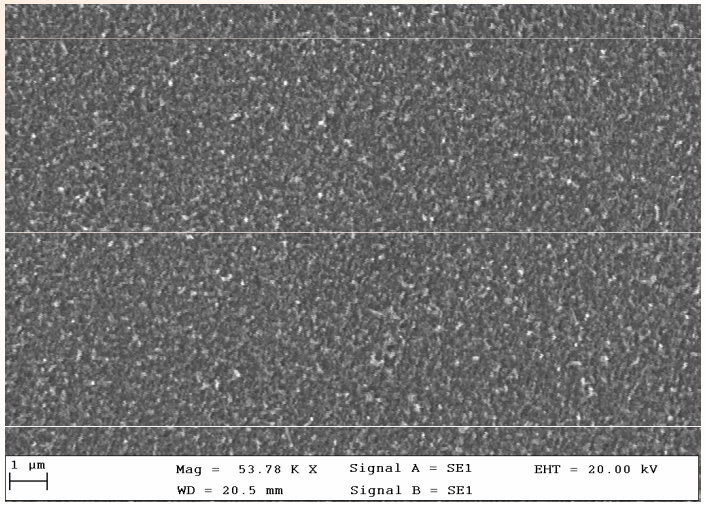

Be-CW25

SEM and EDS characterization of the Be-C-W films

Cod probă	SEM 10.000 X	SEM 50.000 X	EDS	Concentration (at%)
22.02.2010 Be+C+W on Si substrate Sample nr. 2	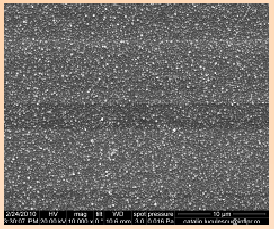	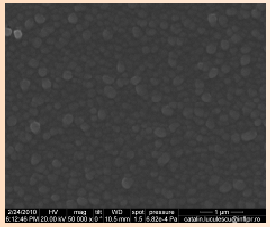	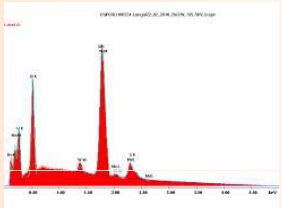	Be - 25.34at% C – 27.21at% W – 23.31at% O – 23.64 at%
22.02.2010 Be+C+W on Si; Sample nr. 5	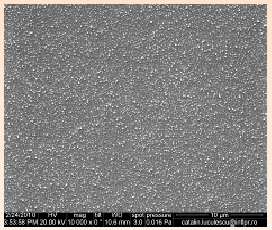	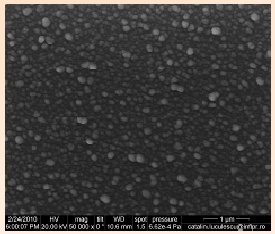	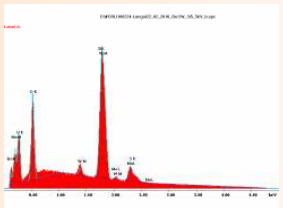	Be - 22.00 at% C – 30.44 at% W – 25.27 at% O – 22.29 at%
23.02.2010 Be+C+W on Si; Sample nr. 2	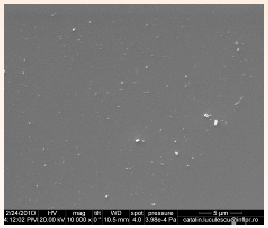	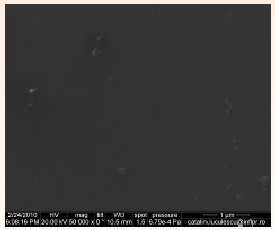	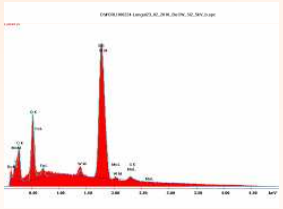	Be – 19.70 at% C – 29.20 at% W – 27.65 at% O – 23.42 at%

TEM image of the Be-C-W film

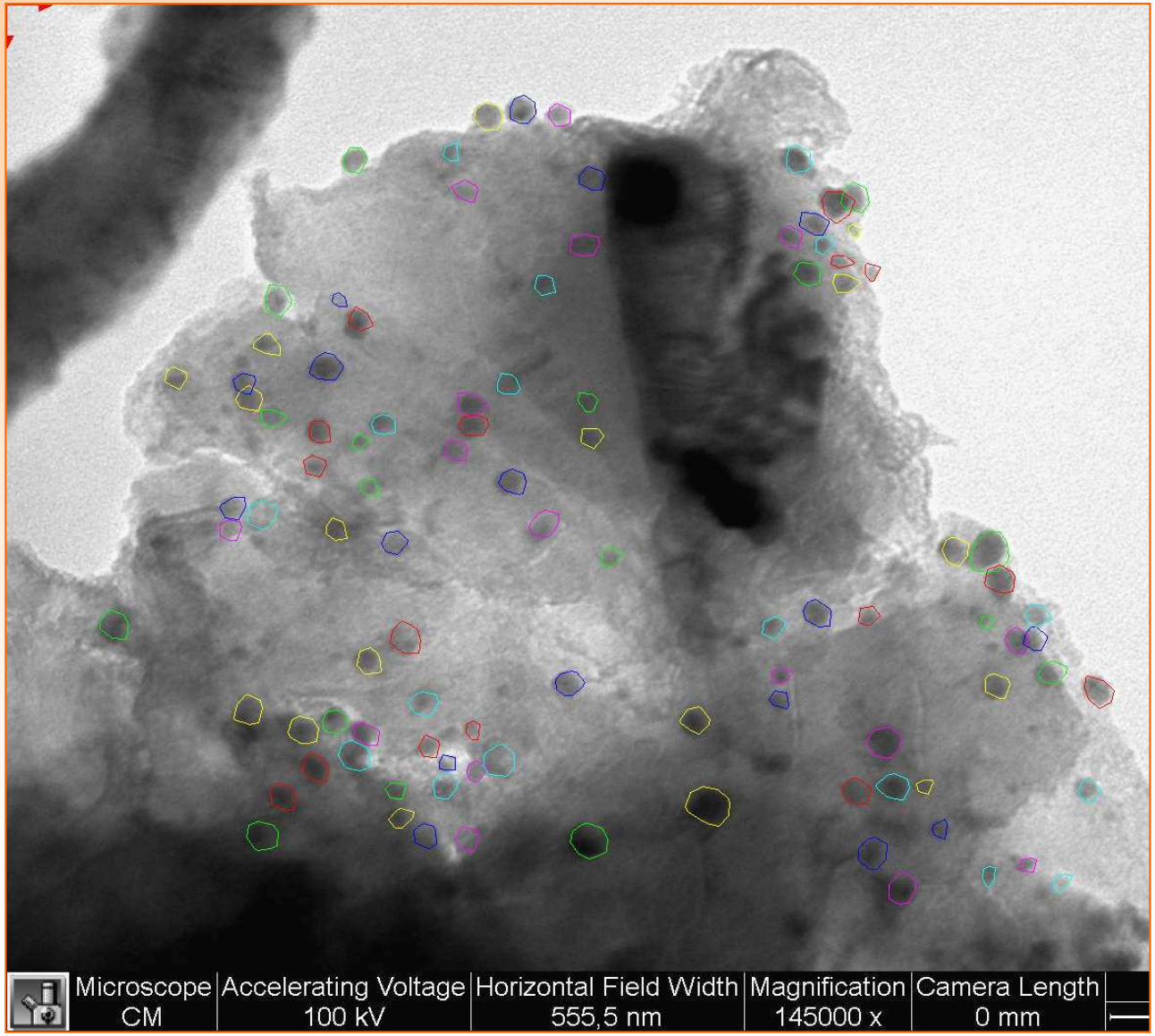

Elemental mapping (EDS analysis) and concentration compositions of Be-C-W films

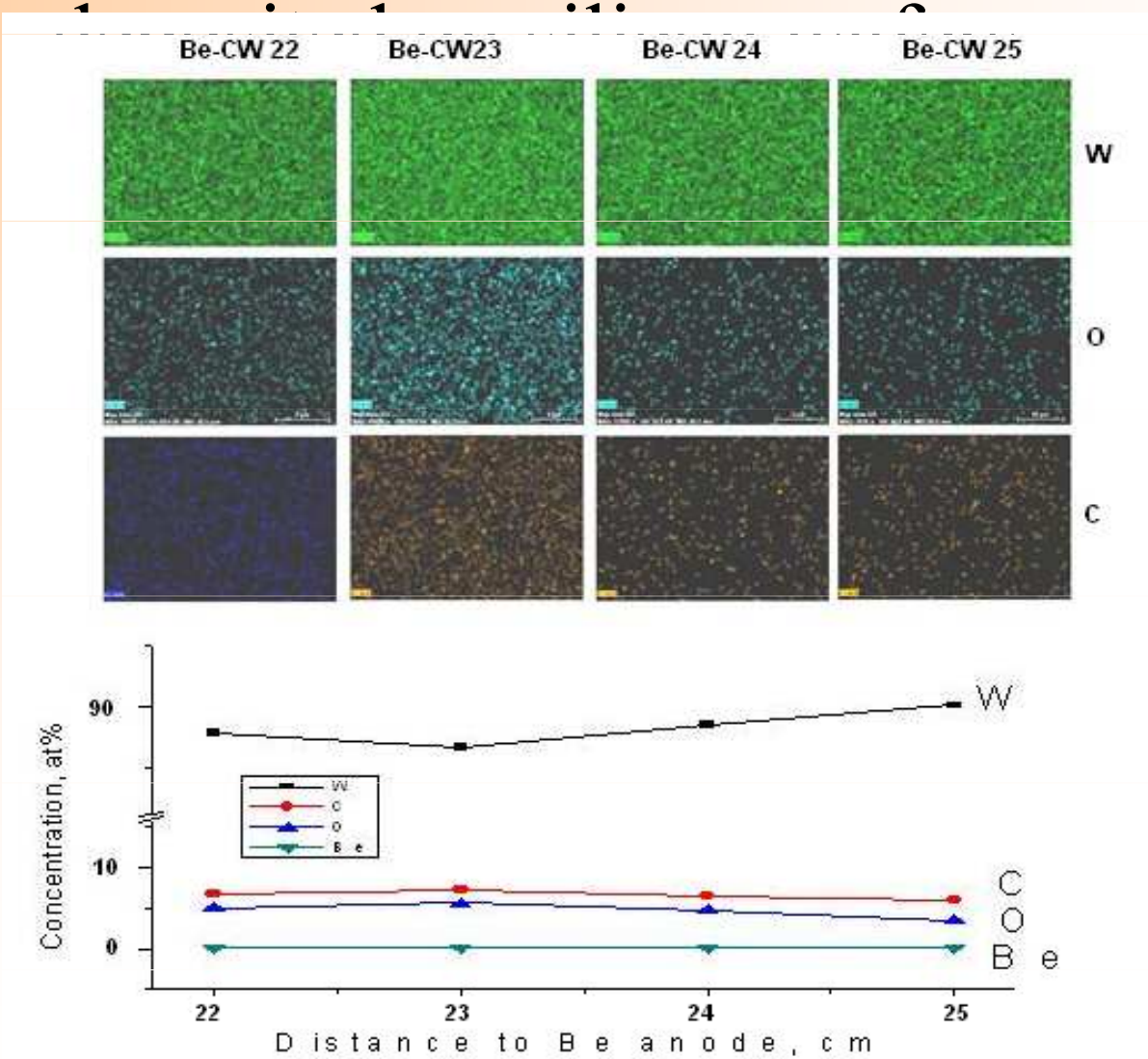

Be-C-W depth profile film analysis by XPS

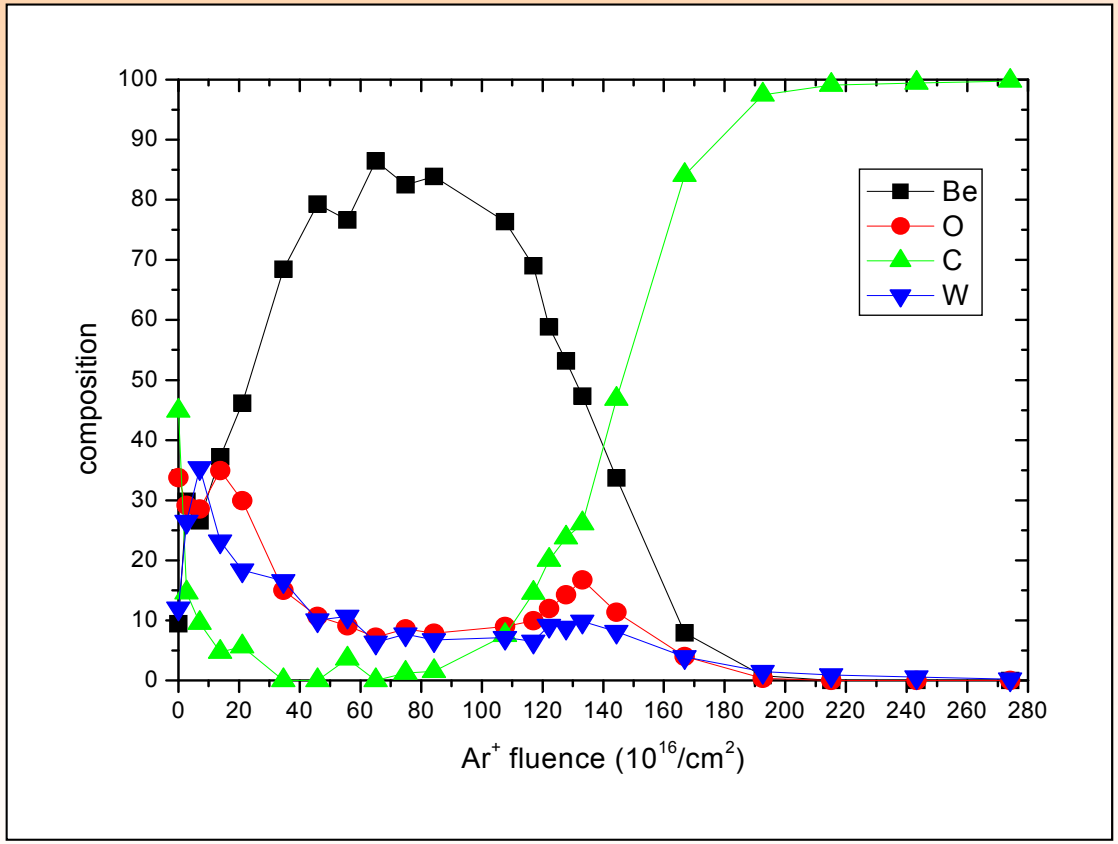

Be-C-W depth profile film analysis by SIMS

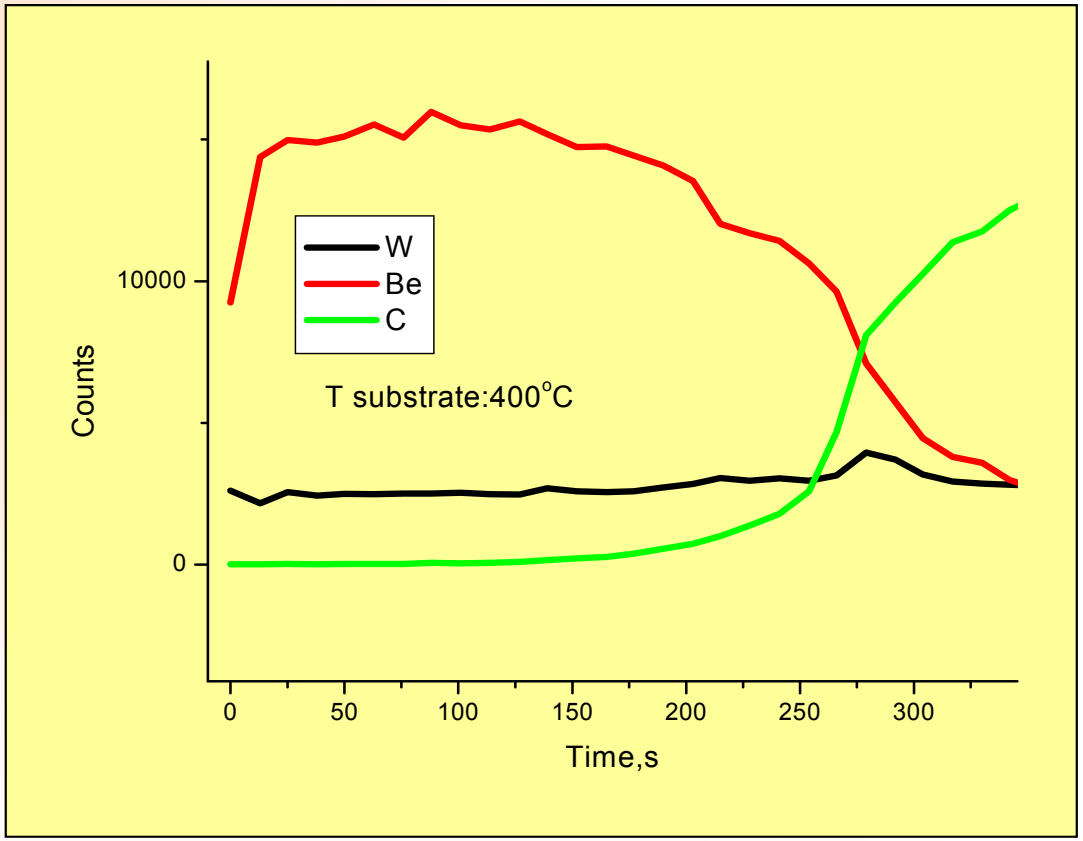

XPS depth profile

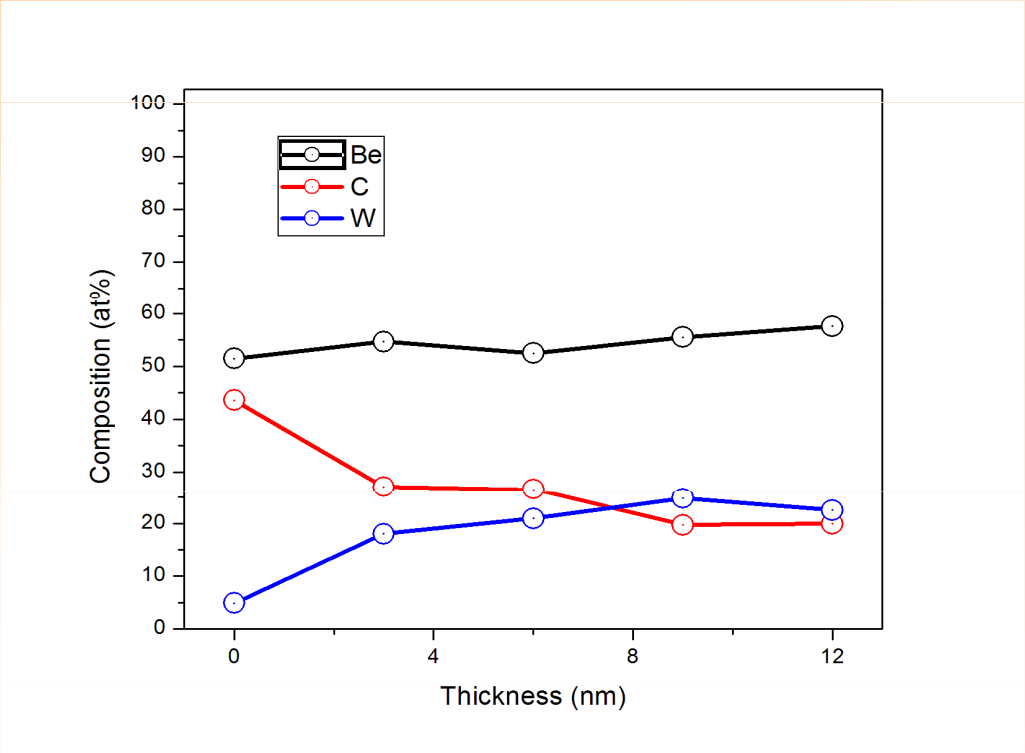

RBS depth profile

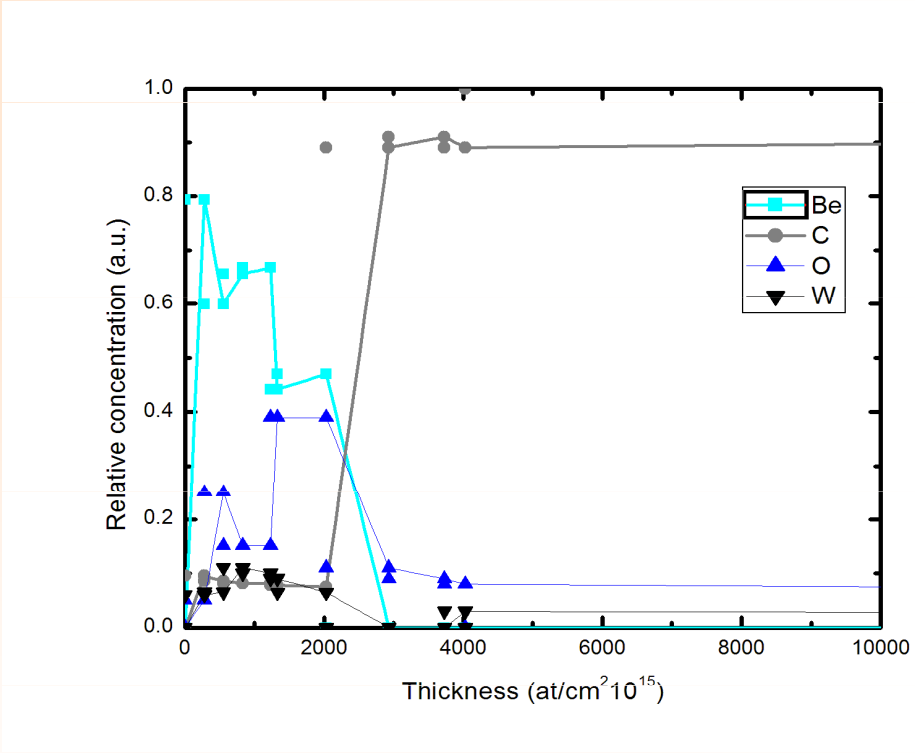

E-Beam irradiation/annealing

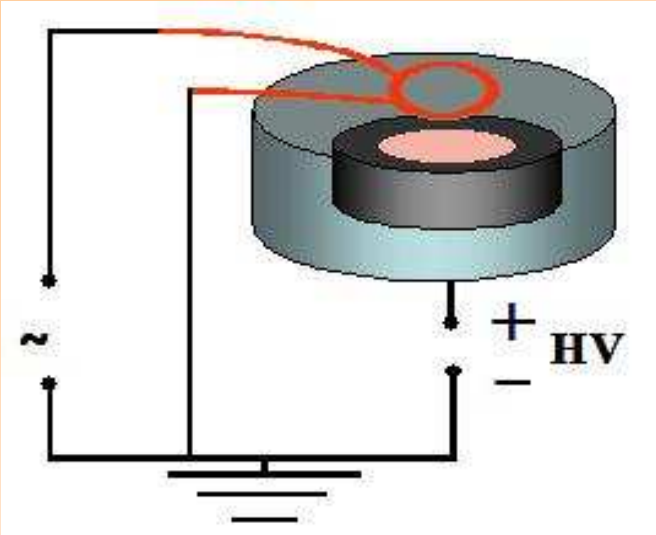

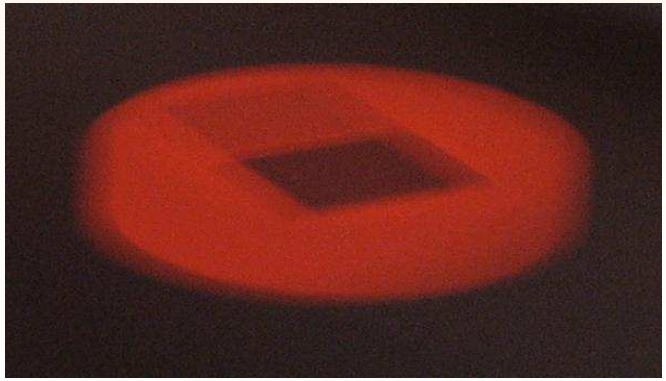

Before annealing

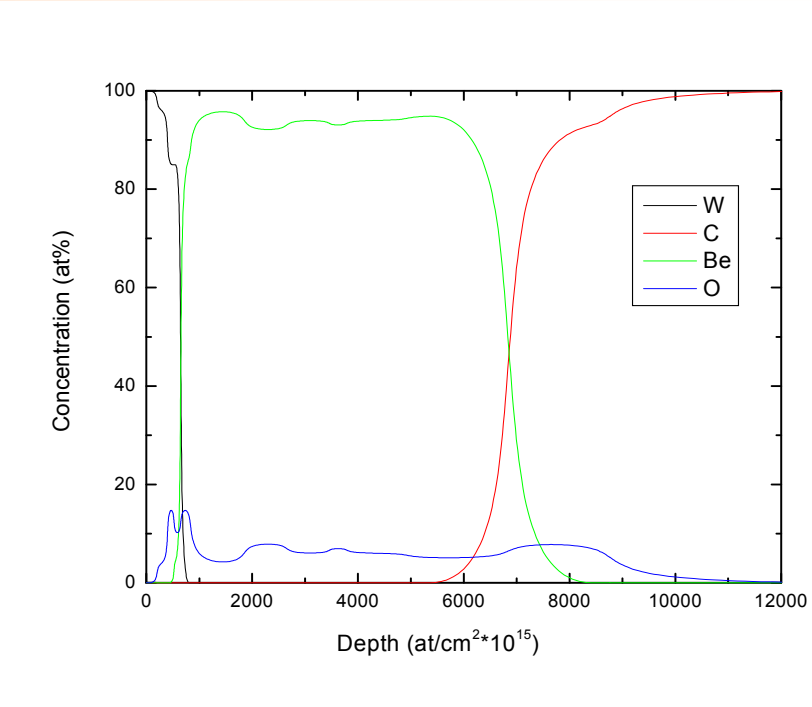

After annealing

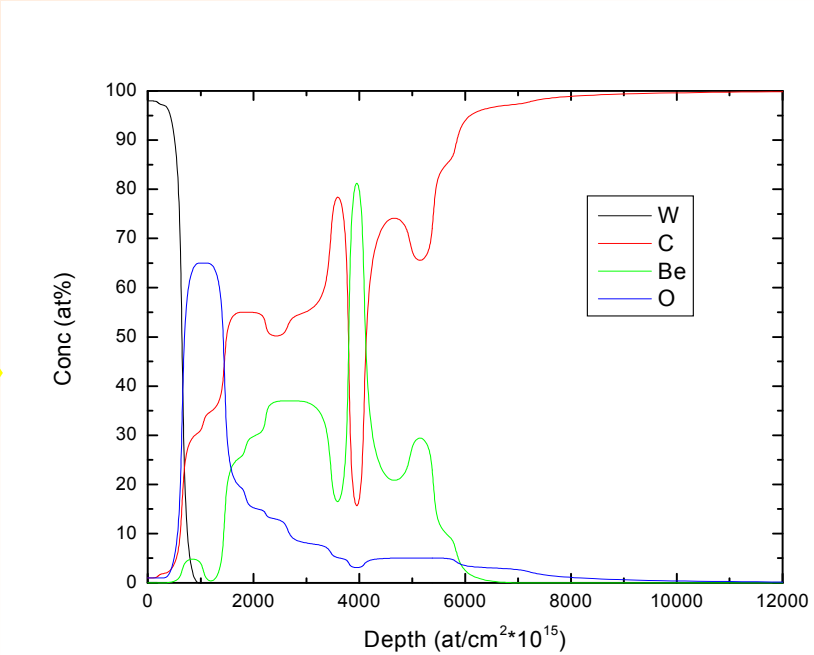

CONCLUSIONS

- Thermionic Vacuum Arc method (TVA), was used for preparation of composite films for fusion programme.
- RBS and XPS analysis proved the formation of binary/ternary mixtures at interfaces and as prepared and annealed films.
- At RT the films were oxidized only at the surface and at the interface, while for the heated substrates the oxygen was present at the surface, and diffuses into the material, oxidizing the beryllium and the tungsten in the whole film. In addition, the oxygen present at interfaces begins to migrate into the substrate as the temperature increased.
- In the case of 350 ^{o}C annealing of Be/graphite, Be_2C compound occurs only at the interface but the thickness of the mixed layer increases with the duration of the thermal treatment.
- Annealing Be/graphite samples at 750 ^{o}C, Be_2C was formed in the whole film
- Oxygen from the interface migrates into the film forming BeO
- The films were stable after annealing

PULSED LASER BEAM INTERACTION WITH CARBON, TUNGSTEN AND BERYLLIUM COATINGS

The the behavior of the 0.5 - 10 μm thickness carbon, tungsten and beryllium layers in interaction with single or multiple terawatt laser beam pulses in vacuum was studied. Terawatt laser system (Tewalas), a modern facility of the National Institute for Laser, Plasma and Radiation Physics (NILPRP) is a high power, 20-360 x 10^{-15} s pulse duration, 100-450 mJ pulse energy, 10 Hz repetition rate. The 10^{12} - 10^{14} W/cm^2 density power laser beam was focalized, in vacuum, on the W, C, Be coatings prepared using the orginal technology of thermionic vacuum arc (TVA) developed at NILPRP.

The laser pulses were programmed to have durations of pico or femtoseconds, in order to obtain duration and power densities compared to the fusion plasma instabilities.

The spectroscopy of plasmas produced by laser breakdown using pico and femtosecond laser pulses reveal features not observed with longer (nanosecond) laser pulses. Were studied the effects of the laser produced plasmas with pure C, W and Be films. The coatings characterizations before and after exposures were performed using modern techniques as: atomic force microscopy (AFM), scanning electron microscopy (SEM), transmission electron microscopy (TEM), X-ray photoelectron spectroscopy (XPS) and Raman spectroscopy.

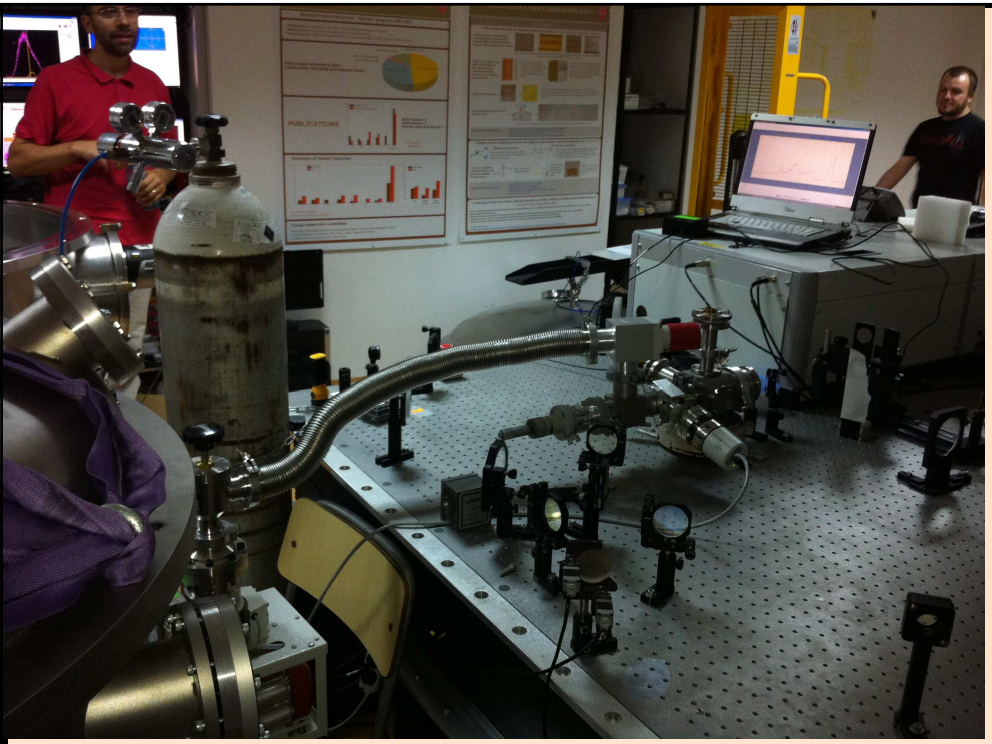

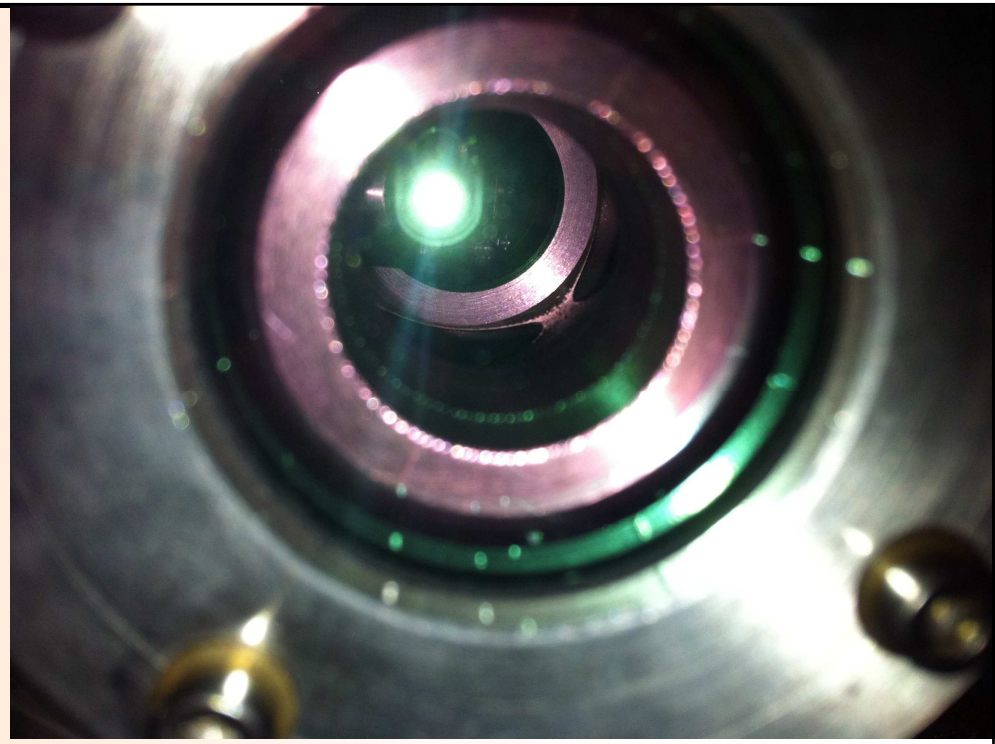

IMG_1440.MOV

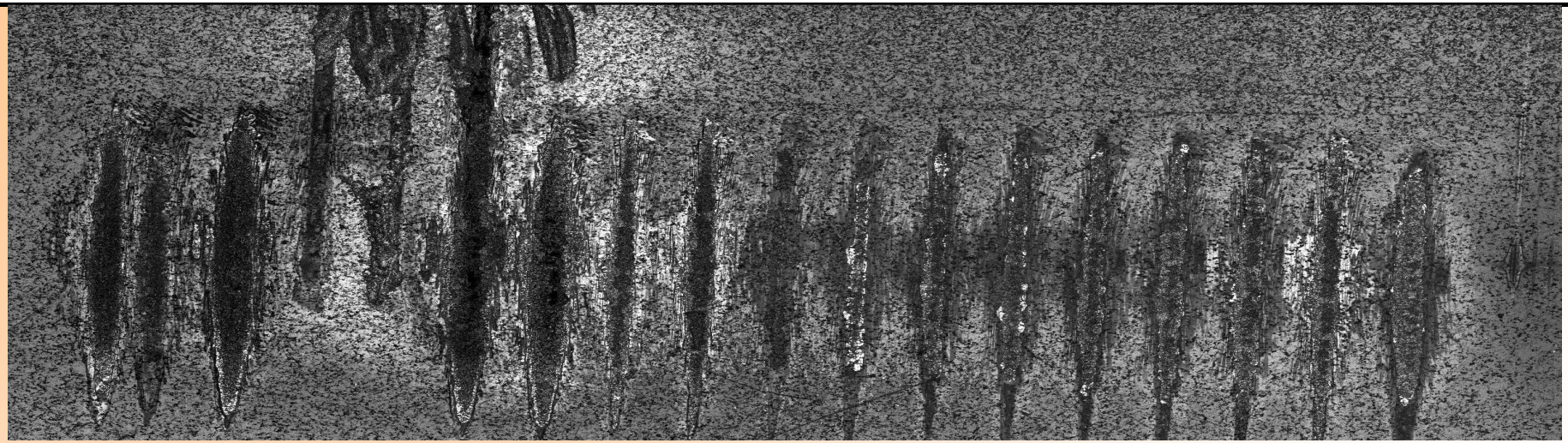

Scanning electron microscopy (SEM) images taken with a SUPRA VP 40 microscope (ZEISS) on the laser irradiated zones (craters) are shown

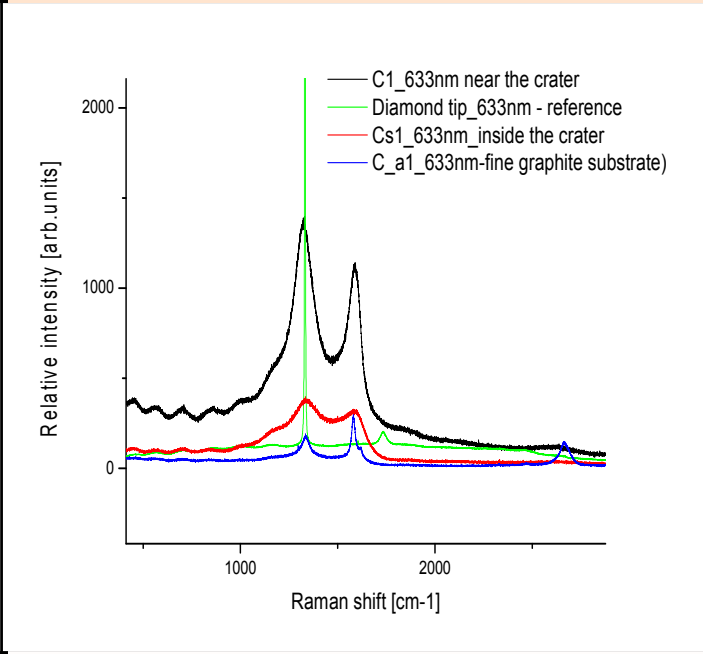

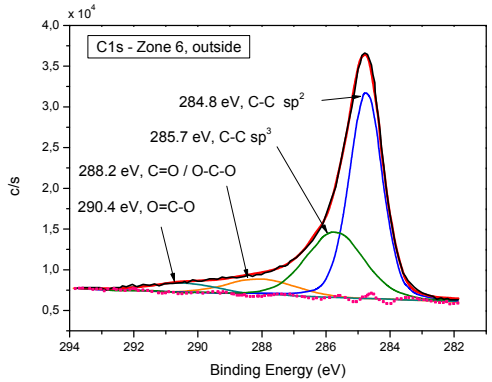

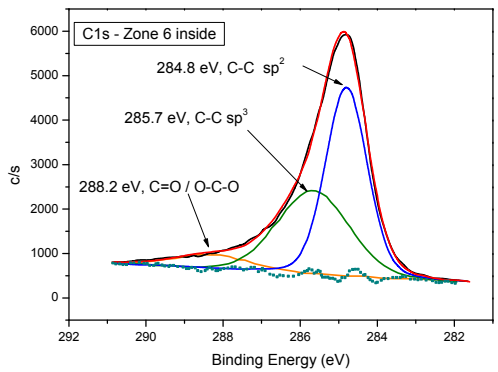

The sp3 content is estimated from the area corresponding to diamond and the sum of the areas of the overlapping peaks of graphite and CO phases. An estimation of sp3 content results in 39.4% at the raw surface on the inside crater of the irradiated zone 6, compared to 30.8% of the non-radiated zone

Conclusions: Carbon films with the thickness of about 2500 nm were coated on top of 200 nm tungsten films deposited on fine grain graphite substrates and were irradiated using ultra-short laser pulses of as The craters produced by the laser irradiation contain ordered structures as observed in the SEM images, which correspond to rhombohedral structures with lattice parameters a =0.25221 nm, c = 4.3245nm (diamond) as identified by SAED analysis. The micro-Raman scattering measurements performed on the craters in comparison with the spectrum of a diamond tip show the 1330 cm-1 wide enough to allow a discontinuous diamond structure interpretation. SEM images associated with EDS analysis prove the existence of W particles in the diamond-graphite structure of the irradiated zones. The ratio of sp3/sp2 bonds estimated using XPS was found larger than 60%.

The Raman characterization leads to the conclusion that the films are built of NCD and NC graphite as a result of hysteresis. .